Laboratory of Metallomics and Nanotechnologies
Mendel University in Brno

CONFERENCE PROCEEDINGS

Metallomics Technology Conference 2015: Recent Advances and Strategies

Vojtěch Adam, René Kizek

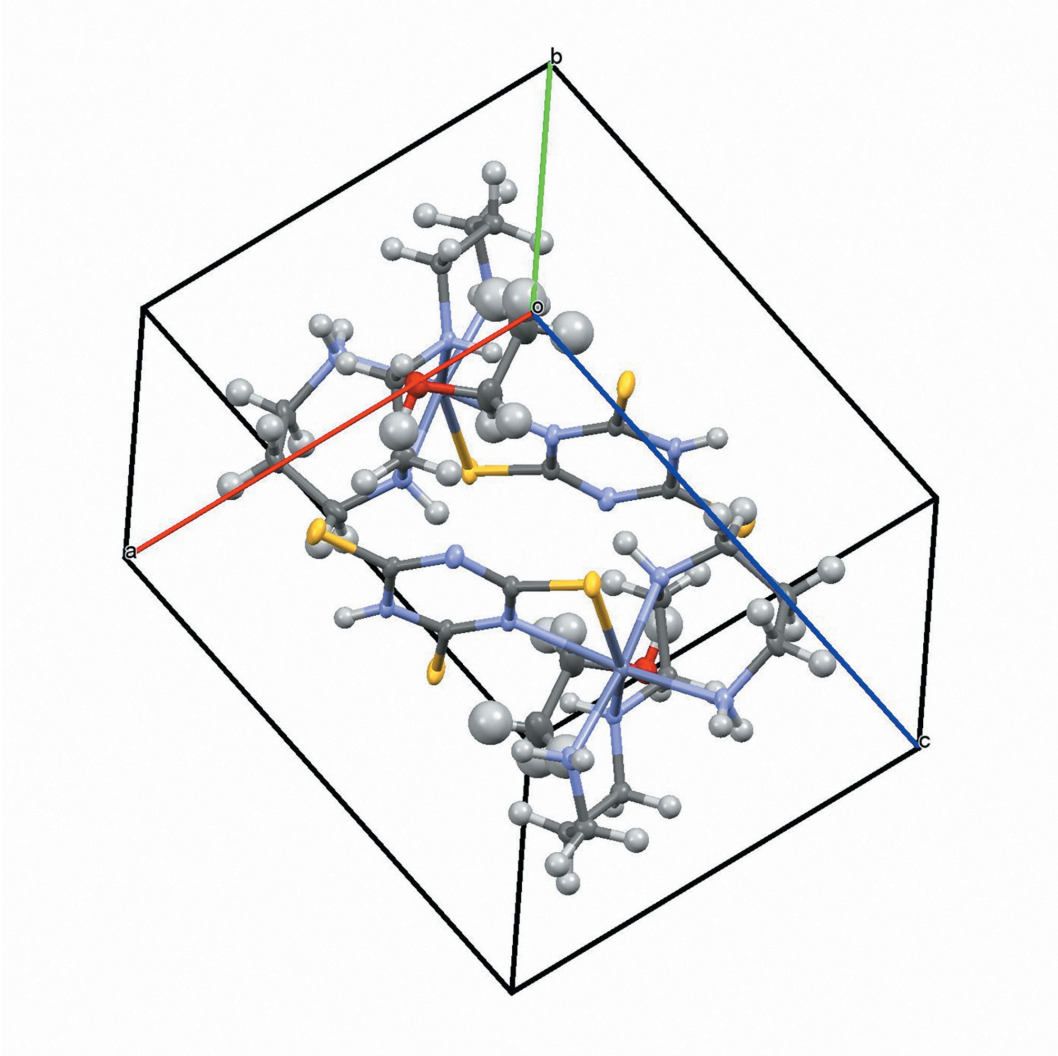

14. – 18. 6. 2015, Brno, Czech Republic

The project is supported by International Visegrad Fund
www.visegradfund.org

Laboratory of Metallomics and Nanotechnologies
Mendel University in Brno

CONFERENCE PROCEEDINGS

Metallomics Technology Conference 2015: Recent Advances and Strategies

Vojtěch Adam, René Kizek

14. – 18. 6. 2015, Brno, Czech Republic

The project is supported by International Visegrad Fund
www.visegradfund.org

Organizer committee
Department of Chemistry and Biochemistry, Faculty of Agronomy,
Mendel University in Brno
Editors are not responsible for language correction. Contents of the contributions are the authors' responsibility.

Editors: Vojtěch Adam, René Kizek
Publisher: Mendel University in Brno, Zemědělská 1, 613 00 Brno

ISBN 978-80-7509-309-7
ISBN 978-80-7509-314-1 (on-line)

“Small grant” Metallomic Scientific Network

No. 11440027

Visegrad Fund

The project is supported by International Visegrad Fund
www.visegradfund.org

Metallomics Scientific Network is a newly created network concerned with research in the field of metallomics and nanotechnologies, which can effectively apply the benefits of cross-border cooperation and joint coordination, education, innovation and research activities. Metallomics is a novel and highly perspective research field which, however, currently lacks support from an established platform in countries of V4. Therefore, we consider it highly desirable to form a functional structure that will strengthen the role and importance of these countries in the scope of V4, and also in whole Europe. The aim resolved by the partners forming the network are future related experiments in metallomics, nanotechnologies, conducted through another V4 and European projects.

Content

Introduction

Dear Colleagues,

Metallomics Technology Conference is an international forum for scientific discussion focused on understanding the relationship and connections between metals and their binding species inducing amino acids, peptides, proteins and nucleic acids.

The aim of this multidisciplinary conference is to bridge the gaps between the specialists and fields of science as diverse as inorganic chemists, biochemists and clinicians.

There is a need for sensitive and reliable analytical methods which would help us to determine what bioactive metal-binding compounds are found in an organism, as well as for trace analysis methods in complex biological matrices to follow the bioactive compounds and their metabolites in the human body. Moreover, we need to understand how disorders and illnesses can influence these.

It is evident that enormous progress has been made in metallomics over the last decade. Recent challenges for scientists in this field are to develop analytical technologies that would allow us to understand our personal metabolism, in connection with specific biomarkers, with the overall aim to personalize medicine as generalized recommendations and to discover how to influence metal metabolism for treatment of civilization diseases.

We are looking forward to meeting you in Brno.

Vojtěch Adam

Articles

Zinc signals and the control of immune cell functions

Hajo Haase

Department of Food Chemistry and Toxicology, Berlin Institute of Technology, Gustav-Meyer-Allee 25, D-13355 Berlin, Germany

The last 50 years have seen a continuous increase of knowledge on the myriad of functions that zinc has for immunity. Starting with the observation that zinc deficiency can cause malfunction of the immune system, the role of zinc in several hundred enzymes and an even greater number of transcription factors has been explored. Here, tightly protein bound zinc ions serve catalytic or structural functions in a multitude of different proteins. In addition, a role for free or loosely bound zinc ions as second messengers in signal transduction has been backed up by increasing evidence for a regulatory role of free zinc, in particular in cells of the immune system. Several molecular targets for zinc signals have been identified, including protein tyrosine phosphatases, cyclic nucleotide phosphodiesterases, caspases, and kinases. While the knowledge about the biochemistry of zinc signaling has grown considerably, in-depth research into the regulation of free intracellular zinc, and thereby zinc signals themselves, is still in its infancy. The important players in zinc homeostasis are known: these are transport proteins from the SLC30 (ZnT) and SLC39 (Zrt, Irt-like protein, ZIP) families, and the group of small cysteine-rich metallothioneins, which act as an intracellular reservoir for protein-bound zinc that may be released upon stimulation. Together these proteins have the capacity to tightly regulate zinc availability. Yet, the mechanisms by which zinc signals are controlled are still unresolved. First results point toward phosphorylation of transporters and oxidation of cysteine thiols in metallothioneins as mechanisms for altering free zinc levels. A more detailed understanding of the molecular events leading to changes of the intracellular free zinc concentration will be important future steps toward understanding the multiple aspects of zinc as a regulator of immunity.

Acknowledgement

The work was supported by V4 Metallomic Scientific Network TD 11440027.

Metallothionein and neuroinflammation

Juan HIDALGO[1*]

[1] Department of Cellular Biology, Immunology and Physiology, Autonomous University of Barcelona, Campus UAB, ES-081 93 Barcelona, Spain, European Union

*juan.hidalgo@uab.cat

Metallothionein (MT) is an ubiquitous protein [1], and its physiological role remains a matter of intense study and debate 50 years after its discovery [2]. This is particularly true of its function in the central nervous system (CNS), where the challenge remains to link its known biochemical properties of metal binding and free radical scavenging to the intricate workings of brain [3].

Metallothioneins (MTs) are a family of low molecular weight, cysteine-rich, metal-binding proteins that have a wide range of functions in cellular homeostasis and immunity [4]. Metallothioneins (MTs) constitute a superfamily of proteins that specifically bind to closed shell metal ions (Zn^{2+}, Cd^{2+}, Cu^{+}) via the sulfur atoms of their rich cysteine residues [5]. They are involved in metal-related tasks including metal ion detoxification and homeostasis [6], radical scavenging [7] and stress response [8]. Their specific physiological role may vary among animal species, the tissues in which they are expressed and the MT family to which they belong [9].

MT has the potential to contribute to a variety of processes, including neuroprotection, regeneration, and even cognitive functions [3]. In humans, the MT genes are tightly clustered in the q13 region of chromosome 16, consisting of seven functional MT-I genes (MT-1A, -B, -E, -F, -G, -H and -X) and a single gene encoding each of the other MT isoforms, namely MT--II (the MT-2A gene), MT-III and MT-IV. Mice have a much simpler MT gene structure, with only one functional gene for each isoform MT-I–MT-IV, all located on chromosome 8 [10].

One of the most active areas of research is the involvement of these proteins in the inflammatory response in general, and in neuroinflammation in particular [2]. Traumatic brain injury is one of the leading causes of injury-related death and disability, especially in young people [11], and thus continued efforts to characterize all factors involved are essential. The general response of the brain to traumatic injury is relatively well-known: inflammation, gliosis, blood-brain barrier disruption, alteration of cytokine expression, and oxidative stress are prototypical changes [12-14].

Previously it has been shown that the antioxidant proteins metallothioneins (MTs) are potent neuroprotective factors in animal models of brain injury. The exogenous administration of MTs causes effects consistent with the roles proposed from studies in knock-out mice.

Acknowledgement

The work was supported by V4 Metallomic Scientific Network TD 11440027.

References

[1] J.Z. Lindeque, J. Hidalgo, R. Louw, F.H. van der Westhuizen, Metabolomics 9 (2013) 418.
[2] Y. Manso, P.A. Adlard, J. Carrasco, M. Vasak, J. Hidalgo, Journal of Biological Inorganic Chemistry 16 (2011) 1103.

[3] A.K. West, J. Hidalgo, D. Eddins, E.D. Levin, M. Aschner, Neurotoxicology 29 (2008) 489.
[4] M.A. Lynes, J. Hidalgo, Y. Manso, L. Devisscher, D. Laukens, D.A. Lawrence, Cell Stress & Chaperones 19 (2014) 605.
[5] J.H.R. Kaegi, Evolution, structure and chemical activity of class I metallothioneins: An overview, Birkhaeuser Boston, Inc., 175 Fifth Avenue, New York, New York 10010, USA; Birkhaeuser Verlag, P. O. Box 133, CH-4010 Basel, Switzerland, 1993.
[6] C.D. Klaassen, J. Liu, B.A. Diwan, Toxicology and Applied Pharmacology 238 (2009) 215.
[7] S.K. Baird, T. Kurz, U.T. Brunk, Biochemical Journal 394 (2006) 275.
[8] C.J. Fu, W. Miao, Protist 157 (2006) 193.
[9] R. Dallinger, Comparative Biochemistry and Physiology C-Toxicology & Pharmacology 113 (1996) 125.
[10] C.J. Quaife, S.D. Findley, J.C. Erickson, G.J. Froelick, E.J. Kelly, B.P. Zambrowicz, R.D. Palmiter, Biochemistry 33 (1994) 7250.
[11] M.L. Prins, D.A. Hovda, Journal of Neurotrauma 20 (2003) 123.
[12] J.T. Coyle, P. Puttfarcken, Science 262 (1993) 689.
[13] C.W. Olanow, Trends in Neurosciences 16 (1993) 439.
[14] S.M. Lucas, N.J. Rothwell, R.M. Gibson, British Journal of Pharmacology 147 (2006) S232.

Metallothionein in cancer development

Michal MASARIK[1,2], Jaromir GUMULEC[1,2], Martina RAUDENSKA[1,2], Marketa SZTALMACHOVA[1,2], Tomas ECKSCHLAGER[4], Vojtech ADAM[2,3*] and Rene KIZEK[2,3]

[1] Department of Pathological Physiology, Faculty of Medicine, Masaryk University, Kamenice 5, CZ-612 00 Brno, Czech Republic, European Union
[2] Central European Institute of Technology, Brno University of Technology, Technicka 3058/10, CZ-616 00 Brno, Czech Republic, European Union
[3] Department of Chemistry and Biochemistry, Mendel University in Brno, Zemedelska 1, CZ-613 00 Brno, Czech Republic, European Union
[4] Department of Paediatric Haematology and Oncology, 2nd Faculty of Medicine, Charles University, Prague, Czech Republic

*vojtech.adam@mendelu.cz

Metallothioneins (MTs) are low molecular, cysteine-rich proteins that have naturally-occurring Zn^{2+} in both clusters. They may serve as a reservoir of metals for synthesis of apoenzymes and zinc-finger transcription regulators. MTs are also involved with several important proteins e.g. p53, NF-κB, PKCl, and GTPase Rab3A. New biological roles for these proteins have been identified including those needed in the carcinogenic process. However, their use as a predictive marker remains controversial. But one may suggest that MTs may lead to a protection of tumor cells against apoptosis and support the metastatic behaviour of tumors and/or cancer cell proliferation. Several reports have disclosed MTs expression as a prognostic factor for tumor progression and drug resistance in a variety of malignancies particularly breast, prostatic, ovarial, head and neck, non-small cell lung cancer, melanoma, and soft tissue sarcoma. The role of MTs as a tumor disease marker or as a cause of resistance in cancer treatment will be discussed.

Acknowledgement

The work was supported by V4 Metallomic Scientific Network TD 11440027.

Pathways in zinc resistance

Monika HOLUBOVA[1,2] , Martina AXMANOVA[1], Jaromir GUMULEC[1,2], Martina RAUDENSKA[1,2], Marketa SZTALMACHOVA[1,2], Vojtech ADAM[2,3*], Rene KIZEK[2,3] and Michal MASARIK[1,2]

[1] Department of Pathological Physiology, Faculty of Medicine, Masaryk University, Kamenice 5, CZ-612 00 Brno, Czech Republic, European Union
[2] Central European Institute of Technology, Brno University of Technology, Technicka 3058/10, CZ-616 00 Brno, Czech Republic, European Union
[3] Department of Chemistry and Biochemistry, Mendel University in Brno, Zemedelska 1, CZ-613 00 Brno, Czech Republic, European Union

*vojtech.adam@mendelu.cz

Zinc ions participate in essential cellular processes like intermediary metabolism, cell division and differentiation, or apoptosis in prostatic tissue. However, the relationship was examined only in short-term zinc(II) treatments. The short term treatment induces apoptosis in prostate cancer cells *in vitro* and *in vivo*. The aim of this study was to create zinc-resistant prostatic cell lines at various stages of the disease (22Rv1 and PC-3) and a normal prostate epithelium (PNT1A) using a long-term zinc exposure. The cell lines were continuously cultivated for at least one month with one to three times their common IC_{50} in the medium. Thus, with a positive selection, a unique model of zinc resistant PNT1A, 22Rv1 and PC-3 cell lines was created. On this model we studied wide range of regulatory genes expressions and cytotoxicity of zinc and cisplatin. The flow cytometry analysis and "scratch" assays to detect the migration differences were performed. Cells were also natively stained to describe their morphology on fluorescent microscopy. The mechanisms of resistance are still to clarify, but the genes responsible for long term adaptation were detected to be mainly k-RAS ($p < 0{,}001$) and Nf-kB ($p < 0{,}001$). The resistant cells behaved differently than the cells exposed to only short term treatment. The expression and cytotoxicity results indicated, that the resistant cells showed more aggressive phenotype than the common cells. The elucidation of complex processes involved in the development of the resistance in these cells will be the subject of further research. The overall impact of zinc treatment is more complex than expected and this has to be considered when discussing the final therapeutic effect.

Acknowledgement

The work was supported by V4 Metallomic Scientific Network TD 11440027.

Metallothionein – immunohistochemical cancer biomarker: a meta-analysis

Jaromir GUMULEC[1,2], Martina RAUDENSKA[1,2], Vojtech ADAM[2,3*], Rene KIZEK[2,3], Michal MASARIK[1,2]

[1] Department of Pathological Physiology, Faculty of Medicine, Masaryk University, Kamenice 5, CZ-612 00 Brno, Czech Republic, European Union
[2] Central European Institute of Technology, Brno University of Technology, Technicka 3058/10, CZ-616 00 Brno, Czech Republic, European Union
[3] Department of Chemistry and Biochemistry, Mendel University in Brno, Zemedelska 1, CZ-613 00 Brno, Czech Republic, European Union

*vojtech.adam@mendelu.cz

Metallothionein (MT) has been extensively investigated as a molecular marker of various types of cancer. Accordingly, zinc ions were also intensively studied. Nevertheless, studies give us inconsistent results regarding the association of neoplasms and zinc(II) and metallothionein levels. Therefore, results of to-date studies were summarized using meta-analysis. And obtained results were discussed from the perspective of diagnostic and therapeutic approach. A total of 77 studies regarding metallothionein with 8,015 tissue samples (4,631 cases and 3,384 controls) and 114 studies regarding zinc levels of 22737 participants were included and analysed using meta-analytical approach. Web of science, PubMed, Embase and CENTRAL databases were searched and the eligibility of individual studies and heterogeneity among the studies was assessed. Random and fixed effects model meta-analysis was employed depending on the heterogeneity, and publication bias was evaluated using funnel plots and Egger's tests.

A significantly positive association between MT staining and tumors (vs. healthy tissues) was observed in head and neck (odds ratio, OR 9.95; 95 % CI 5.82–17.03) and ovarian tumors (OR 7.83; 1.09–56.29), and a negative association was ascertained in liver tumors (OR 0.10; 0.03–0.30). No significant associations were identified in breast, colorectal, prostate, thyroid, stomach, bladder, kidney, gallbladder, and uterine cancers and in melanoma. Decreased serum zinc level was found in patients with lung (standardized mean difference, SMD = –1.04), head and neck (SMD = –1.43), breast (SMD = –0.93), liver (SMD = –2.29), stomach (SMD = –1.59), and prostate (SMD = –1.36) cancers; elevation was not proven in any tumour. More specific zinc patterns are evident at tissue level, showing increase in breast cancer tissue (SMD = 1.80) and decrease in prostatic (SMD = –3.90), liver (SMD = –8.26), lung (SMD = –3.12), and thyroid cancer (SMD = –2.84).

This study provides evidence on cancer-specific tissue zinc and metallothionein level alteration. Although serum zinc decrease was associated with most tumours mentioned herein, further – prospective - studies are needed.

Acknowledgement

The work was supported by V4 Metallomic Scientific Network TD 11440027.

Electrochemistry of metallothioneins

Vojtech ADAM[1,2*] and Rene KIZEK[1,2**]

[1] Department of Chemistry and Biochemistry, Mendel University in Brno, Zemedelska 1, CZ-613 00 Brno, Czech Republic, European Union
[2] Central European Institute of Technology, Brno, University of Technology, Technicka 3058/10, CZ-616 00 Brno, Czech Republic, European Union

*vojtech.adam@mendelu.cz, **kizek@sci.muni.cz

Metallothioneins (MT) are a family of ubiquitous, biologically interesting proteins which have been isolated and studied in a wide variety of organisms, including prokaryotes, plants, invertebrates and vertebrates. Due to the property of MT being metal-inducible and, also, due to their high affinity to metal ions, homeostasis of heavy metal levels is probably their most important biological function. In addition, MT are involved in other important biochemical pathways including scavenging of reactive oxygen species, activation of transcription factors or participation in carcinogenesis. Detection and quantification of MT is not simple due to the high content of cysteine and relatively low molecular mass. These proteins can be detected very sensitively by electrochemical methods. Moreover, MT can be used as a part of biosensors.

Determination of MT by electrochemical methods is based on electroactivity of –SH moieties, which tend to be oxidized or catalyse evolution of hydrogen from a supporting electrolyte. To prevent interferences and lower detection limits, an adsorptive transfer stripping technique (AdTS) is often coupled with electrochemical methods. The main improvement of AdTS is based on removing the electrode from a solution after accumulation of a target molecule on its surface, rinsing of the electrode and transferring it to a pure supporting electrolyte, where no interferences are present [1]. To detect MT, linear sweep, cyclic, differential pulse and square wave voltammetry have been used. Usage of these techniques was reviewed by Sestakova and Navratil [2]. Besides the previously mentioned voltammetric methods, differential pulse voltammetry with a modification called after its founder "Brdicka reaction" is the most commonly used electrochemical method for detection of MT in various types of samples since Olafson optimized it on fish tissues [3]. Over several decades, the method has been optimized with detection limit under fM [4]. Temperature of the supporting electrolyte (app. 5 °C) and concentration of cobalt(III) ions (app. 1 mM) play the key role in the reaching the lowest detection limit. Raspor attempted to elucidate the exact mechanisms of this reaction [5]. Based on these results, Raspor and her colleagues have done a lot of work to propose physical and chemical conditions to achieve comparable results in various laboratories [6]. Moreover, sample-preparation-steps including heat treatment (mentioned in chapter 2) must precede a measurement. Measurements can be also automated and thus used for larger set of samples, as was shown by Fabrik et al. [7]. In spite of the fact that Brdicka reaction is commonly used for detection of MT, Pedersen et al. showed that differential pulse polarography was found to be unsuitable for crustacean tissues due to unidentified interfering compounds which led to 5- to 20-fold overestimation of metallothionein levels [8]. The interfering compounds such as other low molecular mass thiols, ionic strength or surfactants contained in a sample can be considered [9].

Besides voltammetric methods, chronopotentiometric stripping analysis (CPSA) can be also utilized for detection of MT. This method is the most sensitive analytical tool for detection and determination of MT with detection limits estimated as units of aM [10].

Reaction and therefore sensitivity of determination depends on many parameters such as pH and ionic strength of a supporting electrolyte, and isoelectric point of measured protein. Temperature is not a concern compared to Brdicka reaction. Another study discovered that addition of $[Co(NH_3)_6]Cl_3$ to a supporting electrolyte can increase sensitivity up to 30 % [11]. The signal amplification is probably caused by complex inorganic salt-protein formation [12]. AdTS coupled with the CPSA method was used for detection of MT expressed in yeast Yarrowia lipolytica exposed to Zn, Ni, Co and Cd [13]. However, Petrlova et al. found that the CPSA signal of MT is dependent on content of metals in the sample, because MT-metal complex gives lower CPSA signal compared to metal free MT [14]. However, the results can be re-calculated on the content of metals.

Acknowledgement

The work was supported by V4 Metallomic Scientific Network TD 11440027.

References

[1] V. Adam, S. Krizkova, O. Zitka, L. Trnkova, J. Petrlova, M. Beklova, R. Kizek, Electroanalysis 19 (2007) 339.
[2] I. Sestakova, T. Navratil, Bioinorg. Chem. Appl. 3 (2003) 43.
[3] R.W. Olafson, P.E. Olsson, Methods in Enzymology 205 (1991) 205.
[4] J. Petrlova, D. Potesil, R. Mikelova, O. Blastik, V. Adam, L. Trnkova, F. Jelen, R. Prusa, J. Kukacka, R. Kizek, Electrochim. Acta 51 (2006) 5112.
[5] B. Raspor, J. Electroanal. Chem. 503 (2001) 159.
[6] B. Raspor, M. Paic, M. Erk, Talanta 55 (2001) 109.
[7] I. Fabrik, Z. Ruferova, K. Hilscherova, V. Adam, L. Trnkova, R. Kizek, Sensors 8 (2008) 4081.
[8] K.L. Pedersen, S.N. Pedersen, J. Knudsen, P. Jerregaard, Environmental Science & Technology 42 (2008) 8426.
[9] S. Krizkova, I. Fabrik, V. Adam, J. Kukacka, R. Prusa, L. Trnkova, J. Strnadel, V. Horak, R. Kizek, Electroanalysis 21 (2008) 640.
[10] R. Kizek, L. Trnkova, E. Palecek, Anal. Chem. 73 (2001) 4801.
[11] M. Tomschik, L. Havran, E. Palecek, M. Heyrovsky, Electroanalysis 12 (2000) 274.
[12] P. Sobrova, L. Vyslouzilova, O. Stepankova, M. Ryvolova, J. Anyz, L. Trnkova, V. Adam, J. Hubalek, R. Kizek, PLoS ONE 7 (2012) 1.
[13] M. Strouhal, R. Kizek, J. Vecek, L. Trnkova, M. Nemec, Bioelectrochemistry 60 (2003) 29.
[14] J. Petrlova, S. Krizkova, O. Zitka, J. Hubalek, R. Prusa, V. Adam, J. Wang, M. Beklova, B. Sures, R. Kizek, Sensors and Actuators B-Chemical 127 (2007) 112.

Metalothionein and its role in metabolism of free radicals

Branislav Ruttkay-Nedecky[1,2], Lukas Nejdl[1,2], Marketa Vaculovicova[1,2], Vojtech Adam[1,2] and Rene Kizek[1,2*]

[1] Department of Chemistry and Biochemistry, Mendel University in Brno, Zemedelska 1, CZ-613 00 Brno, Czech Republic
[2] Central European Institute of Technology, Brno University of Technology, Technicka 3058/10, CZ-616 00 Brno, Czech Republic

*kizek@sci.muni.cz

Metallothionein (MT) is a low molecular weight protein (about 6.5 kDa), which was isolated in 1957 by Margoshes and Vallee from horse kidney [1]. This protein contains in its primary structure cysteins and coversely have no aromatic amino acids [2]. It was found that the loss of the MT protective effects leads to exacerbation of pathogenic processes [3,4]. MT also has antioxidant properties [5]. At the organism intoxication by heavy metals (Cd, Hg, Pb) MT can bind to these metals and thus neutralize them [6]. Detoxification of the organism via MT likely occurs in the kidney. MT main function in the body, however, is homeostasis of heavy metal levels and maintaining of redox conditions [2,7].

Four major isoforms (MT-1 through MT-4) have been identified in mammals. In addition, at least thirteen known closely related MT proteins in humans have been described [8]. MT genes are tightly linked, and at a minimum they consist of eleven MT-1 genes (MT-1A, B, E, F, G, H, I, J, K, L and X), and one gene for each of the other MT isoforms (the MT-2A gene, MT-3 gene, and MT-4 gene). Differences between individual isoformes arise mainly from posttranslational modifications, small changes in the primary structure, affinity to various heavy metals and degradation rate [9]. Different biological functions of MT isoforms are ensured by their distinct localization in the cell compartments and individual tissues. MT-1 and MT-2 are widespread in almost all tissues; MT-3 is expressed in brain tissue, cardiac muscle, kidney tissue and reproductive organs. At least explored is the isoform MT-4, which was discovered in epithelial cells [9]. MT form without bound metal ion (apo-MT) is present in cells that are exposed to a lack of Zn^{2+}.

Significant progress in MT research was the demonstration of the redox regulation of Zn-S interaction and the coupling of zinc and redox metabolism in eliminating of free radicals. MT quenches free radicals by oxidation of its thiol groups, which leads to the release of zinc ions and MT-disulfide is formed. MT-disulfide is then in the cell reduced to MT-thiol, to which zinc ions are bound and MT redox cycle continues [10]. Willingness of MT to react with superoxide radical is relatively low, but the MT very efficiently eliminates hydroxyl radicals, which are more dangerous for the cell [11]. For this reason the MT expression is also regulated by the effect of oxidative factors [11,12]. From the physical point of view, this includes the X-ray, UV and gamma radiation, which was confirmed by several studies [13]. In mice an experiment was carried out in which their body was irradiated with X-rays [13]. Based on X-ray exposure an elevated mRNA expression of MT-1 in mice was found. It is assumed that the MT acts as a quencher of free radicals and also as a donor of zinc to enzymes that are involved in repair processes. Induction of MT expression by chemicals inducing oxygen radicals has been also demonstrated [14].

Acknowledgement

The work was supported by V4 Metallomic Scientific Network TD 11440027.

References

[1] M. Margoshes, B.L. Vallee, Journal of the American Chemical Society 79 (1957) 4813.
[2] P. Babula, M. Masarik, V. Adam, T. Eckschlager, M. Stiborova, L. Trnkova, H. Skutkova, I. Provaznik, J. Hubalek, R. Kizek, Metallomics 4 (2012) 739.
[3] P. Coyle, J.C. Philcox, L.C. Carey, A.M. Rofe, Cellular and Molecular Life Sciences 59 (2002) 627.
[4] T. Eckschlager, V. Adam, J. Hrabeta, K. Figova, R. Kizek, Current Protein & Peptide Science 10 (2009) 360.
[5] M. Ebadi, M.P. Leuschen, H. ElRefaey, F.M. Hamada, P. Rojas, Neurochemistry International 29 (1996) 159.
[6] S.R. Davis, R.J. Cousins, Journal of Nutrition 130 (2000) 1085.
[7] K. Ghoshal, S.T. Jacob, Progress in Nucleic Acid Research and Molecular Biology, Vol 66 66 (2001) 357.
[8] R. Nath, D. Kumar, T.M. Li, P.K. Singal, Toxicology 155 (2000) 17.
[9] N. Thirumoorthy, A.S. Sunder, K.T.M. Kumar, M.S. Kumar, G.N.K. Ganesh, M. Chatterjee, World Journal of Surgical Oncology 9 (2011).
[10] Y.J. Kang, Experimental Biology and Medicine 231 (2006) 1459.
[11] M. Sato, I. Bremner, Free Radical Biology and Medicine 14 (1993) 325.
[12] W. Maret, Journal of Biological Inorganic Chemistry 16 (2011) 1079.
[13] L. Cai, M. Satoh, C. Tohyama, M.G. Cherian, Toxicology 132 (1999) 85.
[14] J.W. Bauman, J. Liu, Y.P. Liu, C.D. Klaassen, Toxicology and Applied Pharmacology 110 (1991) 347.

Metal nanoparticles in soils and cells

Miguel Angel MERLOS RODRIGO[1,2], Sylvie SKALICKOVA[1,2], Ondrej ZITKA[1,2], Vojtech ADAM[1,2], Rene KIZEK[1,2*]

[1] Department of Chemistry and Biochemistry, Laboratory of Metallomics and Nanotechnologies, Mendel University in Brno, Zemedelska 1, CZ-613 00 Brno, Czech Republic, European Union
[2] Central European Institute of Technology, Brno University of Technology, Technicka 3058/10, CZ-616 00 Brno, Czech Republic, European Union

*kizek@sci.muni.cz

Nanostructured materials, such as nanoparticles have been employed in the field of many applications ranging from medicine to electronics. Nanoparticles (NPs) are generally defined as particulate matter with at least one dimension that is less than 100 nm [1].

The investigations in nanoscience have been focused on NPs forming, their characterization and application in vitro. A recently research have been shown, the NPs could be formed by anthropogenic origin including photochemical reactions, volcanic eruptions, forest fires, simple erosions, by plants or by animals [2]. A new approach of nanoparticle synthesis is their formation in living organisms. Due to the organization of living cells, the biosynthesis seems to be a sophisticated level of molecular control over the various inorganic nanomaterials. In this field of research is the most discussed soil microbiota or soil invertebrates which are able to transport of metal ions of soils and their subsequent accumulation in their tissues. In particular, the environmental pollution by anionic contaminants [arsenic (As), chromium, lead (Pb), mercury, selenium, copper (Cu), uranium], natural organic matter, organic acids, and heavy metals [3, 4] could be used to be absorbed by soil organisms. Thus, the three main reasons to produce nanoparticles are: i) chemolithotrophy for energy production, ii) use of these particles for special functions, and iii) detoxification for survival in toxic environments [5]. Into this process are involved electrostatic interaction of the negative charged cell wall and positive charge of the metal ions. The presented enzymes are able to reduce ions to NPs and newly formed particles get diffused off through the cell wall [6, 7]. The uptake of nanoparticles by different types of cells is mediated by endocytic phagocytosis and pinocytosis. Mammalian cells are able to phagocytize the senescent cells, disabled particles, and infectious microorganisms as an immunity response mechanism [8]. This process is initiated through the contact of the receptors on cell-surface with particular ligands presented by the foreign agents and employs attractive forces (i.e., ionic, electrostatic, hydrophobic/ hydrophilic, van der Waals) between the surfaces of nanoparticle and cells. In some cases, the phagocytosis can be initiated by the receptor-mediated recognition of opsonins adsorbed on the nanoparticle surfaces. The process is terminated by forming the endocytosed vesicles (>250 nm) which is known as phagosomes [9]. The geometry of the particle can help in controlling their cellular uptake via phagocytosis. It was found, the different shapes of particles can generate different angles between the membrane and them at the point of cell attachment and this angle of contact shows significant effects on the ability of macrophages to uptake particles via actin-driven movement of the membrane of macrophages [10, 11]. Pinocytosis can be further classified as clathrin-mediated endocytosis, caveolae-mediated endocytosis, clathrin/caveolae-independent endocytosis, and macropinocytosis. Macropinocytosis is an endocytic process regulated by actin. Using this process the cells internalize significant volumes of extracellular fluid through macropinosomes

(diameter of 0.5 – 10 μm) [12]. Macropinocytosis can be considered as the main route to internalize apoptotic cell fragments [13], bacteria [14] and viruses [15]. The process is initiated by the activation of a tyrosine kinase receptor helps to increase the actin polymerization, actin-mediated ruffling, and subsequently macropinosome formation [16], but is not dependent on direct action of a receptor or cargo molecules. Micron-size particles are commonly known to be taken up by macropinocytosis [17]. However, nanoparticles are generally internalized by cells via more than one endocytic pathway. Eukaryotic cells use clathrin-mediated endocytosis (CME) for trafficking of materials which includes intercellular signaling, membrane recycling, and uptake of nutrients [18]. Different proteins are employed to initiate a curvature in the membrane and subsequently some vesicles are formed [19, 20]. After internalization through this process, the uncoated vesicles can be directed to early endosomes and in some cases they can be recycled to the plasma membrane surface also. CME was proven as a suitable process of nanoparticles cellular uptake [21]. Clathrin-independent endocytosis (CIE) pathway can be considered as an entry point for different cell surface proteins and bacterial toxins [22]. Generally, CIE delivers the cargos first to the early endosomes, and later to late endosomes and lysosomes. The cargos can also be moved to the trans-Golgi network or recycled back to the plasma membrane [23]. Employing of this pathway for nanoparticles uptake was studied using trisaccharide-substituted chitosan oligomers (SBTCO) which had higher uptake and better transfection efficacy than nanoparticles derived from a linear chitosan (LCO). SBTCO were mostly internalized by cells through CIE and were effectively released from the endocytic vesicles. On the other hand, LCO suspension in the cell culture medium caused aggregation of nanoparticle and less cellular uptake compared to SBTCO. Nanoparticles cellular uptake was also proven by Caveolae which is able to perform transendothelial transport and can be exploited for the release of nanoparticles in subendothelial tissues [24]. The caveolin-mediated pathway helps in localization of endocytosed materials initially into caveosomes, whose neutral pH avoids the hydrolytic environment of lysosomes. The cellular internalization via caveolae is generally triggered by negative surface charges [25]. The phenomena of nanoparticles have been employed in many fields of research and application. Their biosynthesis in living organisms provide them exceptional properties, while also offers a lot of questions on molecular level included their transport, synthesis or cellular uptake. However, future research is needed to answer these questions.

Acknowledgement

The work was supported by V4 Metallomic Scientific Network TD 11440027.

References

[1] Borm, P.J.A., et al., The potential risks of nanomaterials: a review carried out for ECETOC. Particle and fibre toxicology, 2006. 3: p. 11-11.
[2] Hochella, M.F., et al., Nanominerals, mineral nanoparticles, and Earth systems. Science, 2008. 319(5870): p. 1631-1635.
[3] Chang, Y.C. and D.H. Chen, Preparation and adsorption properties of monodisperse chitosan-bound Fe3O4 magnetic nanoparticles for removal of Cu(II) ions. Journal of Colloid and Interface Science, 2005. 283(2): p. 446-451.
[4] Yang, K., L.Z. Zhu, and B.S. Xing, Adsorption of polycyclic aromatic hydrocarbons by carbon nanomaterials. Environmental Science & Technology, 2006. 40(6): p. 1855-1861.
[5] Krumov, N., et al., Production of Inorganic Nanoparticles by Microorganisms. Chemical Engineering & Technology, 2009. 32(7): p. 1026-1035.
[6] Hulkoti, N.I. and T.C. Taranath, Biosynthesis of nanoparticles using microbes-A review. Colloids

and Surfaces B-Biointerfaces, 2014. 121: p. 474-483.
[7] Narayanan, K.B. and N. Sakthivel, Biological synthesis of metal nanoparticles by microbes. Advances in Colloid and Interface Science, 2010. 156(1-2): p. 1-13.
[8] Silverstein, S.C., Phagocytosis of microbes: insights and prospects. Trends in Cell Biology, 1995. 5(3): p. 141-142.
[9] Rabinovitch, M., Professional and non-professional phagocytes: an introduction. Trends in Cell Biology, 1995. 5(3): p. 85-87.
[10] Champion, J. and S. Mitragotri, Shape Induced Inhibition of Phagocytosis of Polymer Particles. Pharmaceutical Research, 2009. 26(1): p. 244-249.
[11] Champion, J.A. and S. Mitragotri, Role of target geometry in phagocytosis. Proceedings of the National Academy of Sciences of the United States of America, 2006. 103(13): p. 4930-4934.
[12] Falcone, S., et al., Macropinocytosis: regulated coordination of endocytic and exocytic membrane traffic events. Journal of Cell Science, 2006. 119(22): p. 4758-4769.
[13] Fiorentini, C., et al., Activation of Rho GTPases by Cytotoxic Necrotizing Factor 1 Induces Macropinocytosis and Scavenging Activity in Epithelial Cells. Molecular Biology of the Cell, 2001. 12(7): p. 2061-2073.
[14] Kolb-Mäurer, A., et al., Interaction of human hematopoietic stem cells with bacterial pathogens. Vol. 100. 2002. 3703-3709.
[15] Mercer, J. and A. Helenius, Virus entry by macropinocytosis. Nat Cell Biol, 2009. 11(5): p. 510-520.
[16] Kerr, M.C. and R.D. Teasdale, Defining Macropinocytosis. Traffic, 2009. 10(4): p. 364-371.
[17] Gratton, S.E.A., et al., The effect of particle design on cellular internalization pathways. Proceedings of the National Academy of Sciences, 2008. 105(33): p. 11613-11618.
[18] Kirchhausen, T., Clathrin. Annual Review of Biochemistry, 2000. 69(1): p. 699-727.
[19] Marsh, M. and H.T. McMahon, The Structural Era of Endocytosis. Science, 1999. 285(5425): p. 215-220.
[20] Stowell, M.H.B., et al., Nucleotide-dependent conformational changes in dynamin: Evidence for a mechanochemical molecular spring. Nature Cell Biology, 1999. 1(1): p. 27-32.
[21] Harush-Frenkel, O., et al., Targeting of nanoparticles to the clathrin-mediated endocytic pathway. Biochemical and Biophysical Research Communications, 2007. 353(1): p. 26-32.
[22] Sandvig, K., et al., Clathrin-independent endocytosis: from nonexisting to an extreme degree of complexity. Histochemistry and Cell Biology, 2008. 129(3): p. 267-276.
[23] Grant, B.D. and J.G. Donaldson, Pathways and mechanisms of endocytic recycling. Nat Rev Mol Cell Biol, 2009. 10(9): p. 597-608.
[24] Oh, P., et al., Live dynamic imaging of caveolae pumping targeted antibody rapidly and specifically across endothelium in the lung. Nat Biotech, 2007. 25(3): p. 327-337.
[25] Sahay, G., D.Y. Alakhova, and A.V. Kabanov, Endocytosis of nanomedicines. Journal of Controlled Release, 2010. 145(3): p. 182-195.

Immunohistochemical detection of metallothioneins

Gabriella EMRI[1]* and Eszter EMRI[1]**

[1] Department of Dermatology, Faculty of Medicine, University of Debrecen, Nagyerdei krt. 98., H-4032 Debrecen, Hungary, European Union

*gemri@med.unideb.hu, **emeszti@gmail.com

The metallothionein (MT)/thionein pair, which is an important component of cellular Zn (II) homeostasis, is critical to sequester or release Zn(II) depending on the local redox state, thereby influencing the function of numerous enzymes and transcription factors that control cell proliferation, apoptosis and signalling pathways [1]. Abnormal MT function and expression have been implicated in various human diseases, including cancer [2].

There are at least 10 isoforms of MT in human body, which are expressed in a tissue specific pattern and may play distinct roles in the different cell types. MT-I and MT-II isoforms are present in all cells throughout the body, MT-III is found primarily in the central nervous system, MT-IV is located in the skin and upper gastrointestinal tract [2]. MT is a cytosolic protein in resting cells, but it can be translocated transiently to the cell nucleus during cell proliferation and differentiation [3].

Immunohistochemical (IHC) detection of MT in tissue samples is a very important method to study the role of MT in disease pathogenesis. Immunohistochemistry identifies the expression as well as location, cellular and tissue distribution of various proteins, while morphology of tissue can also be assessed precisely [4]. Multiple immunolabelling using serial sections of tissue blocks or double staining technique provides an opportunity to study correlations between the expression of MT and important cell and tissue functions. Tissue microarray allows simultaneous examination of large number of tissues on a single microscope slide, therefore it is very suitable to evaluate diagnostic, prognostic or predictive biomarkers. The IHC technique is a combination of immunologic and chemical reactions visualized with a photonic microscope [4]. It can be divided in pre-analytical, analytical and post-analytical phases. It starts with tissue fixation, embedding, and tissue sectioning, followed by deparaffination, antigen retrieval, blocking of nonspecific activities, incubation with the primary antibody, and labelling of the antigen-antibody reaction, and ends with slide counterstaining, cover-slipping and evaluation. Most commonly, formalin-fixation and paraffin-embedding is used for its ability to preserve tissue indefinitely for morphologic examination [5]. The IHC detection of antigens fixed in cross-linking fixatives is hindered, but heat-induced epitope retrieval was proved to restore the immunoreactivity of tissues [4]. Monoclonal antibodies reacting with a single and highly conserved epitope of MT-I and MT-II are used to investigate MT protein expression in tissues, antibodies that are specific to the different MT-I isoforms, are not available. Immunohistochemical detection of MT-III protein expression is also feasible using a monoclonal antibody specific to this isoform. MT expression in tissues is studied most intensively in human cancers [6]. Changes in MT expression (up- or down-regulation) seems to be associated with a more aggressive phenotype and therapeutic resistance, ultimately resulting in a worse prognosis [2, 7]. We have found that MT-I/II overexpression in melanoma cells is significantly more frequent in primary cutaneous malignant melanomas with haematogenous metastases [8]. The role of MT in metastasis formation remains to be confirmed, and experimental evidence for its oncogenic role is still lacking. IHC provides an excellent opportunity for further investigations.

Acknowledgement

The work was supported by V4 Metallomic Scientific Network TD 11440027.

References

[1] Maret, W., The function of zinc metallothionein: a link between cellular zinc and redox state. J Nutr, 2000. 130(5S Suppl): p. 1455S-8S.
[2] Thirumoorthy, N., et al., A review of metallothionein isoforms and their role in pathophysiology. World J Surg Oncol, 2011. 9: p. 54.
[3] Cherian, M.G., The significance of the nuclear and cytoplasmic localization of metallothionein in human liver and tumor cells. Environ Health Perspect, 1994. 102 Suppl 3: p. 131-5.
[4] Ramos-Vara, J.A. and M.A. Miller, When tissue antigens and antibodies get along: revisiting the technical aspects of immunohistochemistry--the red, brown, and blue technique. Vet Pathol, 2014. 51(1): p. 42-87.
[5] Bass, B.P., et al., A review of preanalytical factors affecting molecular, protein, and morphological analysis of formalin-fixed, paraffin-embedded (FFPE) tissue: how well do you know your FFPE specimen? Arch Pathol Lab Med, 2014. 138(11): p. 1520-30.
[6] Cherian, M.G., A. Jayasurya, and B.H. Bay, Metallothioneins in human tumors and potential roles in carcinogenesis. Mutat Res, 2003. 533(1-2): p. 201-9.
[7] Pedersen, M.O., et al., The role of metallothionein in oncogenesis and cancer prognosis. Prog Histochem Cytochem, 2009. 44(1): p. 29-64.
[8] Emri, E., et al., Correlation among metallothionein expression, intratumoural macrophage infiltration and the risk of metastasis in human cutaneous malignant melanoma. J Eur Acad Dermatol Venereol, 2013. 27(3): p. e320-7.

Capillary electrophoresis of metallothionein

Marta KEPINSKA* and Halina MILNEROWICZ**

Department of Biomedical and Environmental Analysis, Faculty of Pharmacy, Wroclaw Medical University, Borowska 211, Wrocław 50-556, Poland

*zalewska.m@gmail.com, **halina.milnerowicz@umed.wroc.pl

Metallothionein (MT) was first isolated in 1957 from the horse kidney by Margoshes and Vallee [1], subsequently MT presence was demonstrated in other animals, in higher plants, eukaryotic microorganisms, and in some prokaryotes [2]. Mammalian MT belongs to a group of proteins of low molecular weight (6000-7000 Da) with 30% content of cysteine [3]. The sulfhydryl groups of cysteine form with metals closely packed spatial structure in which metals are within the molecule [2]. It serves as the reservoir of metals for the body (mainly Zn and Cu) which are the part of many enzymes and proteins involved in the removal of DNA damage, replication or transcription. MT protects the body against the toxicity of heavy metals (Cd, Pb, Hg) by binding them. Slight differences in amino acid composition, hydrophobicity and isoelectric point allowed to separate the four major isoforms: MT-1, MT-2, MT-3 (also known as, growth inhibitory factor GIF), and MT-4 [2,3].

To identify MT, sensitive and selective analysis techniques are applied. Low molecular weight of protein, and the heterogeneity of the biological material to be analyzed (serum, erythrocyte lysate, urine, tissue), also causes a variety of methods used for its quantitative determination.

Electrochemical methods such as differential pulse and cathodic stripping voltammetry, saturation analysis methods based on Cd, Ag and Hg, spectrophotometric methods as well as chromatographic and electrophoretic techniques are used [4]. Among immunological techniques used in MT analysis are: immunoenzymatic ELISA, immunofluorescence assay (FIA) and radioimmunoassay (RIA). These methods are highly sensitive and can detect even small amounts of MT in the tested material [5]. One of the most widely used techniques in the analysis of proteins including MT is two-dimensional polyacrylamide gel electrophoresis or capillary electrophoresis (CE) often coupled with mass spectrometry (MS). CE allows analysis of both MT as MT in complexes with metals. As the determination of various isoforms is concerned, there must be very sophisticated detection system connected with separation one.

For the separation of MT isoforms, different CE techniques in combination with appropriate detectors are used. It provides a wide range of possibilities to optimize the degree of resolution by selecting the pH, temperature, buffer, electrolyte and the type of capillary. Two types of capillaries have been used: capillary uncoated and coated. The use of uncoated capillaries gives advantages in terms of their stability and the shorter time of analysis, while the use of surface-modified capillaries increases the resolution of MT isoforms separation [6]. The choice of method for determining MT isoforms in CE depends on the required degree of reproducibility, sensitivity and specifics. The techniques of detection which are used in the analysis of MT isoforms are UV detection, diode array detector and mass spectrometers.

The absorbance detection is highly universal especially in the deep UV range of spectra, its sensitivity is dependent on the optical pathlength, which is given by the capillary diameter. MT absorbance detection is mostly carried out at 200 nm employing the light absorption by the peptide bond [4]. MT does not disclose the absorbance at 280 nm, as it does not contain aromatic amino acids. The most common method of MT isoforms identification is

use of diode-array detector. Simultaneous monitoring of spectra at different wavelengths: 200, 214, and 254 nm can be done to see apoproteins at absorbance at 220 nm, Zn-MT - at 214 nm, Cd-MT - at 254 nm [7]. Another problem is the type of buffer used. Organic buffers as HEPES, Tricine strongly absorbs UV light below 230 nm. This limits the use of lower wavelength. In contrast, buffers as phosphate and sodium borate do not absorb UV light and are suitable for the determination in wavelength less than 230 nm. A mixture of alkaline borate and SDS shows a good separation and repeatability of migration times.

A very good method for determining isoforms of MT is to use of MS. The device separates the beam of charged particles according to a weight value of the particle charge by means of electric and magnetic fields. There are many types of mass spectrometers differing in the type and direction of fields, shape their area of operation and the distribution of the intensities. With MS, monomers and polymers of MT isoforms can be identify.

The spectrometer analyzes very small sample volumes, making it possible to obtain more detailed information about the fraction obtained after separation on CE, compared with UV or DAD detection. Furthermore, the combination of MS with various techniques for CE gained a lot of important information on MT. CZE-MS shows the molecular structure of MT and inductively coupled plasma (ICP)-MS binding of MT with metal. The application of CE-ICP-MS has made significant progress in MT analysis in last few decades. The metals complexes of two major MT isoforms, MT-1 and MT-2, were separated and elements contained in the isoforms selectively detected by CE-ICP-MS coupled via various interface designs [8].

MTs are considered as medical or environmental pollution biomarkers therefore methods of their effective determination are needed.

Acknowledgement

The work was supported by V4 Metallomic Scientific Network TD 11440027.

References

[1] M. Margoshes, B.L. Vallee, J. Am. Chem. Soc. 79 (1957) 4813.
[2] C.D. Klaassen, J. Liu, S. Chaudhuri, Ann. Rev. Pharmacol. Toxicol. 39 (1999) 267.
[3] M. Dabrio, A.R. Rodriquez, G. Bordin, M.J. Bebianno, M.D. Ley, I. Sestakova, M. Vasak, M. Nordberg, J. Inorg. Biochem. 88 (2002) 123.
[4] M. Ryvolova, V. Adam, R. Kizek. J Chromatogr A. 1226 (2012) 31.
[5] H. Milnerowicz, A. Bizoń, Acta Biochim Pol.57 (2010) 99.
[6] M.P. Richards, J.H. Beattie, J. Chromatogr. B. 669 (1995) 27.
[7] M. Zalewska, A. Bizoń, H. Milnerowicz, J Sep Sci. 34 (2011) 3061.
[8] X. Guo, H.M. Chan, R. Guevremont, K.W. Siu, Rapid Commun Mass Spectrom. 13 (1999) 500.

DNA based biosensor for an evaluation of damage to DNA by quantum dots

Lenka HLAVATA[1], Ivana STRIESOVA[1], Teodora IGNAT[1,2], Rene KIZEK[3,4*], Jan LABUDA[1]

[1] Institute of Analytical Chemistry, Faculty of Chemical and Food Technology, Slovak University of Technology in Bratislava, Radlinského 9, SK-81237 Bratislava, Slovak republic
[2] National Institute for Research and DeveloPMent in Micro- and Nanotechnology IMT-Bucharest, 126A, Erou Iancu Nicolae Street, RO-077190, Bucharest, Romania
[3] Department of Chemistry and Biochemistry, Mendel University in Brno, Zemedelska 1, CZ-613 00 Brno, Czech Republic
[4] Central European Institute of Technology, Brno University of Technology, Technicka 3058/10, CZ-616 00 Brno, Czech Republic, European Union

*kizek@sci.muni.cz

QDs are semiconductors made out of the elements from groups II and VI or groups III and V in periodic table. They are known for their small size (1-10nm) and size-dependent optical and electronic properties caused by quantum confinement [1]. By now QDs have been confirmed as suitable alternative for fluorophores used in FRET based biosensors and other fluorescence techniques. They offer several advantages over organic dyes; some of them will be discussed according to FRET desirable characteristics and are presented in the Table 1.

QDs as new generation of fluorophores have several advantages over conventional ones. Also, QDs have one characteristic unique to them and incomparable with organic fluorophores, the ability of tuning emission range as a result of core size regulation during synthesis follows quantum confinement. QDs broad excitation spectra and narrow defined emission peak allow multicolor QDs to be excited from one source without emission signal overlap [2,3], also 10-100 times lager molar extinction coefficient than fluorophores has as a result brighter probes comparing the conventional fluorophores [4,5].

This induce large Stokes shift (difference between peak absorption and peak emission wavelengths) of QDs in a range of 300-400 nm as well valuable for multiplexing [6].

These advantages enable imaging and/or tracking multiple molecular targets at the same time as well as elimination of background autofluorescence which can emerge in biological samples causing detection of mixed signals from autofluorescence and fluorophores fluorescence. Therefore fluorescence lifetime plays an important role and QDs, with their lifetime of 20-50 ns lifetime, have superiority over fluorophores with their few nanoseconds fluorescence lifetime, as well as size-tunable absorption and emission spectra [7]. Further notable advantage is high quantum yield from 40% to 90% and due to their inorganic core they are highly resistant to the photobleaching and/or chemical degradation [8,9].

QDs are not flawless, they suffer of luminescence intermittency known as blinking which can cause problems in applications and usually have been overcome by shell engineering and/or decreasing the excitation intensity [10,11], and then their inorganic nature and insolubility has been successfully mitigated by different coating and capping agents. QDs are an order of magnitude bigger that organic dyes, which represents a problem if the probe size is important [7]. Further as shortcomings, their synthesis costs and high toxicity of the used precursors are usually stated. Their overall toxicity remains a subject of discussions although possible solutions are given by development of alternative ways of synthesis such as “green synthesis” [12-14] or biosynthesis [15-16] of QDs.

Due to unique physical properties, quantum dots (QDs) and generally nanomaterials

have received enormous attention for their applications in technology, medicine, cosmetics, and other areas. Nevertheless, potential toxicity of QDs is still of great interest and represents one of the major issues that limits their use in clinical studies.

In the present work, DNA-based biosensor composed of glassy carbon electrode and a surface-attached dsDNA layer was constructed and applied for the detection of damage to DNA by UV-C radiation (λ = 254 nm) both, in the absence and the presence of CdTe QDs of different size present as a colloid in the aqueous medium. The DNA biosensor response is based on square-wave voltammetric intrinsic signal of the guanine moiety as well as on the voltammetric response of the redox indicator $[Fe(CN)_6]^{3-/4-}$ in the solution.

Depending on the QDs size, they have exhibited a significant effect on the degradation of dsDNA by UV-C and even daily light. Time depending deep DNA structural changes include opening of the helix indicated by an increase in the guanine moiety response due to its redox correspondence with the electrode and by an increase in the voltammetric peak current of the $[Fe(CN)_6]^{3-/4-}$ anion after degradation of the negatively charged DNA layer at the electrode.

The QDs behavior has been verified using two types of dsDNA (salmon sperm and calf thymus) and confirmed also by experiments with irradiation of DNA solution in the presence of QDs. Test of other nanomaterials are in progress. By this study, potentialities of the DNA biosensor and DNA biosensing for toxicologic investigations will be documented.

Acknowledgement

The work was supported by V4 Metallomic Scientific Network TD 11440027.

References

[1] F.C. Adams, C. Barbante, Spectrochimica Acta Part B: Atomic Spectroscopy 86 (2013) 3.
[2] A.P. Alivisatos, W.W. Gu, C. Larabell, in Annual Review of Biomedical Engineering, Annual Reviews, Palo Alto, 2005, p. 55.
[3] C.E. Probst, P. Zrazhevskiy, V. Bagalkot, X.H. Gao, Advanced Drug Delivery Reviews 65 (2013) 703.
[4] W.W. Yu, L.H. Qu, W.Z. Guo, X.G. Peng, Chemistry of Materials 15 (2003) 2854.
[5] J. Sun, E.M. Goldys, Journal of Physical Chemistry C 112 (2008) 9261.
[6] A.H. Fu, W.W. Gu, C. Larabell, A.P. Alivisatos, Current Opinion in Neurobiology 15 (2005) 568.
[7] M.A. Walling, J.A. Novak, J.R.E. Shepard, International Journal of Molecular Sciences 10 (2009) 441.
[8] J.P. Wolfgang, P. Teresa, P. Christian, Nanotechnology 16 (2005) R9.
[9] P. Zrazhevskiy, M. Sena, X.H. Gao, Chemical Society Reviews 39 (2010) 4326.
[10] L. Li, G.J. Tian, Y. Luo, H. Brismar, Y. Fu, Journal of Physical Chemistry C 117 (2013) 4844.
[11] M.H.W. Stopel, J.C. Prangsma, C. Blum, V. Subramaniam, RSC Advances 3 (2013) 17440.
[12] P.C. Huang, Q. Jiang, P. Yu, L.F. Yang, L.Q. Mao, ACS Applied Materials & Interfaces 5 (2013) 5239.
[13] R.K. Beri, P.K. Khanna, Journal of Nanoscience and Nanotechnology 11 (2011) 5137.
[14] M. Ahmed, A. Guleria, M.C. Rath, A.K. Singh, S. Adhikari, S.K. Sarkar, Journal of Nanoscience and Nanotechnology 14 (2014) 5730.
[15] H.F. Bao, N. Hao, Y.X. Yang, D.Y. Zhao, Nano Research 3 (2010) 481.
[16] H.Q. Huang, M.X. He, W.X. Wang, J.L. Liu, C.C. Mi, S.K. Xu, Spectroscopy and Spectral Analysis 32 (2012) 1090.

The composites of graphene oxide with metal or semimetal nanoparticles and their effect on pathogenic microorganisms

Dagmar CHUDOBOVA[1,2], Lukas RICHTERA[1,2], Kristyna CIHALOVA[1,2], Monika KREMPLOVA[1,2], Halina MILNEROWITZ[3], Jan LABUDA[4], Vedran MILOSAVLJEVIC[1,2], Pavel KOPEL[1,2], Vojtech ADAM[1,2*] and Rene KIZEK[1,2]

[1] Department of Chemistry and Biochemistry, Faculty of Agronomy, Mendel University in Brno, Zemedelska 1, CZ-613 00 Brno, Czech Republic, European Union
[2] Central European Institute of Technology, Brno University of Technology, Technicka 3058/10, CZ-616 00 Brno, Czech Republic, European Union
[3] Department of Biomedical and Environmental Analyses, Wroclaw Medical University, Borowska 211, PL-50-556 Wroclaw, Poland, European Union
[4] Department of Analytical Chemistry, Faculty of Chemical and Food Technology STU, Radinskeho 9, SK-812 37, Bratislava, Slovak Republic, European Union

*vojtech.adam@mendelu.cz

Abstract

Herein we describe a synthesis and testing of composites based on graphene oxide as a carrier in composites with metal or metalloid based nanoparticles (Cu, Zn, Mn, Ag, AgP, Se) as an antimicrobial agent for bacterial strains (*Staphylococcus aureus (S. aureus)*, methicillin-resistant *S. aureus* (MRSA) and *Escherichia coli (E. coli)*). The composites were firstly applied in the identical 300 μM concentrations on all types of model organisms and their effect was observed spectrophotometrically by decrease in absorbance values in comparison with the control untreated strain. The most pronounced inhibition of *S. aureus* growth was observed after application of graphene oxide composite with selenium nanoparticles (87.4% decreases) in comparison with control without the addition of the antimicrobial agent. After application of composite with silver nanoparticles, the decrease of 68.8% was observed, and finally, after application of composite of silver phosphate nanoparticles, the decrease of 56.8% was reached. For all tested composites antimicrobial effect, which ranged from 26% to 87.4% was observed. Interestingly, the effects of composites with selenium nanoparticles significantly differed in G^+ and G^- bacteria. While the effects of composites on bacterial cultures of *S. aureus* and MRSA, the representatives of G^+ bacteria, has been with increasing concentration appreciable, the effects of the same composites on G^- bacteria *E. coli* was observed only in the highest applied concentration.

Introduction

In food and textile industries or in hospital facilities, we meet technological processes that should prevent the spread of bacteria between staff, consumers and patients [1-3]. Application of antibiotics is not always a suitable choice, since they can be transferred into the treated material [3]. Another problem arising from using of antibiotics is a presence of bacterial strains resistant towards applied chemical substances. Nanosized materials can be used as a suitable alternative to overcome the multidrug resistance of several organisms.

Aims

The production of nanosized material as a potential antibacterial agent is very important, since it can be used as a suitable alternative to overcome the multidrug resistance of several organisms. The aim of this study was the manufacturing of composites, which partially are themselves antimicrobial agents. Packing of metal or metalloid nanoparticles to the carrier based on the graphene oxides may lead to a gradual release of nanoparticles and therefore to the long-term effects of nanoparticles on various bacterial strains as it was shown in presented study.

The aim of this study was to develop composites with metalloid nanoparticles, which are themselves, partially, antimicrobial agents.

Material and methods

The GO was prepared by chemical oxidation of 5.0 g graphite flakes according to the simplified Hummer's method. Composites of GO with nanoparticles were formed from metal or semimetal salts. Synthesized composites were characterized by different analytical methods (SEM, quasielastic laser light scattering, microscopy in ambient light and DPV. Effect of synthesized composites were observed by microbiological methods on bacterial strains (*Staphylococcus aureus* NCTC 8511, *Escherichia coli* NCTC 13216, methicillin-resistant *Staphylococcus aureus* ST239:SCCmec IIIA) from Collection of Microorganisms, Faculty of Science, Masaryk University, Brno, Czech Republic.

Results and discussion

The size of composites was evaluated by Zetasizer Nano NS with a scattering angle = 173°. At least 200 particles per sample were measured to obtain the size distribution (the standard spherical particle models were used in DLS).

Inserts show their representative SEM images by drying composites dispersions on clean silicon wafers. The length of scale bar is 2 μm. Pie charts show the amount of reduced or precipitated metal or metalloid (green sectors with values) and metal or metalloid ionic form (russet sectors) determined by DPV. The amount of reduced or precipitated metal or metalloid was determined as the difference between total applied amount and amount found by DPV.

Metal ions were detected in their aqueous solutions (supernatants) by anodic or cathodic stripping differential pulse voltammetry. Except silver ions, the metal ions were detected by using a hanging mercury drop electrode (HMDE). The electrochemical peaks of Cu(II), Mn(II), Se(IV) and Zn(II) were evaluated at the potential of –0.05, –1.68, –0.68 and –1.04 V, respectively.

Silver was detected as Ag(I) by glassy carbon electrode, and the electrochemical signal of Ag(I) was observed at the potential +0.18 V.

The most pronounced inhibition of *S. aureus* growth was observed after the treatment of GO-Se composite, since the decrease in comparison with control was up to 87.4%. Furthermore, the highest inhibitions for the composite with silver and silver phosphate nanoparticles observed were 68.8% and 56.8%, respectively. Other tested composites did not reach such inhibitory effect, even though the reduction of *S. aureus* growth was determined (Fig. 3A).

The formation of inhibition zones was determined in *S. aureus* strain treated with GO

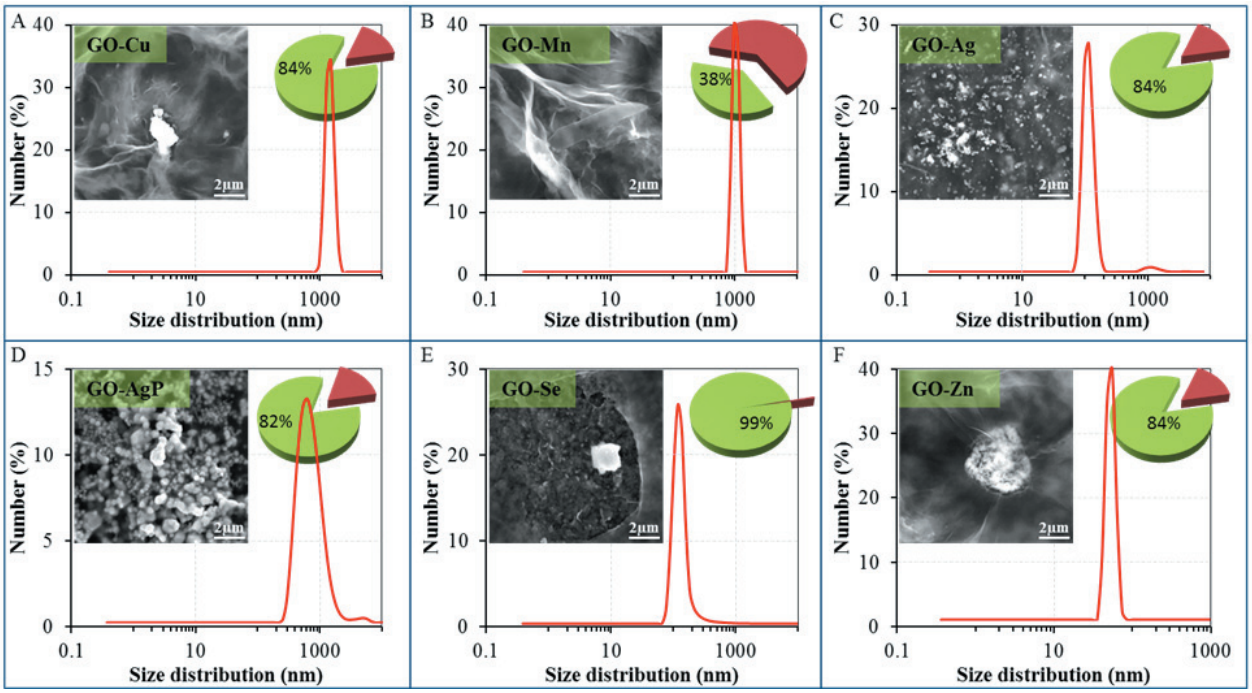

Figure 1: Dynamic light-scattering (DLS) spectra of graphene oxide (GO) composites with metal- or metalloid-based nanoparticles dispersions—size distribution by number: (**A**) GO-Cu; (**B**) GO-Mn; (**C**) GO-Ag; (**D**) GO-AgP; (**E**) GO-Se; and (**F**) GO-Zn.

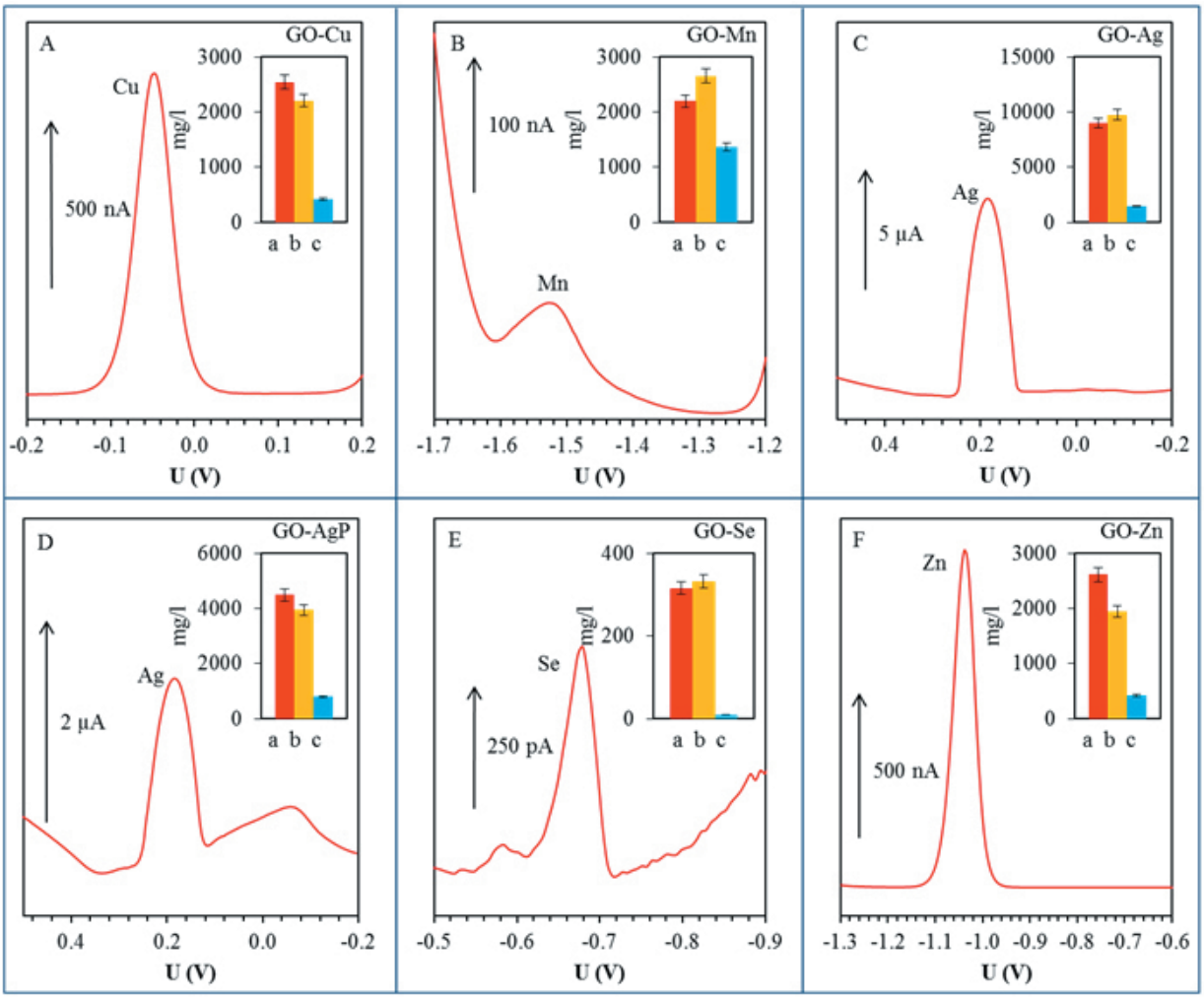

Figure 2: Differential pulse voltammograms of free (non-bonded) metal or metalloid ions in supernatants: (**A**) Cu(II); (**B**) Mn(II); (**C**) Ag(I); (**D**) Ag(I); (**E**) Se(IV); and (**F**) Zn(II). In inserted graphs: (**a**) corresponds to applied concentration (mg/L); (**b**) corresponds to total (free and bonded) metal concentration (mg/L) determined by AAS; (**c**) expresses concentration of free ions in the solution (mg/L) by DPV.

composites except GO-Mn. Based on the inhibition zones results, GO-Se was shown to exhibit the strongest antibacterial activity in G^+ bacteria (13 mm in *S. aureus*, 9 mm in MRSA), while treatment of *E. coli* with GO-Se caused minimal inhibition (2 mm) (Fig. 3B). The highest concentration of the composite even caused almost the total growth inhibition in resistant (MRSA) and non-resistant strain of *S. aureus* (Fig. 3C).

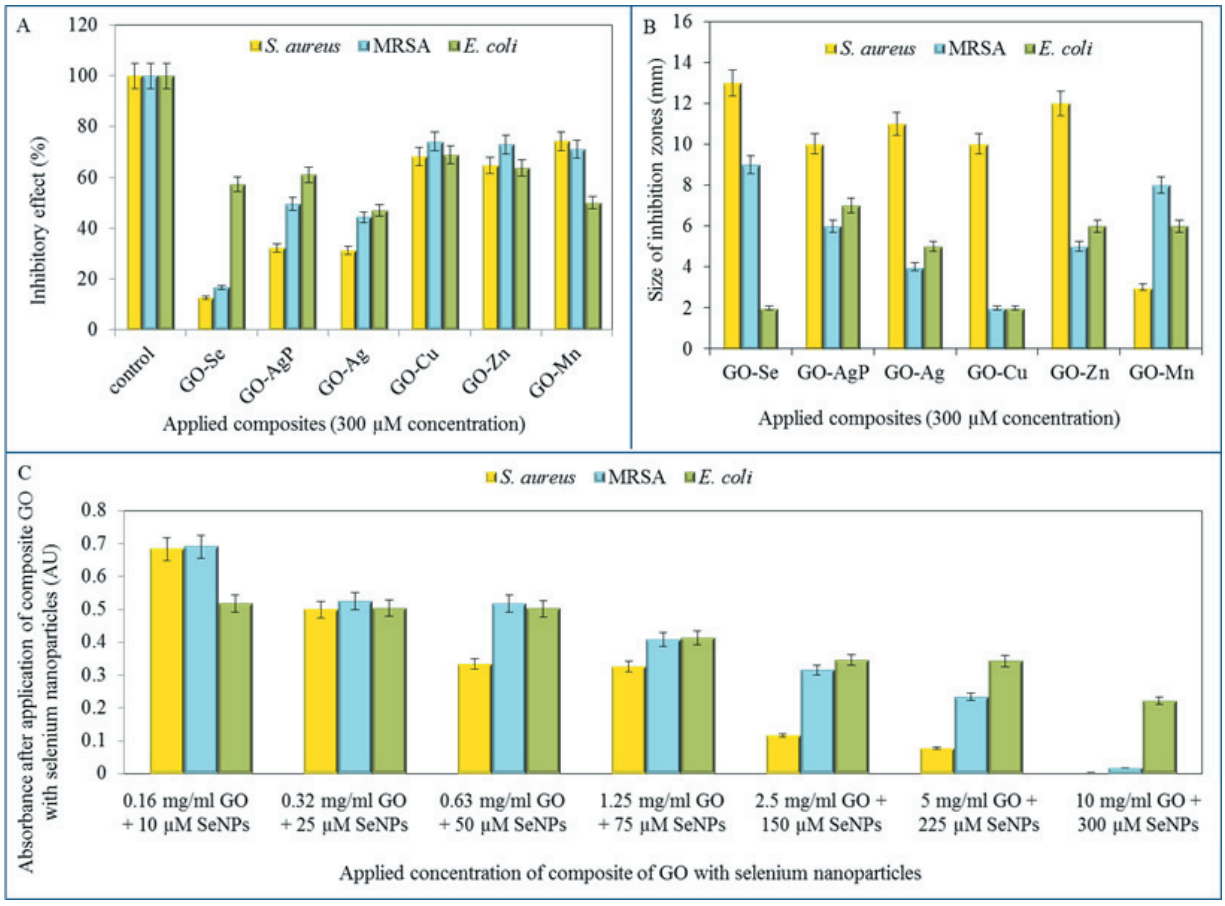

Figure 3: Determination of bacterial growth after the application of GO composites. (**A**) Percentage of bacterial growth after application of 300 µM concentration of composites using method of growth curves (24 h of measurement); (**B**) Determination of inhibition zones after application of 300 µM concentration of tested composites; (**C**) Determination of bacterial growth after the application of various concentrations of GO-Se composite.

Conclusion

Our results pointed to an antimicrobial effect of all tested composites on three tested pathogenic bacterial strains; however, the best results were achieved after the application of GO-Se-based composite. The obtained results can be useful in practice to prevent the risk of the spread and proliferation of bacterial infections. The coating of nanoparticles on graphene oxide may also lead to a slower release of nanoparticles in connection with the gradual decomposition of graphene oxide composite, including prolonged exposure of the composites at the infection site.

Acknowledgement

The work was supported by V4 Metallomic Scientific Network TD 11440027.

References

[1] J. Yip, L.W. Liu, K.H. Wong, P.H.M. Leung, C.W.M. Yuen, M.C. Cheung, Journal of Applied Polymer Science 131 (2014) 8886.
[2] M.R. Nateghi, H. Hajimirzababa, Journal of the Textile Institute 105 (2014) 806.
[3] R. Olar, M. Badea, O. Carp, D. Marinescu, V. Lazar, C. Balotescu, A. Dumbrava, Journal of Thermal Analysis and Calorimetry 92 (2008) 245.

Electrochemical detection of Cr(III) ion using activated glassy carbon electrode

Hoai Viet NGUYEN[1,2], Lukas RICHTERA[1,2], David HYNEK[1,2], Anna BIZON[3], Gabriella EMRI[4], Vojtech ADAM[1,2*], Rene KIZEK[1,2]

[1] Department of Chemistry and Biochemistry, Faculty of Agronomy, Mendel University in Brno, Zemedelska 1, CZ-613 00 Brno, Czech Republic, European Union
[2] Central European Institute of Technology, Brno University of Technology, Technicka 3058/10, CZ-616 00 Brno, Czech Republic, European Union
[3] Department of Biomedical and Environmental Analyses, Wroclaw Medical University, Borowska 211, PL-50-556 Wroclaw, Poland, European Union
[4] Department of Dermatology and Venerology, Faculty of Medicine, University of Debrecen, Nagyerdei krt.98, HU-4012, Debrecen, Hungary, European Union

*vojtech.adam@mendelu.cz

Abstract

Heavy metals are attracting more attention in environmental, toxicological, pharmaceutical and biomedical analysis. Among those, the detection of chromium is of particular interest owing to the high toxicity of it. In aqueous solution, the stable oxidation states of chromium are Cr (III) and Cr (VI). Cr (III) is considered less toxic than Cr (VI) and even essential to human health in trace concentration. However, higher concentration of Cr (III) can cause adverse effects because of its high capability of coordinating with various organic compounds, resulting in inhibiting some metallic-enzyme systems. Electrochemical methods are chosen for analytical purpose, as they are reliable, sensitive and requiring less expensive equipment. In this study, activated glassy carbon electrode was used to determine Cr (III) ion. Limit of detection (LOD) and limit of quantification (LOQ) were also investigated in the present study.

Introduction

There is no report on Cr (III) oxidation at mercury electrodes in the literature as would be expected from the relative ease of oxidation of mercury compared with Cr (III) [1]. Direct Cr(III) electrochemical oxidation has been studied using solid electrode such as Pt [2], MnO_2 [3], diamond paste electrode [4], glassy carbon electrode [1], and gold electrode [1]. Most of these investigations were carried out under alkaline conditions[5]. In this study, Cr (III) ion was detected using activated glassy carbon electrode.

Aims

Electrochemical oxidation could be an attractive alternative method for Cr (III) detection, benefiting from its efficiency, versatility, easy manipulation, environmental compatibility, and cost-effectiveness. The first aim of this study is to characterize electrochemical signal of Cr (III) ion using glassy carbon electrode.

The second aim of this study was to use activated glassy carbon electrode to increase sensitivity of method for determination of Cr (III) ion.

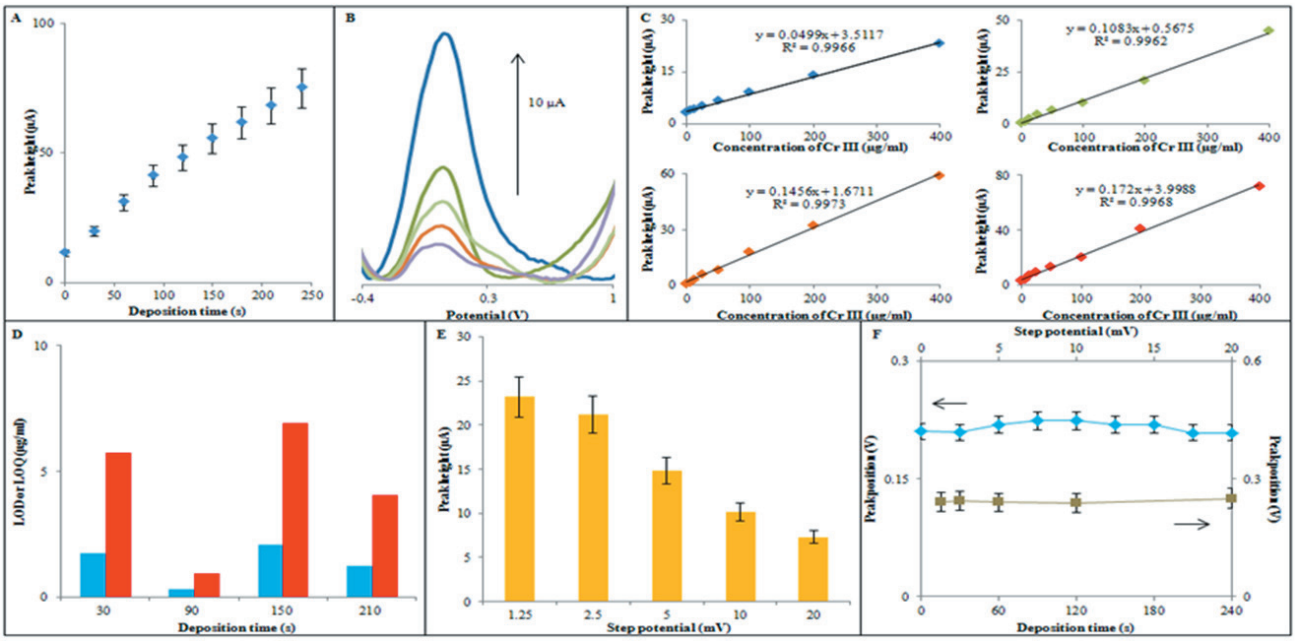

Figure 1: Electrochemical detection of Cr(III) ion (400 μg/ml) measured by GCE in BR buffer pH 6. **A** Dependence of peak height of Cr(III) on depsition time. **B** Differential pulse voltammograms of different concentrations of Cr(III) ion. **C** Calibration curve of Cr(III) ion with deposition time of 30 s (blue square), 150 s (green square), 210 s (orange square), and 210 s (red square). **D** Dependence of LOD (blue column) and LOQ (red column) on deposition time. **E** Dependence of peak height of Cr(III) ion on step potential. **F** Dependence of deposition time (blue rhombus) and step potential (grey square) on peak position.

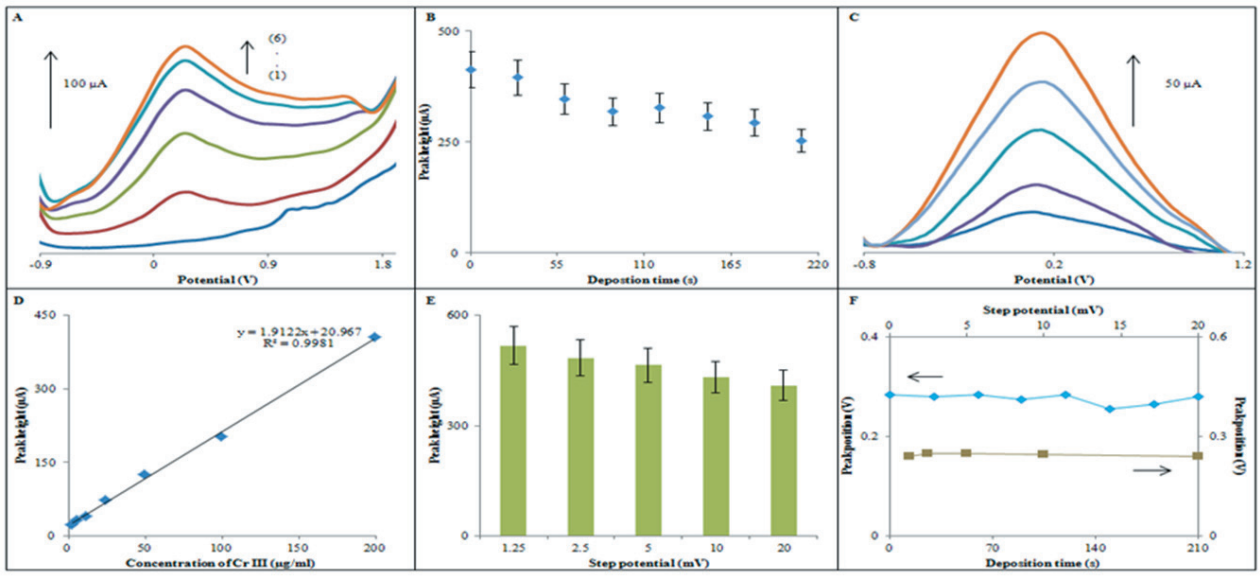

Figure 2: Electrochemical detection of Cr(III) ion (200 μg/ml) measured by activated GCE in BR buffer pH 6. **A** Activation method with six times running DPV. **B** Dependence of peak height of Cr(III) on depsition time. **C** Differential pulse voltammograms of different concentrations of Cr(III) ion. **D** Calibration curve of (Cr III) ion. **E** Dependence of peak height of Cr(III) on.

Material and methods

The electrochemical robotic device (Sensolytics, Bochum, Germany) included three motorized units ST4118M1804 (Nanotec, Munich, Gemany) and positioning system (OWIS, Staufen, Germany). First unit was rigidly connected to the vertical frame of the electrochemical robot; electrode holder was attached to it and enabled precise vertical (z) positioning of electrode holder (up and down). Microtiter plate was placed on horizontally (x/y) positioned board. Coordinates and the precise time of the holder and plate motion were controlled by ELChemRo software (Sensolytics, Bochum, Germany). We used advanced setting of NOVA to prepare script, which enable to set sequence of differential pulse voltammetry measurements with adjustable time interval between individual measurements.manuscript reporting the results of experimental work must include an experimental section. The $Cr(NO_3)_3$ solution was supplied from Sigma Aldrich (Sigma-Aldrich, USA). Differential pulse voltammetry were employed for activating GCE and determination of Cr(III) ion. Activating step for GCE was carried out using six times running of DPV.

Results and discussion

Fig. 1 shows electrochemical detection of Cr(III) (400 µg/ml) ion measured by GCE in BR buffer pH 6. peak position on deposition time and step potential. The using concentration of Cr(III) must be high because sensitivity of it measured by GCE is low. Fig. 1A demonstrated that peak height of Cr(III) ion increased with increasing of deposition time. Based on these results, we tried to increase limit of detection (LOD) and limit of quantification (LOQ) by changing deposition time. Fig. 1B showed typical voltammograms of Cr(III) ion with different concentrations. Fig. 1C showed calibration curves of Cr(III) ion corresponding with different deposition time (30, 90, 150, and 210 s). As we can see from Fig. 1D, LOD and LOQ for electrochemical detection of Cr(III) ion chaning with changing of deposition time. Deposition time of 90 s produced best LOD (0.27539 µg/ml) and LOQ (0.91796) whereas the worst LOD (2.0771) and LOQ (6.92382) appeared with deposition of 150 s. Fig. 1E showed dependenc of step potential on peak height of Cr(III) ion. With increasing of step potential, peak heigh decreased. Fig. 1F showed dependence of step potential. F Dependence of deposition time (blue rhombus) and step potential (grey square) on peak position.

Fig. 2A shows different voltammograms of activating step (6 times running of DPV), it can be seen that signal highly increased after each run. Comparison with signal of Cr(III) ion measured by GCE, signal increased more than 10 times with activated GCE. Fig. 2B showed dependence of peak height on deposition time. Peak height of Cr(III) ion decreased with increasing of deposition time. Fig. 2C calibration curve of Cr(III) ion. LOD and LOQ respectively are 0.05262 and 0.175401 µg/ml. Fig. 2E showed dependenc of step potential on peak height of Cr(III) ion. With increasing of step potential, peak heigh decreased. Fig. 2F showed dependence of peak position on deposition time and step potential. It can be seen that, peak postion does not depend on deposition time and step potential.

Conclusion

Our results showed electrochemical determination of Cr(III) ion by using glassy carbon electrode. Furthermore, by using activated glassy carbon electrode electrochemical signal of Cr(III) ion highly increased. As a results, limit of detection and limit of quantification for detection of Cr(III) ion hiehly increased. Besides, Peak position did not have much influence on the electrochemical signal of Cr(III) ion in both cases using glassy carbon or activated glassy carbon electrode.

Acknowledgement

The work was supported by V4 Metallomic Scientific Network TD 11440027.

References

[1] C.M. Welch, M.E. Hyde, O. Nekrassova, R.G. Compton, Physical Chemistry Chemical Physics 6 (2004) 3153.
[2] P. Zanello, G. Raspi, Analytica Chimica Acta 88 (1977) 237.
[3] F.I. Danilov, A.B. Velichenko, Electrochimica Acta 38 (1993) 437.
[4] R.I. Stefan, S.G. Bairu, J.F. van Staden, Analytical and Bioanalytical Chemistry 376 (2003) 844.
[5] W. Jin, M.S. Moats, S. Zheng, H. Du, Y. Zhang, J.D. Miller, Journal of Physical Chemistry B 116 (2012) 7531.

Magnetic beads based isolation and electrochemical detection of specific influenza sequences labeled by quantum dots

Ludmila KREJCOVA[1,2], Petr MICHALEK[1,2], Pavel KOPEL[1,2], Anna BIZON[3], Gabriela EMRI[4], David HYNEK[1,2], Vojtech ADAM[1,2*] and Rene KIZEK[1,2]

[1] Department of Chemistry and Biochemistry, Faculty of Agronomy, Mendel University in Brno, Zemedelska 1, CZ-613 00 Brno, Czech Republic, European Union
[2] Central European Institute of Technology, Brno University of Technology, Technicka 3058/10, CZ-616 00 Brno, Czech Republic, European Union
[3] Department of Biomedical and Environmental Analyses, Wroclaw Medical University, Borowska 211, PL-50-556 Wroclaw, Poland, European Union
[4] Department of Analytical Chemistry, Faculty of Chemical and Food Technology STU, Radinskeho 9, SK-812 37, Bratislava, Slovak Republic, European Union

*vojtech.adam@mendelu.cz

Abstract

In this study we designed and described two step beads based assay, consists from magnetic isolation, followed by electrochemical detection of isolated target sequences. method magnetic beads modified by oligo-thymine tail was used for isolation process. Two different nanoparticles were used in this study. For capturing of target influenza derived sequence magnetic particles (MPs) were used. For labeling of target sequences quantum dots (QDs) were used. Isolated target sequence as well as QDs labels were analysed by voltammetry.

Introduction

Influenza viruses belonging to the family Orthomyxoviridae, including three genera: influenza A, B and C. The type A viruses are the most virulent and cause annualy epidemics as well as more rarely pandemis [1]. The influenza A viruses are subdivided into different subtypes based on the surface antigens: neuraminidase (NA) and haemagglutinin (HA), which represent the platform for mutation changes [2]. Mutations pose a risk of origination of new, pandemic subtype, like was Spain flu in 1918 [3]. In this study we design a assay for multi target detection of influenza sequences, where magnetic particles (MPs) and quantum dots (QDs) were employed. The assay contains three steps: first step was hybridization of target DNA on modified MPs. Next step was hybridisation of antisense labeled by QDs (ODN-QDs). The end-point was electrochemical detection of ODN sequences and QDs labells by voltammetry.

Aims

Globalization together with population growth and the increased frequency of airplane transportation may potentiate the emergence of rapid spread of potential pandemic. We will able to fight against epidemiological and pandemic spread of infectious diseases, but for this rapid and sensitive method is required. The aim of this study was to design and

develop fast, easy to use and sensitive method for influenza detection, where magnetic particles and quantum dots were employed.

Material and methods

QDs were prepared with a method published in [4]. Thereafter they were used for labeling of anti-sense sequences (ODN). MPs: Oligo $(dT)_{25}$ (Invitrogen, Oslo) was dispensed in selected wells in the microplate, and washed by phosphate buffer (PB 1). The first hybridization was the next step. AAAAA-modified target sequence and hybridization buffer (HB) were added and then the plate was incubated. This was followed by a washing (PB 1) and the second hybridization. ODN-QDs and HB were added and the plate was incubated. Procedure was followed by a washing by PB1. Then, elution solution was added and plate was incubated (5 min, 85°C). Thereafter plate was transferred to the magnet; product of isolation was separated and measured by electrochemical analysis.

Results and discussion

We described multi target assay for the isolation and detection of three different influenzas' sequencees in one sample. Isolation of target sequences was performed by modified MPs (Fig.1/A) and then was hybridized anti sense strand modified by QDs. Targets (influenzas' derived ODN) were incubated with the probe modified by three different QDs (ZnS, CdS, and PbS) see Fig.1/B. Complex anti-sense modified by QDs and target may be determined electrochemicaly (Fig.1/Part1D). Two different electrochemical methods brought two diverse signals. One corresponds to ODN (CA peak) measured by SWV and the second one QDs (metal peak) measured by DPV. We detected CA signal at the potential about -1.4V. ODN--QDss provide sufficient signal (metal part QDs): -1.03 V (Zn), -0.63 V (Cd) and -0.45 V (Pb). Effect of ODN concentration on the CA peak height is shown in Fig. 2/Part 1.

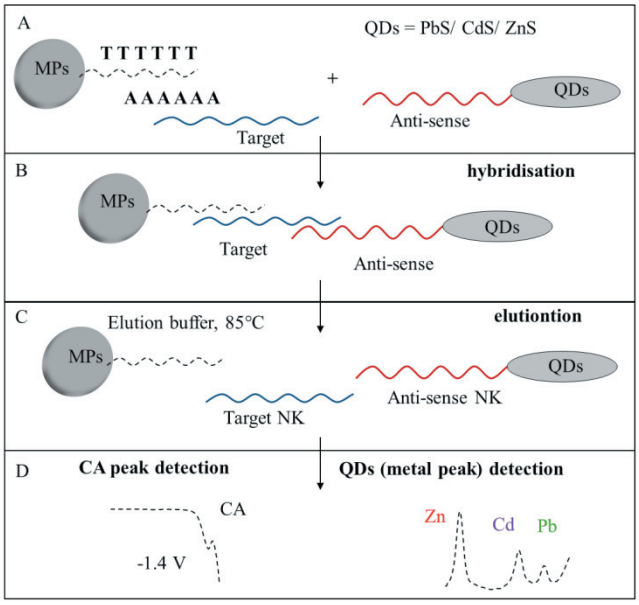

Figure 1: Scheme of multi target isolation and detection of influenza subtypes. **A** hybridization of target on modified MPs (based on T-A binding). **B** hybridization between target and QDs labeled anti--sense. **C** Elution hybridized molecule out of MPs. **D** Electrochemical detection of NPs and target influenza ODN.

The effect of hybridization temperature on the hybridisation of anti-sense ODN-QDs was deteriminated. Target ODN interacted with 2.5; 5; 10 and 20 µg/ml of ODN-SH-QDs by the temperature of 15°C, 20°C, 25°C and 30°C. Subsequently, the CA signal (Fig. 3. A, C, E) and Cd, Zn and Pb signal responses were determined (Fig. 3 B, D, F). The highest response of ODN-SH-NPs was determined for the hybridization temperature of 25 °C.

On the other hand, the lowest ODN-SH-QDs response was detected for the hybridization temperature of 30°C. We expected that the higher temperature of hybridization increased hybridization effect. This direct correlation can be applied only to the temperature of 25 °C because the oligonucleotide Tm was 28 °C.

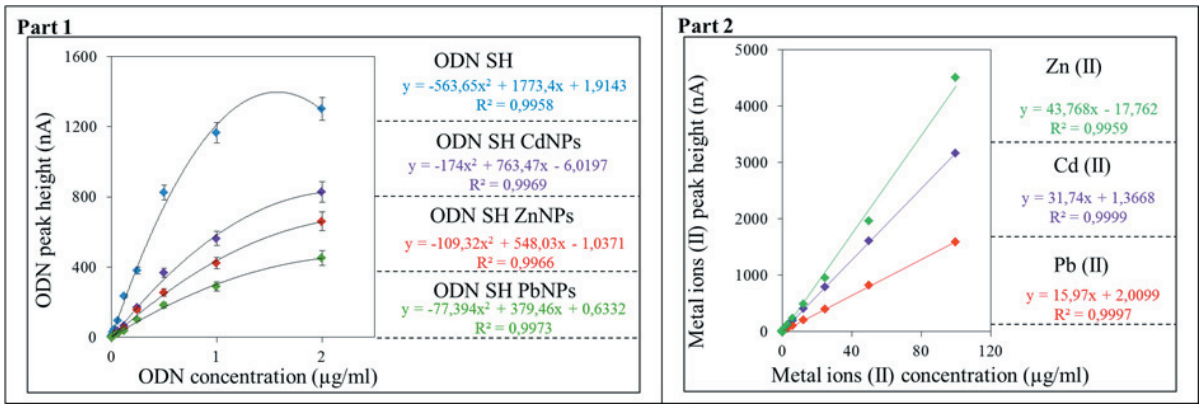

Figure 2 Part 1 Dependence of CA peak height on concentration of ODN (µg/ml). CA peak height for ODN-SH or ODN-SH-NPs. **Part 2** Dependence of metal peak height on concentration of metal ions (µg/ml). Peak height for metal ions Pb (II); Zn (II) and Cd (II).

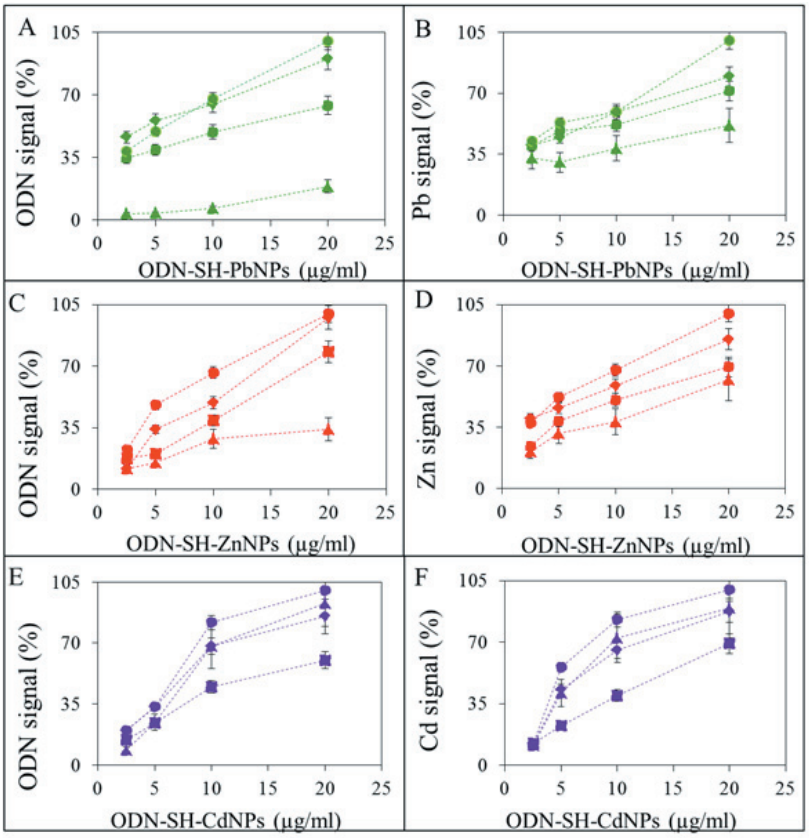

Figure 3: Dependence of relative peak height (%) on concentration of ODN-SH-NPs (µg/ml), (left side - ODN peak height; right side – metal peak height). Hybridization temperatures: ▲30°C; ● 25°C; ♦20°C; ■15°C.

Conclusion

It was designed and optimized multi target isolation and detection of three different influenza oligonucleotides labeled by QDs. It was observed the effect of hybridization temperature (second hybridization) on CA and metal peak height. The temperature optimum of second hybridization was 25°C. Combination of MPs, QDs, automated pipetting system and electrochemical detection represented unique tool for the detection of specific sequences More sensitive answers provides metal from QDs label, than influenza derived target sequences.

Acknowledgement

The work was supported by V4 Metallomic Scientific Network TD 11440027.

References

[1] S. Bhatt, T.T. Lam, S.J. Lycett, A.J.L. Brown, T.A. Bowden, E.C. Holmes, Y. Guan, J.L.N. Wood, I.H. Brown, P. Kellam, O.G. Pybus, I. Combating Swine, Philosophical Transactions of the Royal Society B-Biological Sciences 368 (2013).

[2] X. Chen, Z. Yang, Y. Lu, Q. Xu, Q. Wang, L. Chen, Plos One 8 (2013).

[3] D. Butler, Nature 465 (2010) 672.

[4] L. Krejcova, D. Hynek, R. Guran, P. Michalek, A. Moulick, P. Kopel, K. Tmejova, H. Nguien Viet, V. Adam, J. Hubalek, J. Kynicky, R. Kizek, International Journal of Electrochemical Science 9 (2014) 3349.

Influence of oxidation stage and exfoliation extent of carbon-based materials on electrochemical detection of As(III)

Monika KREMPLOVA[1,2], Lukas RICHTERA[1,2], Pavel KOPEL[1,2], Renata KENSOVA[1,2], Marta KEPINSKA[3], Gabriela EMRI[4], Vedran MILOSAVLJEVIC[1,2], David HYNEK[1,2], Vojtech ADAM[1,2*], Rene KIZEK[1,2]

[1] Department of Chemistry and Biochemistry, Faculty of Agronomy, Mendel University in Brno, Zemedelska 1, CZ-613 00 Brno, Czech Republic, European Union
[2] Central European Institute of Technology, Brno University of Technology, Technicka 3058/10, CZ-616 00 Brno, Czech Republic, European Union
[3] Department of Biomedical and Environmental Analyses, Wroclaw Medical University, Borowska 211, PL-50-556 Wroclaw, Poland, European Union
[4] Department of Dermatology and Venerology, Faculty of Medicine, University of Debrecen, Nagyerdei krt. 98, HU-4012, Debrecen, Hungary, European Union

*vojtech.adam@mendelu.cz

Abstract

This study deals with the electrochemical detection of As(III) and especially with its interaction with carbon-based materials such as graphene oxide, graphite oxide and partially reduced graphene oxide in connection with the adsorption of As(III) to their surface. Using differential pulse voltammetry, it was found that the As(III) reaches the best adsorption efficiency on the carbon-based materials surfaces at very acidic pH after interaction time 1 hour. We decided to use this promising ability of graphene oxide to design a new method for As(III) detection using a modified glassy carbon electrode. In order to enable detection of As(III) the surface of glassy carbon electrode was firstly modified by gold nanoparticles (AuNPs). After this step the working electrode was modified for a second time by graphene oxide to enhance the electrochemical signal of As(III). Compared to the working electrode modified only by gold nanoparticles, the electrochemical signal of As(III) on the GCE/AuNPs/GO increased by 50%. Interaction time of As(III) with graphene oxide on the surface of the working electrode demonstrated the process of As(III) adsorption to the surface o, which is manifested by increasing electrochemical signal of As(III) in individual time intervals.

Introduction

Higher concentrations of arsenic in the environment are a result of anthropogenic activities. Its occurrence is mainly associated with the combustion of fossil fuels and metallurgical processes. With regard to environmental importance of arsenic still makes sense to seek new ways of detection, because it is important to design methods that allow rapid, inexpensive and routine detection of this element [1,2].

Aims

The aim of this study was the monitoring of the trivalent arsenic, especially its adsorption on the surface of the carbon-based materials such as graphene oxide, graphite oxide and partially reduced graphene oxide. For determination of As(III) on glassy carbon electrode this electrode was modified by gold nanoparticles and graphene oxide.

Material and methods

Graphite oxide, graphene oxide and partially reduced graphene oxide were used in this study for As(III) adsorption on its surface. These materials were characterized usign microscopy in ambient light and SEM analysis. The efficiency As(III) adsorption was determined using difference pulse voltammetry on HMDE electrode and AAS in different time and pH. Samples for time interaction were prepared as follows: To 250 µL (5 mg/mL) of carbon materials 375 µL of As(III) standard solution (100 µM) was pipetted followed by addition of 375 µl of concentrated hydrochloric acid. Interaction of arsenic and carbon material was carried out in five different time intervals (0, 30, 60, 90 and 120 minutes).

Results and discussion

For detection of arsenic in aqueous solutions and for the verification of sorption properties of carbon-based materials an electrochemical method differential pulse voltammetry as one of the most sensitive techniques for the determination of metal ions, metalloids and other electrochemically active substances have been used. For obtaining higher sensitivity of the method an individual parameters were optimized. The addition of copper ions was the first optimized parameter (Fig. 1A). The volume of $CuSO_4$ (concentration of Cu(II) 1g/L) to the supporting electrolyte was gradually increased in the range 60 - 130 mL and At applied volume 110 mL stable electrochemical response was recorded. Further, the deposition potential was tested (Fig. 1B), the best electrochemical response was observed at deposition potential -0.1 V. Figure 1C shows an increasing electrochemical signal of As (III) depending on the increasing deposition time. The increase in peak height of As(III) does not exceed 25%, therefore deposition time 0 s was used in all subsequent measurements. The calibration curve of As(III) in concentration range 0.78 – 100 µg/mL was determined. Between 12.5 – 100 mg/mL the concentration dependence has a linear course with regression equation $y = 4.4798x + 36.168$. At the slot in figure 1D there is shown a calibration curve in the lower concentration range (0.78 – 12.5 µg/mL).

For a more detailed description of the structure of carbon materials SEM analysis were used. in Figure 2Aa was noticeable bumpy surface of a material but it can be seen that this material contains partially exfoliated proportion which shows only locally transparent veil structure (Fig 2Ab). Figure 2Ba and 2Bb shows the characteristic structure formed by evaporating the solvent from a solution of graphene oxide. The structure of the partially reduced graphene oxide (Fig 2C) is quite similar to the starting material (Fig 2B), but it is clearly visible that the partially reduced graphene oxide have more pronounced gossamer texture (Fig 2Ca and 2Cb).

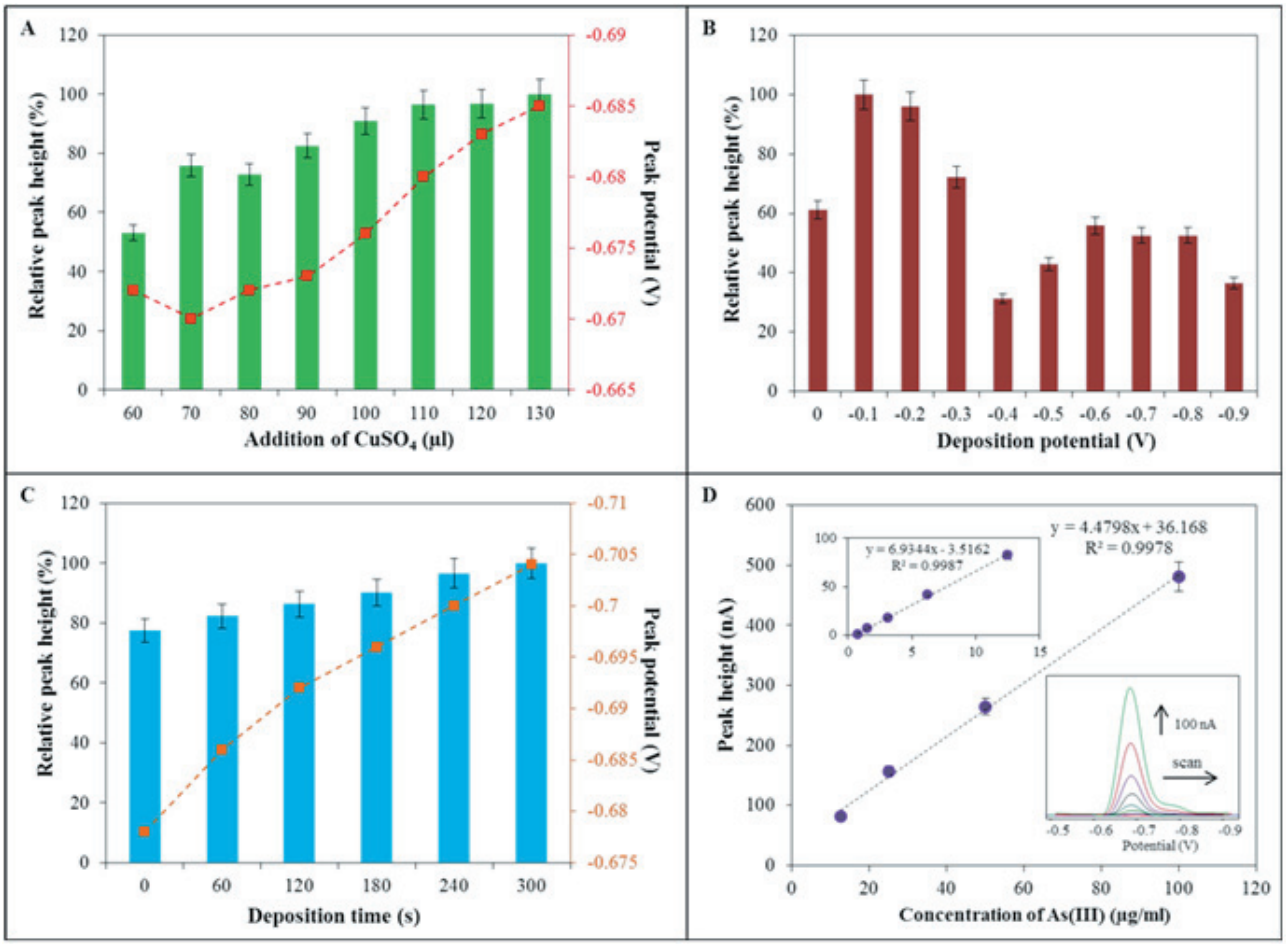

Figure 1: Optimization of the parameters of the method for As(III) determination: (A) dependence of relative peak height on the addition of $CuSO_4$ (1g/L),; (B) influence of deposition potential; (C) dependence of relative peak height of As(III) on deposition time; (D) calibration curves in concentration range 0.78 – 12.5 µg/mL and 12.5 – 100 µg/mL containing inserted voltammograms.

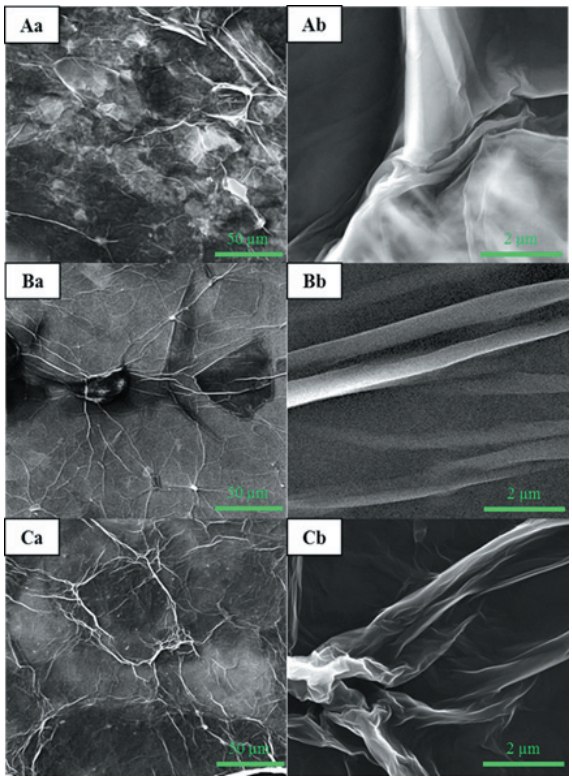

Figure 2: SEM micrographs of (**A**) graphite oxide, (**B**) graphene oxide, (**C**) partially reduced GO. Magnification (**a**) 1000×, (**b**) 30 000×.

The interaction of carbon-based materials with As(III) in the pH range 0-7 was carried out. The graph in Figure 3A shows the strongest adsorption onto the carbon surface at the lowest pH. From Figure 3B can be seen the efficiency of adsorption reaches the maximum after 60-90 min. Graphene oxide with the adsorption efficiency of 30.8% after 1 hour interaction seemed to be the most effective. For determination of As(III) on GCE, this electrode was modified with AuNPs and GO to increase the As(III) signal (Fig 3C). The initial signal of As(III) measured at time 0 was increased with increasing interaction time. Electrochemical signal reached a maximum in 60 minutes (Fig 3D).

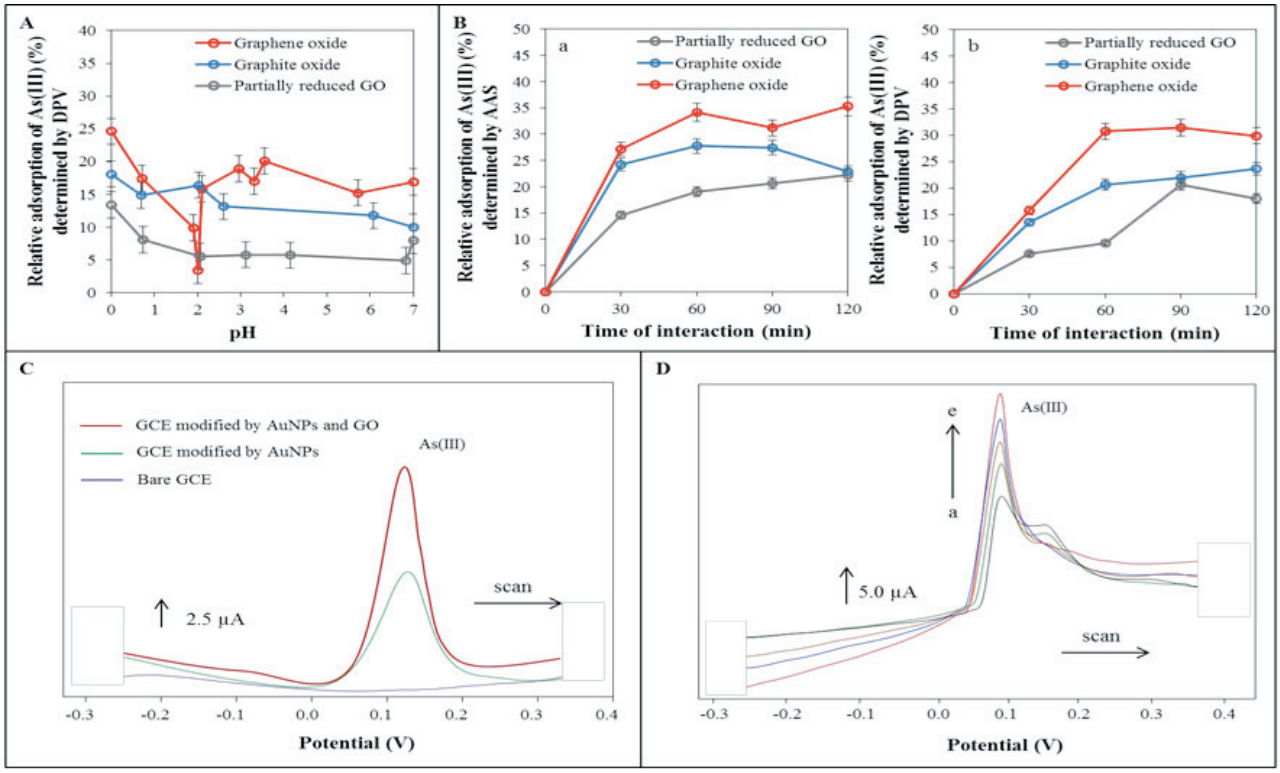

Figure 3: (**A**) relative adsorption of As(III) depending on pH; (**B**) relative adsorption of As(III) depending on time interaction (0, 30, 60, 90 and 120 minutes); (**C**) voltammograms of As(III) signal determined using bare GCE, GCE+AuNPs and GCE+AuNPs+GO; **(D)** voltammograms of As(III) signal depending on time interaction with GO on the GCE surface, (a) 0, (b) 15, (c) 30, (d) 45, (e) 60 minutes.

Conclusion

With regard to environmental importance of arsenic it still makes sense to seek new ways of detection and it is also important to design methods that allow rapid, inexpensive, routine detection of this element. In this study, an alternative method for detection of As (III) using GC/AuNPs/GO electrode has been proposed. This method of double modification resulted in a twofold increase of the electrochemical signal of As(III) in comparison with a simple modification of GCE using gold nanoparticles only.

Acknowledgement

The work was supported by V4 Metallomic Scientific Network TD 11440027.

References

[1] A. Vahidnia, G.B. Van der Voet, F.A. de Wolf, Human & Experimental Toxicology 26 (2007) 823.
[2] S. Wang, C.N. Mulligan, Science of the Total Environment 366 (2006) 701.

The study of interaction of graphene oxide with selenite anion using DPV

Monika KREMPLOVA[1,2], Lukas RICHTERA[1,2], Renata KENSOVA[1,2], David HYNEK[1,2], Halina MILNEROWITZ[3], Jan LABUDA[4], Rene KIZEK[1,2*]

[1] Department of Chemistry and Biochemistry, Faculty of Agronomy, Mendel University in Brno, Zemedelska 1, CZ-613 00 Brno, Czech Republic, European Union
[2] Central European Institute of Technology, Brno University of Technology, Technicka 3058/10, CZ-616 00 Brno, Czech Republic, European Union
[3] Department of Biomedical and Environmental Analyses, Wroclaw Medical University, Borowska 211, PL-50-556 Wroclaw, Poland, European Union
[4] Department of Analytical Chemistry, Faculty of Chemical and Food Technology STU, Radinskeho 9, SK-812 37, Bratislava, Slovak Republic, European Union

*kizek@sci.muni.cz

Abstract

Selenium is essential nutrient element for human organism, but higher concentrations are toxic and can cause serious health problems. High concentrations of selenium can enter into the environment through the metal processing industries, burning of fossil fuels as well as agriculture activities. Through this way selenium can release into the soil and water, and then could be transferred to the plants, animals, organisms and life cycles. The removal of selenium from surface and waste water is one of the worldwide problems. Carbon-based adsorbents have attracted much attention and demonstrate recently promising performance in removal of heavy metals. Due to its properties like high surface area, abundant surface hydroxyl and carboxyl functional groups, and easy modification, graphene oxide can be considered as an adsorbent candidate for selenium removal.

Introduction

Increased concentrations of heavy metals and transition elements in the environment is high risk to the human organism and remove these substances from the surface and waste water is one of the world questions [1-3]. Selenium belongs to the transition elements which are very beneficial in trace concentrations, but at higher concentrations are very toxic [4]. In nature the selenium occurs in organic and inorganic forms and is an integral part of the flora and fauna. The organic forms of selenium include amino acids selenomethionine and selenocysteine. Inorganic forms are selenite (SeO_3^{2-}), selenide (Se^{2-}), selenate (SeO_4^{2} and elementary selenium (Se^0) [5,6]. In the human body selenium plays an important role in many biological processes and biochemical pathways, such as antioxidant activity, formation of thyroid hormones, DNA synthesis and reproductive cycle. Very important is function of selenium in the muscles, which improves endurance and slows the aging process [7,8]. High concentrations of selenium are released into the environment due to anthropogenic activities. It can cause short or long term damages to human health. Short-term health effect includes the hair loss, nail deterioration and damage, damage to the peripheral nervous system, fatigue and irritability. Prolonged exposure to high concentrations of selenium can cause kidney and liver damage, as well as the nervous system and circulatory system [9-11]. Carbon-based adsorbents have attracted much attention and demonstrate recently promising performance in removal of heavy metals. Due to its properties like high surface

area, abundant surface hydroxyl and carboxyl functional group, high adsorption capacity, strong affinity and easy modification, graphene oxide can be considered as an adsorbent candidate for selenium removal [12-16].

Material and methods

Preparation of large area graphene oxide – smaller particles (more exfoliated) modified by iron nanoparticles (MGOJ)

Nanoparticles from 5 mL of Fe_2O_3 was magnetically separated, washed three times with ACS water and diluted to initial volume. 5 mL of large area graphene oxide with smaller particles was added to this sample, the resulting concentration of graphene oxide was 2 mg/mL. This mixture was stirred for 24 hours.

Preparation of partially reduced graphene oxide modified by iron nanoparticles (MrGO)

Nanoparticles from 5 mL of Fe_2O_3 was magnetically separated, washed three times with ACS water and diluted to initial volume. 5 mL of partially reduced graphene oxide was added to this sample, the resulting concentration of partially hydrazine-reduced graphen oxide was 2 mg/mL. This mixture was stirred for 24 hours.

Preparation of samples for Se (IV) removal from aqueous solution

250 µL of ACS water and 500 µL of standard solution of sodium selenite with concentration of Se 15 µg/mL was added to 250 µL of carbon based material or iron nanoparticles. This sample was shaken for chosen time period using Thermomixer Comfort (Eppendorf, Germany). After the time interaction the solid part of the sample was separated by centrifugation or magnetic separation according to the type of carbon material. The supernatant was removed using a syringe and filtred through the membrane filter with pore size 0.45 µm to separate potential non-sedimenting nanoparticles. The concentration of Se(IV) was determined by differencial pulse voltammetry in purified supernatant and using this information the concentration of Se(IV) adsorbed on the adsorbent surface was calculated (Fig 1).

Electrochemical determination of Se(IV) using differencial pulse voltammetry (DPV)

Determination of selen by differential pulse voltammetry were performed with 797 VA Computrace instrument connected to 889 IC Sample Center (Metrohm, Switzerland), using a standard cell with three electrodes. A hanging mercury drop electrode (HMDE) with a drop area of 0.4 mm^2 was the working electrode. An Ag/AgCl/3M KCl electrode was the reference and platinum electrode was auxiliary. The analyzed samples were deoxygenated prior to measurements by purging with argon (99.999%). 0.128 M ammonium sulphate, 0.123 mM copper sulphate and sulfuric acid (to adjust pH to 2.2) as a supporting electrolyte were used. The supporting electrolyte was exchanged after each analysis. The parameters of the measurement were as follows: initial potential of -0.4 V, end potential -0.9 V, deoxygenating with argon 120 s, accumulation time 200 s, deposition potential -0.6 V, time interval 0.05 s, voltage step 6 mV, pulse amplitude 30 mV, volume of injected sample: 20 µl, volume of measurement cell 2 ml (20 *µl* of sample + 1980 *µl* electrolyte).

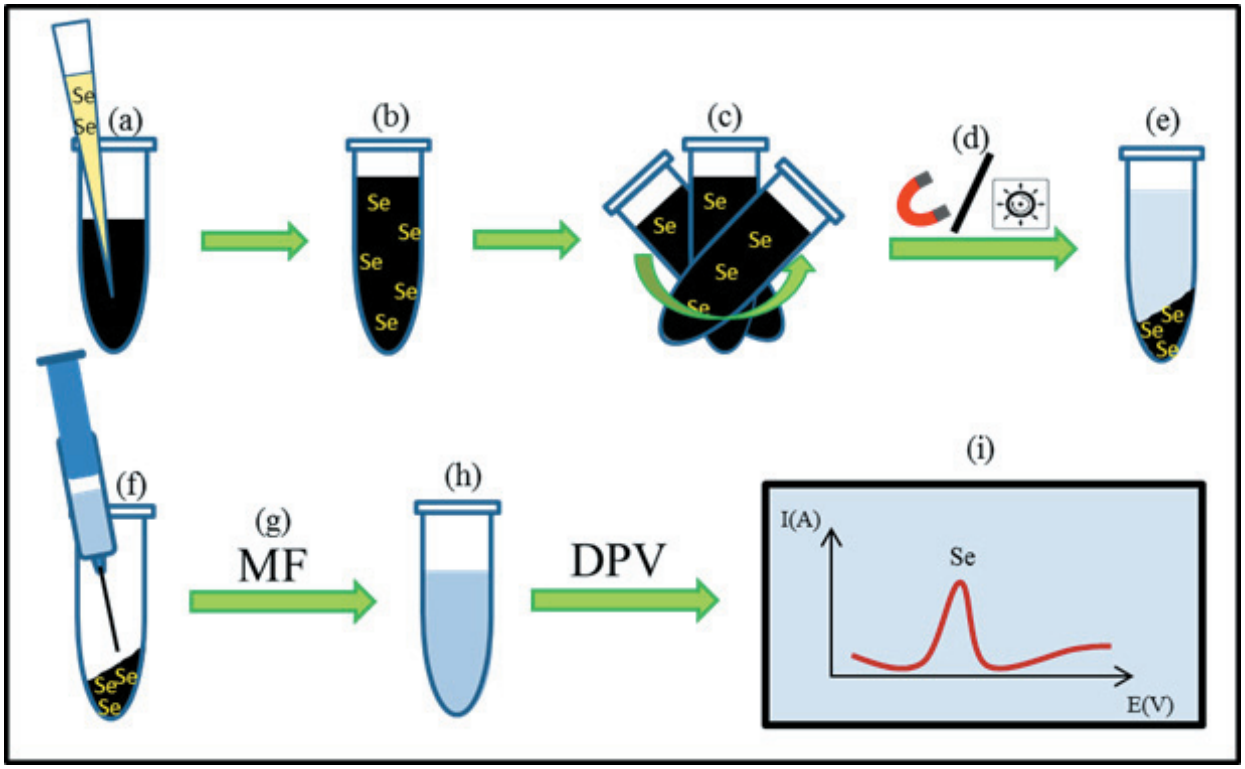

Figure 1: The scheme of selenium removal from aqueous solution using different types of adsorbents. (**a**) carbon based adsorbent; (**b**) mixture of adsorbent and standard solution of sodium selenite; (**c**) shaking and mixing of the sample; (**d**) centrifugation or magnetic separation; (**e**) separated solid part; (**f**) removal of supernatant using syringe; (**g**) filtration using membrane filter 0.45 μm; (**h**) purified supernatant; (**i**) electrochemical determination of Se(IV) by DPV.

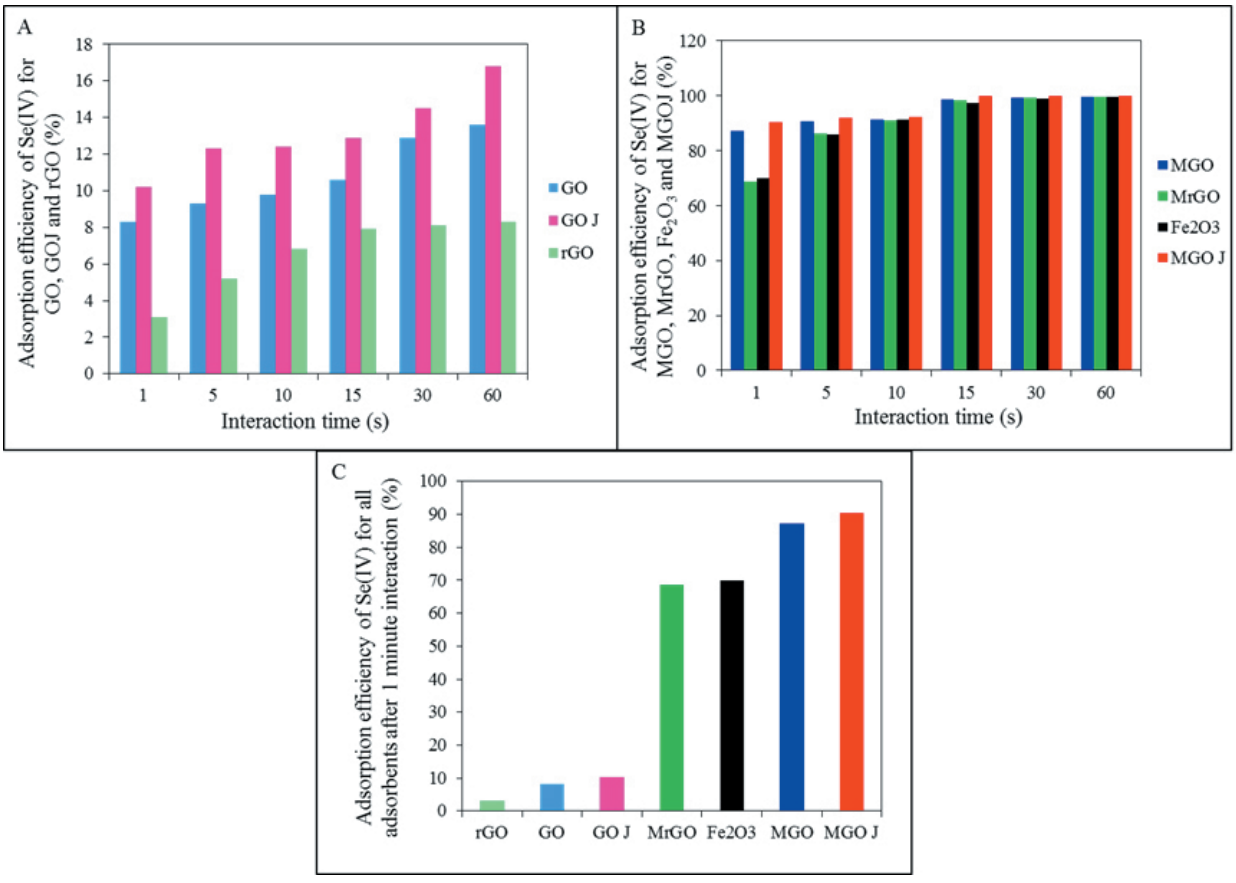

Figure 2: The adsorption efficiency of Se(IV) depending on interaction time 1, 5, 10, 15, 30 and 60 minutes for (A) starting materials GO, GOJ and rGO and (B) iron nanoparticles and GO based materials modified by iron nanoparticles (MGO, MGOJ and MrGO). (C) The adsorption efficiency of Se(IV) for all used nanomaterials after 1 minute interaction time. Determined by difference pulse voltammetry using 0.128 M ammonium sulphate, 0.123 mM copper sulphate and sulfuric acid, pH 2.2 as supporting electrolyte with parameters of the method as follows: initial potential -0.4 V, end potential -0.9 V, accumulation time 200 s, deposition potential -0.6 V, time interval 0.05 s, voltage step 6 mV, pulse amplitude 30 mV.

Results and discussion

Materials based on graphene oxide, reduced graphene oxide and iron nanoparticles exhibit sorption ability to heavy metals and can be used e.g. for decontamination of surface water and waste water polluted with these metals and transition elements. In this experiment, seven different nanomaterials (large area graphene oxide, large area graphene oxide with smaller particles (more exfoliated), partially reduced graphene oxide, iron nanoparticles and 3 mentioned GO based materials modified by iron nanoparticles) was tested to their ability to adsorb Se(IV) from an aqueous solution on its surface. To verify these properties the time interaction of the material with a standard solution of sodium selenite was carried out in applied times of 1, 5, 10, 15, 30 and 60 minutes.

The graph in figure 2A recorded the adsorption efficiency of Se(IV) for the starting carbon materials (GO, GOJ and rGO) without modification by iron nanoparticles. For all the adsorbents there is a same trend - with increasing time of interaction the efficiency of adsorption of Se (IV) from an aqueous solution increases but the maximum achieved adsorption efficiency is only 16.5% after 60 minutes interaction for large area GO with smaller particles (more exfoliated), the efficiency of adsorption for GO and rGO did not exceed 15%.

Due to the low adsorption properties of the basic materials to Se(IV), the modification of these adsorbents by iron nanoparticles was performed. In the Fig. 2B, the adsorption efficiency of Se(IV) depending on the interaction time of the metal with different composite materials is mentioned. The graph shows that all of the materials (Fe_2O_3, MGO, MGOJ and MrGO), the efficiency of adsorption reached more than 99% after 60 minutes interaction with Se(IV). The greatest differences in the rate of adsorption were visible after 1 minute interaction where the efficiency of adsorption for the large area GO with larger and smaller particles was 87% and 90%. For iron nanoparticles and MrGO the adsorption efficiency after 1 minute interaction did not exceed 70% (Fig. 2C).

Large area GO with smaller particles modified by Fe_2O_3 was the only material that reached the adsorption efficiency of 100%. In the supernatant of samples with that adsorbent no electrochemical signal of Se(IV) has been recorded. The adsorption capacity for MGOJ was calculated as 15µg of Se(IV) per 1 mg of the adsorbent.

Conclusion

Carbon based materials, especially graphene oxide, are considered to be promising materials for heavy metals or transition metals removal from surface and waste water. This study was focused on removal of Se(IV) from aqueous solution using different nanomaterials based on graphene oxide and its modifications with iron nanoparticles. The large area graphene oxide with smaller particles modified by iron nanoparticles seems to be the most promising nanomaterial for Se(IV) removal, its adsorption efficiency reached 100% from applied concentration of Se(IV) after 60 minutes interaction time. The adsorption capacity of this adsorbent was calculated as 15 µg of Se(IV) per 1 mg of MGOJ. Environmental pollution by heavy metals and transition elements is a serious worldwide problem, so it is necessary to search new materials apply them to real samples.

Acknowledgement

The work was supported by V4 Metallomic Scientific Network TD 11440027.

References

[1] M. Jamil, M.S. Zia, M. Qasim, Journal of the Chemical Society of Pakistan 32 (2010) 370.
[2] S. Khan, Q. Cao, Y.M. Zheng, Y.Z. Huang, Y.G. Zhu, Environmental Pollution 152 (2008) 686.
[3] A. Singh, R.K. Sharma, M. Agrawal, F.M. Marshall, Food and Chemical Toxicology 48 (2010) 611.
[4] L. Schomburg, U. Schweizer, J. Kohrle, Cellular and Molecular Life Sciences 61 (2004) 1988.
[5] Y. Mehdi, J.L. Hornick, L. Istasse, I. Dufrasne, Molecules 18 (2013) 3292.
[6] M. Vinceti, G. Dennert, C.M. Crespi, M. Zwahlen, M. Brinkman, M.P.A. Zeegers, M. Horneber, R. D'Amico, C. Del Giovane, Cochrane Database of Systematic Reviews (2014).
[7] J. Gromadzinska, E. Reszka, K. Bruzelius, W. Wasowicz, B. Akesson, European Journal of Nutrition 47 (2008) 29.
[8] E.J. Underwood, N.F. Suttle, The mineral nutrition of livestock, CABI Publishing, Wallingford, Oxon, OX10 8DE, UK; CABI Publishing, 10 E. 40th Street, Suite 3203, New York, NY, 10016, USA, 1999.
[9] Y. Fu, J.Y. Wang, Q.X. Liu, H.B. Zeng, Carbon 77 (2014) 710.
[10] M.E. Reid, M.S. Stratton, A.J. Lillico, M. Fakih, R. Natarajan, L.C. Clark, Journal of Trace Elements in Medicine and Biology 18 (2004) 69.
[11] I. Zwolak, H. Zaporowska, Cell Biology and Toxicology 28 (2012) 31.
[12] Y. Cao, X.B. Li, Adsorption-Journal of the International Adsorption Society 20 (2014) 713.
[13] P.K. Tripathi, L.H. Gan, M.X. Liu, N.N. Rao, Journal of Nanoscience and Nanotechnology 14 (2014) 1823.
[14] B. Wang, F. Zhang, S.F. He, F. Huang, Z.Y. Peng, Asian Journal of Chemistry 26 (2014) 4901.
[15] H. Wang, X.Z. Yuan, Y. Wu, H.J. Huang, G.M. Zeng, Y. Liu, X.L. Wang, N.B. Lin, Y. Qi, Applied Surface Science 279 (2013) 432.
[16] X. Wang, B. Liu, Q.P. Lu, Q.S. Qu, Journal of Chromatography A 1362 (2014) 1.

Study of the interaction of graphene oxide with chromate anion using AAS

Renata KENSOVA[1,2], Lukas RICHTERA[1,2], Monika KREMPLOVA[1,2], Anna BIZON[3], Gabriella EMRI[4], David HYNEK[1,2], Rene KIZEK[1,2*]

[1] Department of Chemistry and Biochemistry, Faculty of Agronomy, Mendel University in Brno, Zemedelska 1, CZ-613 00 Brno, Czech Republic, European Union
[2] Central European Institute of Technology, Brno University of Technology, Technicka 3058/10, CZ-616 00 Brno, Czech Republic, European Union
[3] Department of Biomedical and Environmental Analyses, Wroclaw Medical University, Borowska 211, PL-50-556 Wroclaw, Poland, European Union
[4] Department of Dermatology and Venerology, Faculty of Medicine, University of Debrecen, Nagyerdei krt. 98, HU-4012, Debrecen, Hungary, European Union

*kizek@sci.muni.cz

Abstract

Metal ions play essential roles in the number of biological processes including DNA synthesis, gene expression, enzymatic catalysis, neurotransmission, and apoptosis. Therefore monitoring of metal concentrations in the biological samples is necessary. For this purpose, different analytical procedures are utilized, especially the methods of atomic spectroscopy and also electrochemical methods. For the isolation of heavy metals from the environment it is possible to use materials which are able to adsorb different metals on and into its surface. These materials include various modifications of carbon, such as graphene or graphene oxide. Atomic absorption spectrometry with electrothermal atomization and Zeeman background correction is appropriate and sensitive method for the determination of wide spectrum of different metals.

Introduction

Chromium is a metal naturally occurring mainly in minerals, rocks, plants, soil, water and volcano dust or gases. Although, chromium exists in all oxidation states from Cr(0) to Cr(VI), the Cr(III) and Cr(VI) species are the most widespread ones in the nature.

Hexavalent chromium Cr(VI) is highly toxic and his compounds are confirmed carcinogens. The toxicity of the Cr(VI) ions is connected with their high oxidation potential and relatively small size, which enables them to penetrate through biological cell membranes [1]. Carbon-based adsorbents have attracted much attention and demonstrate recently promising performance in removal of heavy metals [2]. Due to its properties like high surface area, abundant surface hydroxyl and carboxyl functional group, high adsorption capacity, strong affinity and easy modification, graphene oxide can be considered as an adsorbent candidate for chromium removal.

Aims

The aim of this study was the monitoring of the total chromium, especially its adsorption on the surface of the carbon-based materials such as graphene oxide, partially reduced graphene oxide and their modification with iron nanoparticles. The adsorption efficiency of adsorbents was determined using atomic absorption spectrometry with electrothermal atomization and Zeeman background correction.

Material and methods

For this experiment large area graphene oxide-GO, large area graphene oside with smaller particles-GOJ, partially hydrazine-reduce graphene oxide-rGO and their modifications with iron nanoparticles – MGO, MGOJ and MrGO, and iron nanoparticles were used. These materials were used for Cr(VI) removal from aqueous solution. After the time interaction the solid part of the sample was separated. The supernatant was removed and filtred through the membrane filter. Chromium was determined on 280Z Agilent Technologies atomic absorption spectrometer (Agilent, USA) with electrothermal atomization. Chromium ultrasensitive hollow cathode lamp (Agilent) was used as the radiation source (lamp current 7 mA). The spectrometer was operated at 357.9 nm resonance line with spectral bandwidth of 0.2 nm. Zeeman background correction was used with field strength 0.8 Tesla. Chromium was determined in the presence of palladium chemical modifier. Chromium was determined in the presence of palladium chemical modifier. Graphite oxide, graphene oxide and partially reduced graphene oxide were used in this study for As(III) adsorption on its surface. These materials were characterized usign microscopy in ambient light and SEM analysis. The efficiency As(III) adsorption was determined using difference pulse voltammetry on HMDE electrode and AAS in different time and pH. Samples for time interaction were prepared as follows: To 250 µL (5 mg/mL) of carbon materials 375 µL of As(III) standard solution (100 µM) was pipetted followed by addition of 375 µl of concentrated hydrochloric acid. Interaction of arsenic and carbon material was carried out in five different time intervals (0, 30, 60, 90 and 120 minutes).

Results and discussion

Materials based on graphene oxide, reduced graphene oxide and iron nanoparticles exhibit sorption ability to heavy metals and can be used e.g. for decontamination of surface water and waste water polluted with these metals and transition elements. In this experiment, seven different nanomaterials was tested to their ability to adsorb Cr(VI) from an aqueous solution on its surface. To verify these properties the time interaction of the material with a standard solution of potassium chromate was carried out in applied times of 1, 5, 10, 15 and 30 minutes. The graph in figure 2A recorded the adsorption efficiency of Cr(VI) for the starting carbon materials (GO, GO-J and R-GO) and iron nanoparticles (MP). For the selected carbon materials, the adsorption efficiency is maximal after 10 minutes interaction. From all the unmodified carbon materials, large area graphene oxide (GO) reached the highest adsorption efficiency (60%) of applied Cr(VI) concentration.

To improve the adsorption properties of the basic materials to Cr(VI), the modification of these adsorbents by iron nanoparticles was performed. In the Fig. 2B, the adsorption efficiency of Cr(VI) depending on the interaction time of the metal with different composite materials is mentioned. The graph shows that all of the materials (MGO, MGOJ and MR-GO) reached the efficiency of adsorption more than 50% after 10 minutes interaction with Cr(VI). Large area GO modified by Fe_2O_3 exhibited the highest adsorption efficiency after 10 minutes interaction with Cr(VI) (80%). The adsorption capacity for MGO was calculated as 12 µg of Cr(VI) per 1 mg of the adsorbent.

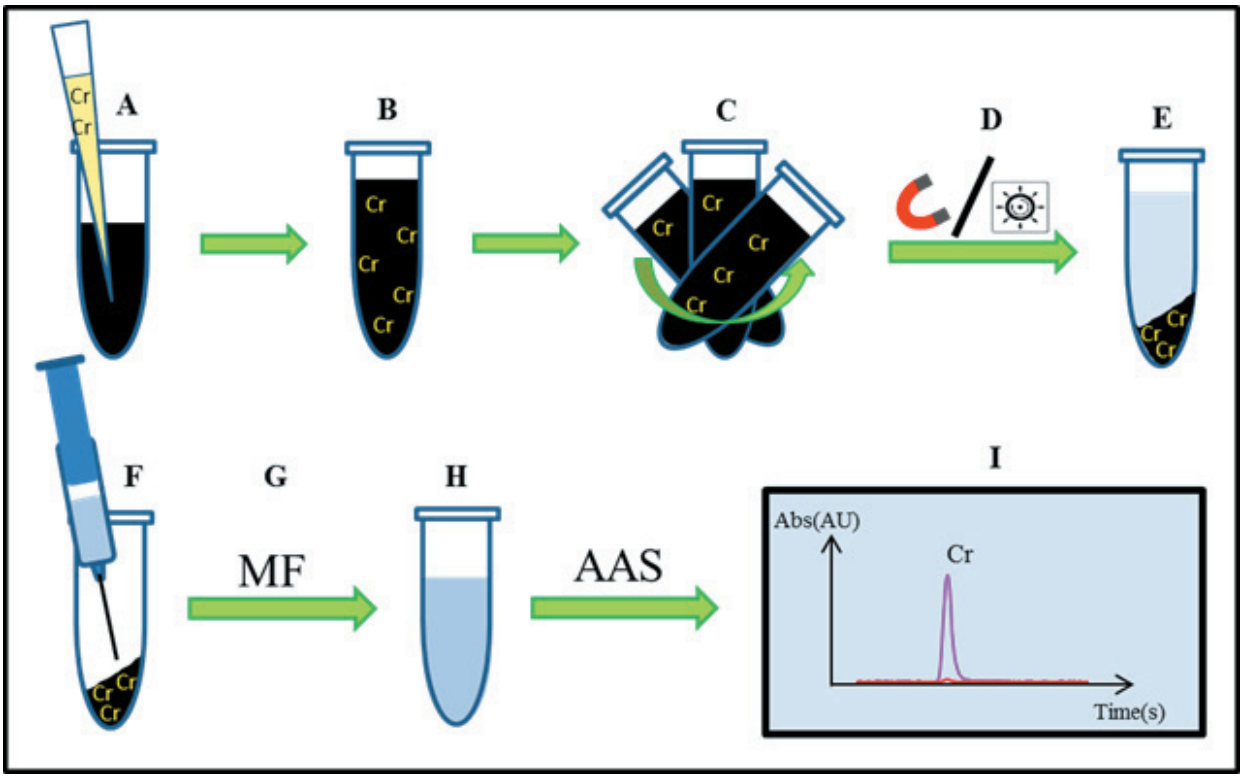

Fig. 1 The scheme of chromium removal from aqueous solution using different types of adsorbents. (**A**) carbon based adsorbent; (**B**) mixture of adsorbent and standard solution of sodium selenite; (**C**) shaking and mixing of the sample; (**D**) centrifugation or magnetic separation; (**E**) separated solid part; (**F**) removal of supernatant using syringe; (**G**) filtration using membrane filter 0.45 µm; (**H**) purified supernatant; (**I**) determination of chromium by AAS.

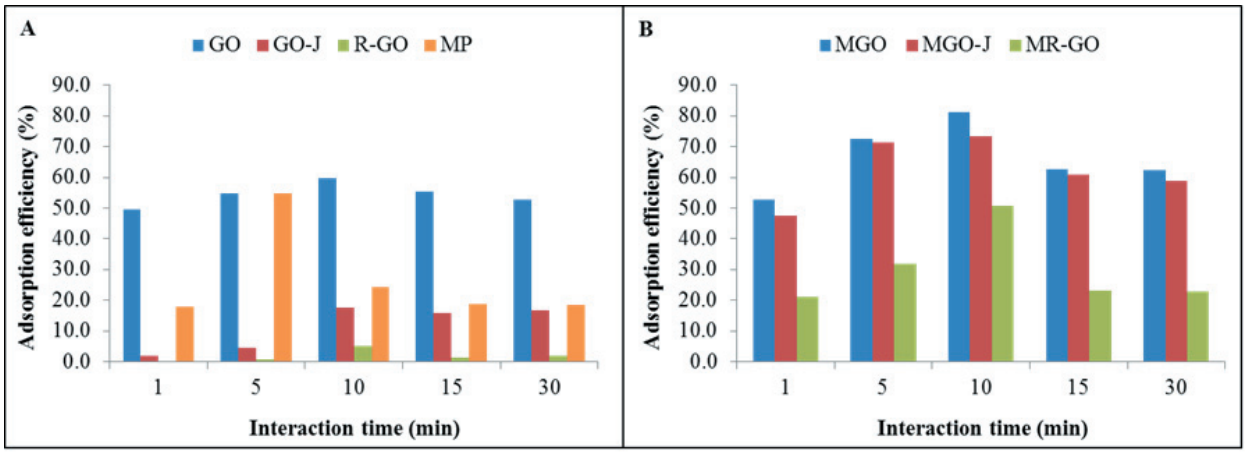

Figure 2: The adsorption efficiency of Cr(VI) depending on interaction time 1, 5, 10, 15 and 30 minutes for (**A**) starting materials GO, GO-J, R-GO and iron nanoparticles and (**B**) GO based materials modified by iron nanoparticles (MGO, MGO-J and MR-GO). The adsorption efficiency of adsorbents was determined using atomic absorption spectrometry with electrothermal atomization and Zeeman background correction.

Conclusion

Carbon based materials, especially graphene oxide, are considered to be promising materials for heavy metals or transition metals removal from surface and waste water. This study was focused on removal of Cr(VI) from aqueous solution using different nanomaterials based on graphene oxide and its modifications with iron nanoparticles. The large area graphene oxide modified by iron nanoparticles (MGO) seems to be the most promising nanomaterial for Cr(VI) removal, its adsorption efficiency reached 80% from applied concentration of Cr(VI) after 10 minutes interaction time. The adsorption capacity of this adsorbent was calculated as 12 µg of Cr(VI) per 1 mg of MGO. Environmental pollution by heavy metals and transition elements is a serious worldwide problem, so it is necessary to search new materials for heavy metals removal and apply them to real samples.

Acknowledgement

The work was supported by V4 Metallomic Scientific Network TD 11440027.

References

[1] S. Khan, Q. Cao, Y.M. Zheng, Y.Z. Huang, Y.G. Zhu, Environmental Pollution 152 (2008) 686.
[2] H. Wang, X.Z. Yuan, Y. Wu, H.J. Huang, G.M. Zeng, Y. Liu, X.L. Wang, N.B. Lin, Y. Qi, Applied Surface Science 279 (2013) 432.

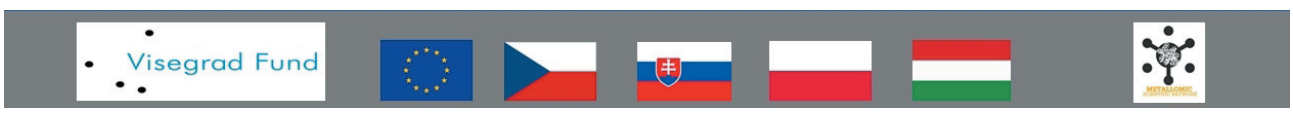

Biological activity and molecular structures of bis(benzimidazoles) and trithiocyanurate complexes

Pavel KOPEL[1,2], Monika KREMPLOVA[1,2], Dorota WAWRZAK[3], Dagmar CHUDOBOVA[1,2], Kristyna CIHALOVA[1,2], Halina MILNEROWICZ[4], Vojtech ADAM[1,2*], Rene KIZEK[1,2]

[1] Department of Chemistry and Biochemistry, Faculty of Agronomy, Mendel University in Brno, Zemedelska 1, CZ-613 00 Brno, Czech Republic, European Union
[2] Central European Institute of Technology, Brno University of Technology, Technicka 3058/10, CZ-616 00 Brno, Czech Republic, European Union
[3] Institute of Chemistry, Environmental Protection and Biotechnology, Jan Dlugosz University of Czestochowa, Armii Krajowej 13/15, Czestochowa PL-42-201, Poland, European Union
[4] Department of Biomedical and Environmental Analyses, Wroclaw Medical University, Borowska 211, PL-50-556 Wroclaw, Poland, European Union

*vojtech.adam@mendelu.cz

Abstract

Heterocyclic compounds are very often used in the development of novel drugs with new mechanisms of action. Benzimidazole and its derivatives are reported to be physiologically and pharmacologically active and some applications are found in the treatment of several diseases. Trithiocyanuric acid ($ttcH_3$), also referred as trimercaptotriazine, has a symmetric structure with three nitrogen atoms and three sulphur atoms in a ring (see Fig. 1). In this paper, we present the possible application of some bis(benzimidazole) and trithiocyanuric complexes in the treatment of bacterial or yeast infections. For the microbiological testing, $[Ni_3(pmdien)_3(\mu\text{-}ttc)](ClO_4)_3$ (3), where pmdien = *N*,*N*,*N*',*N*'',*N*''-pentamethyldiethylenetriamine, was also prepared according to published method [1]. The complex **3** has a similar structure (see Fig 1) to 1 and it was of interest to compare their biological activities.

Introduction

Benzimidazole and its derivatives are reported to be physiologically and pharmacologically active and some applications are found in the treatment of several diseases including epilepsy, diabetes and infertility. These compounds show a wide range of biological activities like antibacterial, antifungal, antitubercular, antitumor and anti-HIV-1 properties. The antitumor activity of the trithiocyanurate complexes was assayed *in vitro* against G-361, HOS, K-562 and MCF-7 tumour cell lines. The IC_{50} values of the Fe(II) and Mn(II) compounds turned out to be lower than those of cisplatin and oxaliplatin [2].

Aims

The major aim of this study was to test the biological activity of these compounds on the commercially supplied microorganisms (*Staphylococcus aureus*, *Escherichia coli* and *Saccharomyces cerevisiae*) and three bacterial strains isolated from patients from non-healing wounds infected by bacterial strains (*Streptococcus agalactiae*, *Corynebacterium striatum* and *Serratia marcescens*). For the microbiological testing, an already known and well characterized coordination compound, $[Ni_3(pmdien)_3(\mu\text{-}ttc)](ClO_4)_3$ (**3**).

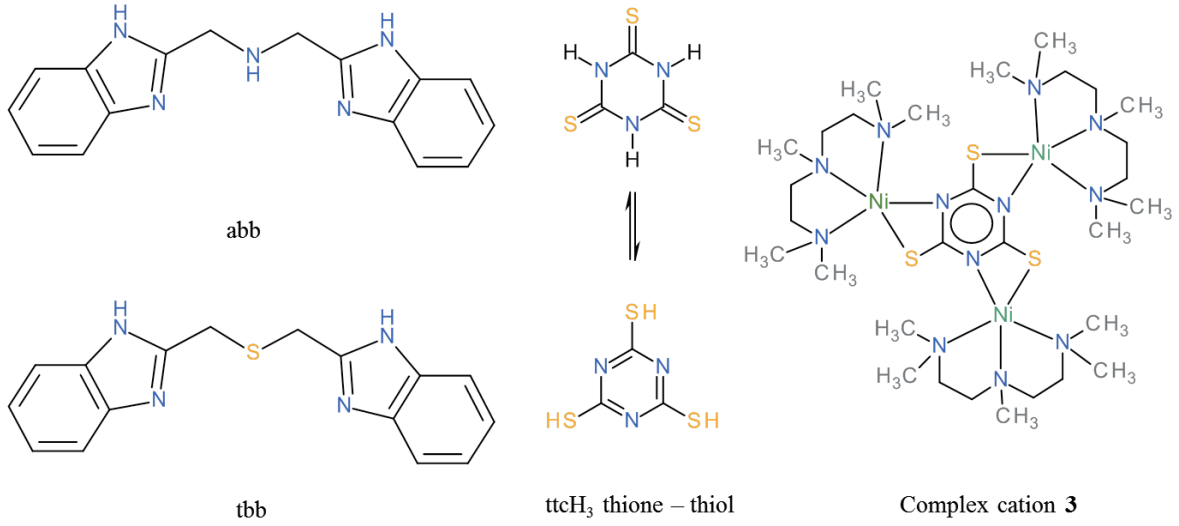

Figure 1: Structural formulas of the ligands used and the complex cation $[Ni_3(pmdien)_3(\mu\text{-ttc})](ClO_4)_3$ (**3**). **abb** = 1-(1*H*-benzimidazol-2-yl)-*N*-(1*H*-benzimidazol-2-ylmethyl)methanamine, **tbb** = 2-(1*H*-benzimidazol-2-ylmethylsulfanyl-methyl)-1*H*-benzimidazole, **ttc**H_3 = trithiocyanuric acid in its thione and thiol forms.

Material and methods

The compounds 1-(1*H*-Benzimidazol-2-yl)-*N*-(1*H*-benzimidazol-2-ylmethyl)- methanamine (abb), 2-(1H-Benzimidazol-2-ylmethylsulfanylmethyl)-1H-benzimidazole (tbb), $[Ni_3(abb)_3(H_2O)_3(\mu\text{-ttc})](ClO_4)_3\cdot 3H_2O\cdot EtOH$ (1), $[(tbbH_2)(ttcH_2)_2(ttcH_3)(H_2O)]$ (2) and $[Ni_3(pmdien)_3(\mu\text{-ttc})](ClO_4)_3$ (3) were prepared. For complexes 1 and 2 the X-ray crystallography was investigated and data were collected on a SMART CCD diffractometer (Siemens, Madison, WI, USA) with Mo-Kα radiation ($\lambda = 0.71073$ Å, graphite monochromator). The procedure for the evaluation of the antimicrobial effect of tested compounds consisted in measuring of the absorbance using the apparatus Multiskan EX (Thermo Fisher Scientific, Vantaa, Finland) and subsequent analysis in the form of growth curves. Bacteria and yeasts were cultivated in GTY medium for 24 h with shaking and were diluted with GTY medium to absorbance 0.1 before analysis using a Specord spectrophotometer 210 at a wavelength of 600 nm. On the microplate, these cultures were mixed with various concentrations of four types of antibiotics or S. aureus alone as a control. The concentrations of antibiotics were 0, 7.8, 15.6, 31.3, 62.5, 125 and 250 µg/mL.The measurements were carried out at time 0, then each half-hourly for 24 h at 37 °C and a wavelength of 600 nm.

Results and discussion

The molecular structure of 1 (see Fig 2) consists of trinuclear nickel(II) complex, ClO^{4-} anions, three crystal water and EtOH molecules. Three central nickel atoms are coordinated by three N atoms of abb, a water molecule O atom and the S,N-donor set of a ttc trianion in a deformed octahedral arrangement. The ttc trianion forms a bridge connecting the nickel centers.

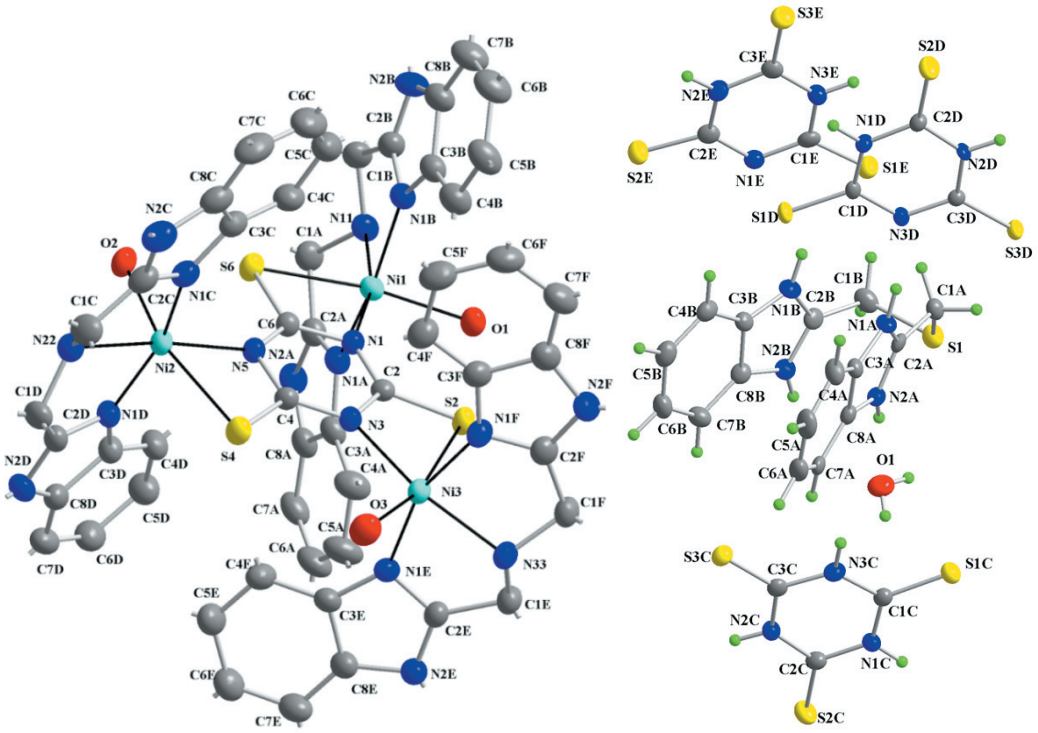

Figure 2: Numbering scheme of complex **1** (left) and complex **2** (right) with atomic displacement ellipsoids drawn at 30% probability level.

The structure of 2 (see Fig 2) consists from protonated tbb, two $ttcH_2$ anions, $ttcH_3$ and a water molecule. The two benzimidazole rings of tbb form a sandwich-like structure probably due to π-π interactions. The crystal structure is stabilized by weak hydrogen bonds. The tbb behaves as a strong base with hydrogen atoms on all nitrogens but from the molecular structure, it is seen that in the structure there are tbb and ttc planes connected through hydrogen bonds.

The biological activity of nickel(II) perchlorate hexahydrate, nickel(II) chloride hexahydrate, the ligands abb, tbb, $ttcNa_3$ and complexes 1–3 was studied (see Fig. 3). The antimicrobial effect of ligands and complexes was tested on commercial Staphylococcus aureus (S. aureus), Escherichia coli (E. coli), Saccharomyces cerevisiae (S. cerevisiae) and on bacteria isolated from the infected wounds Streptococcus agalactiae (*S. agalactiae*), *Corynebacterium striatum* (*C. striatum*) and *Serratia marcescens* (*S. marcescens*).

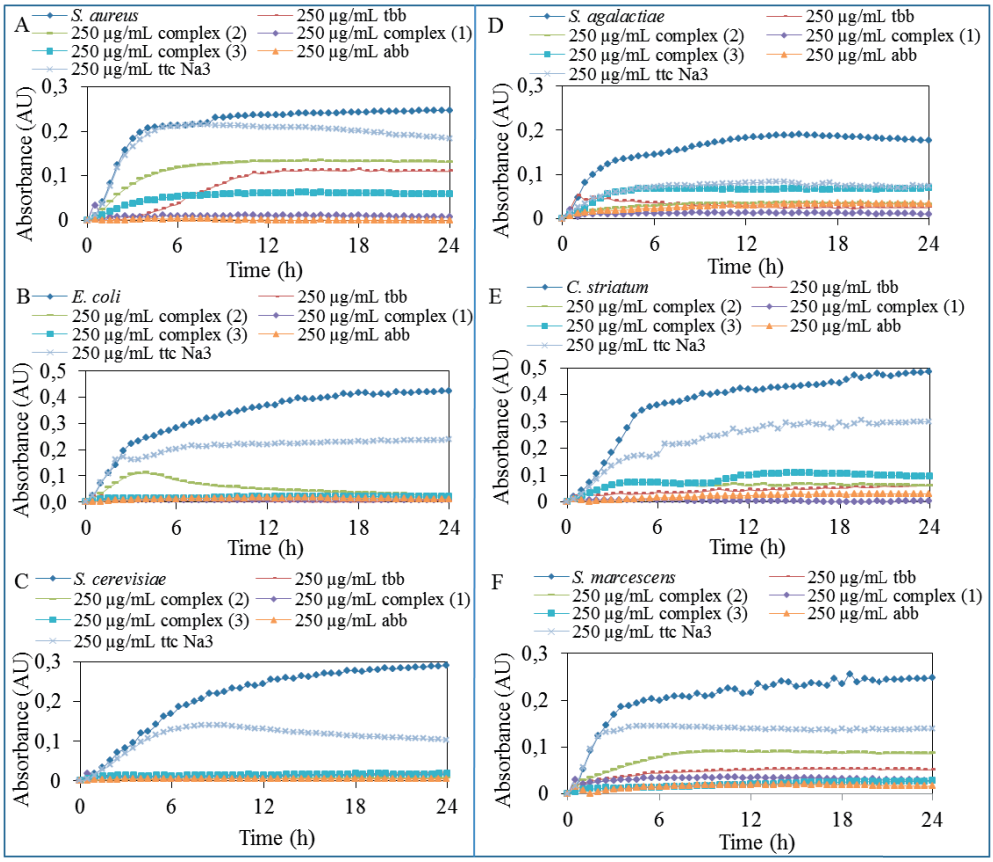

Figure 3: Testing of antimicrobial activity of 250 µg/mL concentration of ligands and complexes after 24 h of treatment on: **(A)** *S. aureus*; **(B)** *E. coli*; **(C)** *S. cerevisiae*; **(D)** *S. agalactiae*; **(E)** *C. striatum*; **(F)** *S. marcescens*.

The salts, ligands and complexes were applied in concentrations of 0; 3.9; 7.8; 15.6; 31.3; 62.5; 125 and 250 µg/mL on the three model organisms and the three bacterial strains isolated from the patient's wounds. The highest inhibition of all tested organisms growth was observed after the treatment of ligand abb and complex 1 and also the lowest IC_{50} values were observed in case of ligand abb and complex 1. These changes in coordination modes and ligands also lead to different biological properties of the complexes. When we compare the activities of abb and tbb, which only differ in the chain atoms in the middle (N or S), the activity of tbb is very low. Complex 1 is active against all the treated microorganisms whereas complex 3 shows no activity against S. aureus, but it shows better activity against E. coli and similar activity against S. cerevisiae in comparison with 1.

Conclusion

The X-ray single crystal analysis proved the structures of trinuclear Ni(II) complex and bis(benzimidazole)—trithiocyanurate co-crystals. It was shown that these compounds are biologically active. Especially the ligand abb and the complex 1, where the ligand is coordinated, showed very good activities against the wide spectrum of commercially available bacterial and yeast strains (S. aureus, E. coli and S. cerevisiae) and clinical specimens from real patients with non-healing infections and complicated courses of treatment.oxide composite, including prolonged exposure of the composites at the infection site.

Acknowledgement

The work was supported by V4 Metallomic Scientific Network TD 11440027.

References

[1] P. Kopel, J. Mrozinski, K. Dolezal, V. Langer, R. Boca, A. Bienko, A. Pochaba, Eur. J. Med. Chem. 44 (2009) 5475.
[2] P. Kopel, K. Dolezal, L. Machala, V. Langer, Polyhedron 26 (2007) 1583.

Automatic electrochemical determination of soil contaminated by heavy metal ions (Cd(II) and Pb(II))

Lukas NEJDL[4,5], Magdalena HABOVA[2], Jiri KUDR[1,4], Branislav RUTTKAY-NEDECKY[1,4], Anna BIZON[3], Lubica POSPISILOVA[2], Vojtech ADAM[1,4*] and Rene KIZEK[1,4]

[1] Department of Chemistry and Biochemistry, Faculty of Agronomy, Mendel University in Brno, Zemedelska 1, CZ-613 00 Brno, Czech Republic, European Union
[2] Department of Agrochemistry, Soil Science, Microbiology and Plant Nutrition, Faculty of Agronomy, Mendel University in Brno, Zemedelska 1, CZ-613 00 Brno, Czech Republic, European Union
[3] Department of Biomedical and Environmental Analyses, Wroclaw Medical University, Borowska 211, PL-50-556 Wroclaw, Poland, European Union
[4] Central European Institute of Technology, Brno University of Technology, Technicka 3058/10, CZ-616 00 Brno, Czech Republic, European Union
[5] Department of Geology and Pedology, Mendel University in Brno, Zemedelska 1, CZ-613 00 Brno, Czech Republic, European Union

*vojtech.adam@mendelu.cz

Abstract

Heavy metal pollution has become one of the most serious environmental problems of today. In this paper, we present low-cost and rapid production of amalgam electrodes, which were used for determination of Cd(II) and Pb(II). Difference pulse voltammetry was used with following settings: initial potential -1,1 V; end potential -0.2 V; step potential 0.005 V; modulation amplitude 0.025 V; modulation time 0.057 s and interval time 0.2 sec. Optimized parameters were implemented in a robotic analyser. Samples were measured in 24-well plates with a flat bottom. The electrochemical robotic device included three motorized units and a positioning system. First unit was rigidly connected to the vertical frame of the electrochemical robot; electrode holder was attached to it and enabled precise vertical (z) positioning of electrode holder (up and down). Microtiter plate was placed on horizontally (x/y) positioned board. The limit of detection (LOD) was calculated for the geometric surface of the working electrode 10.1 mm^2 that can be varied as required for analysis. Application of robotic device allowed us to analyze soil leachates with following LOD: Cd(II) = 80 and Pb(II) = 40 $ng.ml^{-1}$.

Introduction

Heavy metal pollution as a global problem includes contamination of air, soil and surface waters as a consequence of traffic, heavy industry and mining. The main threats to human health from heavy metals are associated with exposure to lead and cadmium [1,2]. These metals along with the mercury and arsenic have been extensively studied and their effects on human health regularly reviewed by international bodies such as the WHO [3]. Even at low concentrations, these metals can be toxic to organisms, including humans. For instance, lead is extremely toxic and can damage the nervous system, kidneys, and reproductive system, particularly in children [4-6].

Recent data from epidemiological studies suggest that intake of cadmium through diet associates to higher risk of endometrial, breast and prostate cancer as well as to osteoporosis in humans [7,8]. Heavy metals occur in the atmosphere and with air can be moved for a long distances and contaminating the land even thousands of kilometres from the source. Due

to this reason it is necessary to find easy to use analytical tools for analysis of heavy metals and to perform automatization of their measurement.

For environmental applications are the most suitable electrochemical detection systems because of their ability to analyse turbid samples [9], they have low energy requirements, and can be variably modified to achieve greater selectivity and sensitivity [10]. For common bench top analytical methods a precise sample preparation is necessary. Analytical method presented in this work is able to electrochemically analyze, Cd(II) and Pb(II) ions in soil leachates or cloudy wastewater by amalgam electrode. The amalgam electrode (Hg/Cu-WE) is alternative mercury hanging drop electrode (HMDE), because amalgam electrode shows similar sensitivity as HMDE and has many advantages. For example amalgam electrodes have a lower toxicity, easy manipulation, can be used multiple times, miniaturizations and flow is possible (automation) [11]. The production of this electrode is cheap and fast (a few seconds).

Aims

In this work, we focused on the production of cheap amalgam electrodes (Hg/Cu-WE). These types of electrodes were used for determined of cadmium and lead by differential pulse voltammetry (DPV). The individual steps of the production (Hg/Cu-WE) and detection of cadmium and lead were optimized step by step. The optimized parameters were implemented in a robotic workstation that can automatically analyze environmental samples.

Material and methods

Chemicals and material

All metal standards including lead(II) nitrate and cadmium(II) sulphate were purchased from Sigma-Aldrich (St. Louis, MO, USA). Stock solutions were prepared in ACS water immediately prior to use. Pipetting was performed by pipettes from Eppendorf (Hamburg, Germany). As electrolyte acetate buffer (0.2 M, pH 5) was utilized. The pH values were measured by using an inoLab Level 3 instrument (Wissenschaftlich-Technische Werkstatten GmbH; Weilheim, Germany).

Preparation of soil samples

The extracted soil sample was spread on a filter paper. After drying it was crushed and sieved through a sieve with a diameter of 2 mm. Two aliquots of the sample were weighed (5 g) into the PET vessel, and one aliquot was then enriched with 100 µl of heavy metal solution (Cd (II) or Pb (II)). The final concentration of metal in the enriched sample was 100 $ng.ml^{-1}$. Samples were incubating 12 hour at 25 ° C and then 100 ml of 0.1 M solvent ($CaCl_2$, NaOH, HCl, and H_2O) was poured on them. PET vessel was placed in a shaker for 30 minutes. Then it was leaved to settle for 24 hours and then centrifuged in a centrifuge MPW - 6.15 (Sigma) for 2 min at 3500 rpm. The solution was then decanted through a coarse sieve into 100 ml flasks and the pellet was discarded.

Modification of electrolytic copper wire as working electrode (Hg/Cu-WE)

Copper wires (Thermo scientific, Cambridge, UK) were used as working electrodes after modification. The copper wire were inserted into 0.01 M $Hg(NO_3)_2$ solution, prepared by the dissolution of 0.086 g mercury(II) nitrate in 25 mL of acidified (5% HNO_3, *v/v*) Milli-Q water. The electrodes were immersed in this solution for 0 – 480 seconds, which resulted in the formation of a thin-film of amalgam on the surface.

Electrochemical robotic device for detection of Cd(II) and Pb(II)

Electrodes were placed into the holder fabricated using the 3D printer (holder, sample loading and electrode system was same as in preceding case). The electrochemical robotic device (Sensolytics) positioning the electrodes included three motorized units ST4118M1804 (Nanotec, Munich, Germany) and positioning system (OWIS, Staufen, Germany). The electrode holder was attached to it and this enabled us to perform precise vertical (z) positioning of the electrode holder (up and down). The microtiter 24-well plate with flat bottom was placed on a horizontally (x/y) positioned board. Coordinates and the precise time of the holder and plate motion were controlled by the ELChemRo software (Sensolytics). We used the advanced settings of NOVA to prepare a script enabling us to set up the sequence of DPV measurements with adjustable time intervals between individual measurements. Electrochemical determination was carried out by differential pulse voltammetry (DPV). The parameters of the DPV measurement were as follows initial potential -1,1 V; end potential -0.2 V; step potential 0.005 V; modulation amplitude 0.025 V; modulation time 0.057 s, deposition time 90 sec and interval time 0.2 s. Cyclic voltammetry was used as a cleaning step (Recovery surface Hg/Cu-WE) between the measurements, unless otherwise indicated. Parameters are follows: start potential -1.1 V, upper vertex potential -0.7 V, lower vertex potential -0.2 V, stop potential -1 V, cycles 50, step potential -0.0024 and scan rate 0.4 V/s.

Results and discussion

Automatic analysis of soil leachates

Optimal parameters of the previous work were implemented in a robotic analyser. Optimum values are summarized in **Table 1** (the top three lines). We analysed four types of soil leachates in different solvents ($CaCl_2$, NaOH, HCl and H_2O). Leachates were prepared according to the methodology mentioned in experimental section. An aliquot of the soil was enriched with a final concentration 100 $ng.ml^{-1}$ of both Cd(II) and Pb(II), (**Table 1, sample 2, 4, 6 and 8**). Other samples (**Table 1, sample 1, 3, 5 and 7**) were analysed without addition of metals. Samples were mixed with 0.2 M acetate buffer pH 5 in a ratio of 1: 1.4 (1 ml of sample and 1.4 ml of buffer) in 24-well plate with a flat bottom. First, the soil leachates were analysed in $CaCl_2$ environment, but electrochemical response was not registered, nor in soil enriched with Cd(II) or Pb(II), **Table 1, sample 1 and 2**.

Furthermore soil leachates in the NaOH environment were analysed with the same result as in the previous case **Table 1, sample 3 and 4**. The best results were achieved in the soil leachate prepared in HCl environment. In this type of leachate 90 $ng.ml^{-1}$ of Pb(II) was detected, Cd(II) concentration was below LOD, **Table 1, sample 5**. By the samples enriched with metals 92 $ng.ml^{-1}$ of Cd(II) and 185 ng $ng.ml^{-1}$ of Pb(II) was determined, **Table 1, sample 5 a 6**. Observed concentrations are in accordance with metal concentration that was added into soil before extract preparations. In this way it was verified that the described electrochemical method is able to determine Cd (II) and Pb (II) in soil extracts prepared in an HCl environment with RSD ≤ 9In the last set of soil leachates prepared in the distilled H_2O environment no electrochemical signal was recorded, **Table 1, sample 7 and 8.** In our experiments we have shown that the metal extraction from soil was most effective in the environment of HCl. It is generally known that the mobility of metals in the soil is closely related to pH [12]. Lower pH facilitates mobility, while at higher pH formation of complexes or sorption to organic particles may occur. Effect of pH and different soil types on the Cd (II) or Pb (II) extraction of will be investigated in subsequent work.

Metal	Electrode area	Deposition time	Amalgamation	Regression equations	Linear dynamic range	R^2	LOD	RSD
Cd(II)	9.5 mm^2	90 s	60 s	y = 0.068x - 3.8886	85 - 3360 $ng.ml^{-1}$	0.9979	80 ng.ml-1	≤9 %
Pb(II)	9.5 mm^2	90 s	60 s	y = 0.0405x + 1.7769	45 - 3360 $ng.ml^{-1}$	0.9929	40 ng.ml-1	≤9 %
sample	solvent	Cd (II) concentration	Pb (II) concentration	sample	solvent	Cd(II) concentration	Pb(II) concentration	
1.	$CaCl_2$	>LD	>LD	2.	$CaCl_2$	>LD	>LD	≤9 %
3.	NaOH	>LD	>LD	4.	NaOH	>LD	>LD	≤9 %
5.	HCL	>LD	90 $ng.ml^{-1}$	6.	HCL	92 $ng.ml^{-1}$	185 $ng.ml^{-1}$	≤9 %
7.	H_2O	>LD	>LD	8.	H_2O	>LD	>LD	≤9 %

Table 1: Analytical table containing investigated parameters (electrode area, deposition time, amalgamation) and analytical data (regression equation, linear range, reliability factor, detection limit and relative standard deviation) at automatic analysis of Cd(II) or Pb(II). The table also lists the samples of soil leachates 1 and 8.

Conclusion

In this work was presented fast and cheap manufacture of amalgam electrodes. The optimized parameters were implemented in a robotic analyser. By this automated method heavy metals (Cd (II) and Pb (II)) in soil leachates have been successfully analysed. It has been found that the best extraction method for Cd (II) and Pb (II) were conducted in the HCl environment.

Acknowledgement

The work was supported by V4 Metallomic Scientific Network TD 11440027.

References

[1] H.F. Sun, Y.H. Li, Y.F. Ji, L.S. Yang, W.Y. Wang, H.R. Li, Transactions of Nonferrous Metals Society of China 20 (2010) 308.
[2] A. Petroczi, D.P. Naughton, Food and Chemical Toxicology 47 (2009) 298.
[3] L. Jarup, British Medical Bulletin 68 (2003) 167.
[4] Y. Finkelstein, M.E. Markowitz, J.F. Rosen, Brain Research Reviews 27 (1998) 168.
[5] J.P. Gennart, A. Bernard, R. Lauwerys, International Archives of Occupational and Environmental Health 64 (1992) 49.
[6] J.A. Thomas, W.C. Brogan, American Journal of Industrial Medicine 4 (1983) 127.
[7] B. Julin, A. Wolk, J.E. Johansson, S.O. Andersson, O. Andren, A. Akesson, British Journal of Cancer 107 (2012) 895.
[8] A. Engstrom, K. Michaelsson, M. Vahter, B. Julin, A. Wolk, A. Akesson, Bone 50 (2012) 1372.
[9] C.Y. Chai, G.Y. Liu, F. Li, X.F. Liu, B. Yao, L. Wang, Analytica Chimica Acta 675 (2010) 185.
[10] C.D. Garcia, C.S. Henry, Electroanalysis 17 (2005) 223.
[11] O. Mikkelsen, K.H. Schroder, Electroanalysis 15 (2003) 679.
[12] K.K. Fedje, L. Yillin, A.M. Stromvall, Journal of Environmental Management 128 (2013) 489.

UV tuning of cadmium telluride quantum dots (CdTe) – assessed by spectroscopy and electrochemistry

Lukas NEJDL[1,3], Lukas RICHTERA[1,2], Renata KENSOVA[1,2], Jiri KUDR[1,2],Branislav RUTTKAY-NEDECKY[1,2], Jindrich KYNICKY[1,3], Gabriela EMRI[4], Vojtech ADAM[1,2*] and Rene KIZEK[1,2]

[1] Central European Institute of Technology, Brno University of Technology, Technicka 3058/10, CZ-616 00 Brno, Czech Republic, European Union
[2] Department of Chemistry and Biochemistry, Mendel University in Brno, Zemedelska 1, CZ-613 00 Brno, Czech Republic, European Union
[3] Department of Geology and Pedology, Mendel University in Brno, Zemedelska 1, CZ-613 00 Brno, Czech Republic, European Union
[4] Department of Dermatology and Venerology, Faculty of Medicine, University of Debrecen, Nagyerdei krt. 98, HU-4012, Debrecen, Hungary, European Union

*vojtech.adam@mendelu.cz

Abstract

In this work the electrochemical analysis (potentiometric stripping analysis – PSA, cyclic voltammetry - CV) and evaluation of fluorescence properties of CdTe – QDs were performed. Using CV it was found that average value of ΔE of QDs is lower than 0.059 V and I is in direct correlation with square root of scan rates, therefore we assume that this system represents rather reversible than quasi-reversible process. Further, it was found that nearly 1.4 electrons are exchanged in both cases, which corresponded with expected electron transfer. Fluorescence analysis showed that UV radiation (254 and 312 nm) significantly changes fluorescence properties of CdTe in time 0 – 60 min. It was found that after 5 min of UV irradiation (λ = 312 nm) the fluorescence intensity increased by 37% and at λ = 254 nm the increase in fluorescence intensity was even bigger, by 45% (compared to the control without irradiation). UV radiation also caused a shift in the emission maximum of CdTe – QDs by approximately 57 nm. This work opens up new ways for tuning the optical properties of QDs.

Introduction

Nanotechnology is the one of the most advanced disciplines. One of the main areas of nanotechnology is the synthesis and characterization of various types of nanoparticles for a broad spectrum of applications [1-3]. Entry into the nano world has opened up a new possibilities for the use of fluorescent nanocrystals (quantum dots - QDs) and their unique properties [4]. The most popular methods for QDs synthesis are organometallic synthesis, aqueous route (low-temperature reaction) and biosyntesis [5]. An interesting complement to these methods can be post-synthesis of QDs by exposure to ultraviolet radiation.

In this way can be activated the surface of the QDs and controlled (tuning) of optical properties. The ability of UV light to change the conformation of the complexes was studied in our previous work [6]. It has been demonstrated that UV radiation activates fluorescence by zinc complexes. The light-induced control of the type (oil or water continuous medium) of emulsions stabilized by an appropriate combination of two polyelectrolyte surfactants was described [7]. Furthermore, a number of photocatalytically active nanoparticles has been reviewed e.g. TiO_2 nanorods [8], ZnO nanoparticles [9] and others [10,11]. Corrosion of the outer sphere caused by photooxidation leading to toxic ion release, formation of

reactive oxygen species (ROS) or induction of genotoxic stress [12-14]. Yin showed that the toxic effect of PbSe - QDs under UV irradiation is caused by release of Pb(II) and generated ROS, inducing DNA damage [15]. Photocatalytic technique can be used for removal metals or transformation of the ions to less toxic species or their deposition on the semiconductor catalyst surface for recovery of expensive and useful metals [16]. The photocatalytic methodology not only provides an on-demand UV-assisted reduction of Cr(VI) [17] or Graphene oxide [18] by TiO_2 suspensions, but also opens up new ways for tuning the optical properties of photo tunable QDs.

Aims

In our experiments, we focused on fluorescent anlysis of QDs exposed to UV radiation at two wavelengths $\lambda = 254$ and $\lambda = 312$ nm in time intervals 0 – 60 minutes.

Material and methods

Chemicals

Working solutions like buffers and standard solutions were prepared daily by diluting the stock solutions. Standards and other chemicals were purchased from Sigma-Aldrich (St. Louis, MO, USA) in ACS purity unless noted otherwise.

Preparation of CdTe QDs

CdTe QDs was prepared according to the following protocol. Briefly, 10 ml of cadmium acetate (5.32 mg/ml) and 1 ml of mercaptosuccinic acid (60 mg/ml) were mixed with 76 ml of deionized water on a magnetic stirrer. 1.8 ml of ammonia (1 M) solution was added to it. 1.5 ml of sodium tellurite (221.6 mg/ml) was also added and mixed very well. 50 mg of sodium borohydride was added later. The solution was stirred for around 2 h until the bubble formation was stopped and subsequently the volume of the solution was made up to 100 ml with deionized water. 2 ml of this solution was taken in a small glass vessel and heated at 60 °C, 300 W for 10 min (ramping time 10 min) under microwave irradiation (Multiwave 3000, Anton-Paar GmbH, Graz, Austria) and finally the CdTe QDs were prepared and stored in dark at 4 °C.

Fluorescence analysis

Fluorescence was acquired by multifunctional microplate reader Tecan Infinite 200 M PRO (TECAN, Switzerland). Wavelength 360 nm was used as an excitation radiation and the fluorescence scan was measured within the range from 400 to 850 nm per 2-nm steps. The detector gain was set to 65. The samples were placed in UV-transparent 96 well microplate with flat bottom by CoStar (Corning, USA). To each well 50 µL of sample was placed. All measurements were performed at 25 °C controlled by Tecan Infinite 200 PRO (TECAN, Switzerland). The QDs were exposed to UV radiation at 254 and 312 nm using transilluminator (VilberLourmat, Marne-la-Vallee Cedex, France). The sample area is 20 × 20 cm illuminated by 6 UV emitting tubes with power of 15 Watts each.

Results and discussion

Fluorescence spectroscopy was employed for monitoring the interaction of UV radiation with CdTe – QDs. Emission spectra in the range of 400 – 800 nm with excitation wavelength 360 nm at temperature 25 ºC were obtained. Conditions mentioned above were used for all measurements. CdTe - QDs were exposed to UV radiation (312 and 254 nm) for 5 minutes in the transilluminator and emission spectra of samples were measured in time of 0 - 60 minutes (every 5 minutes). The samples were placed in UV-transparent 96 well microplate with flat bottom by CoStar. To each well was placed 50 µL of 1 mM QDs. After irradiation the fluorescence properties of QDs (fluorescence intensity and emission maximum) was monitored immediately, this process was repeated twelve times to observe the UV dose dependency. First, transilluminator was set on 312 nm. After that samples (50 ul of 1 mM QDs in UV-transparent 96 well microplate) were inserted into the transilluminator.

It was found that after 5 min UV irradiation (λ =312 nm) the fluorescence intensity increased by 37% (compared to the control without irradiation) and the color was changed from green to light green, **Fig. 1 A.** Another five-minute irradiation caused an increase in fluorescence intensity by a further 9% and the color was change to yellow-green. Another ten-minute irradiation caused an increase in fluorescence intensity by approximately 1% and the color was changed to yellow. Each subsequent irradiation caused a decrease in fluorescence intensity of QDs by about 10%, but the color has not changed. Further, the dependence of the UV radiation on the change of the emission maximum of QDs was observed, **Fig. 1 B.** In control QDs (unirradiated) emission maximum at λ_{em} = 518 nm was found. Five minutes of UV irradiation (312 nm) caused a shift in emission maximum for 14 nm (λ_{em} = 532 nm). Another five-minute exposure to UV radiation caused a shift in emission maximum for another 14 nm (λ_{em} = 546 nm). Another ten-minute irradiation caused shift by 10 nm (λem = 556 nm). After 60 minutes of UV irradiation of QDs emission maximum λ_{em} = 576 nm was achieved. Second, transilluminator was set on 254 nm and same measurements were done as in the previous case.

It was found that after 5 min of UV irradiation (λ = 254 nm) the fluorescence intensity increased by 45% (compared to the control without irradiation) and the color was changed from green to light green, **Fig. 1 B.** Another five-minute irradiation caused an decrease in fluorescence intensity by a 12% and the color was full yellow. Each additional radiation exposure caused a slight decrease (approximately by 2.5%) of QDs fluorescence intensity, but the color did not change. The shift in emission maximum of QDs depending on the UV irradiation length had a similar trend as in the previous case, **Fig. 1 D.** After 60 minutes of UV irradiation of QDs emission maximum λ_{em} = 575 nm was achieved.

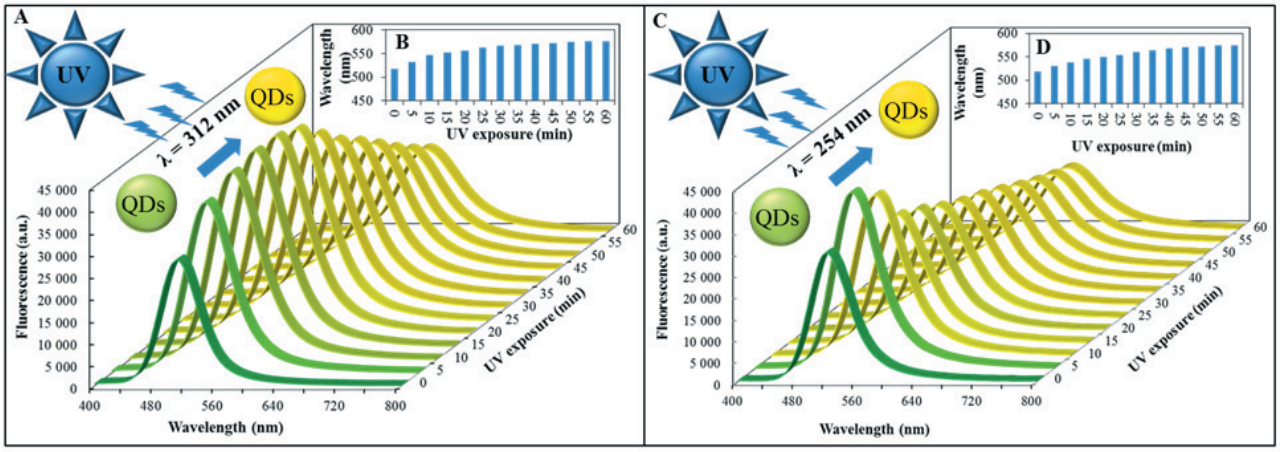

Figure 1: A) The effect of UV radiation (λ = 312 nm) on the change in fluorescence properties of 1 mM QDs and (B) emission maximum of QDs in time UV radiation 0 – 60 min. C) The effect of UV radiation (λ = 254 nm) on the change in fluorescence properties of QDs and (D) emission maximum of QDs in time UV radiation 0 – 60 min.

Conclusion

Using fluorescence spectroscopy a significant relationship between QDs and UV radiation was shown. It was observed that exposure to UV light changes the optical characteristics (radiation intensity and emission) of QDs. In this way QDs can be controlled, tuned for better quantum yield, or to adapt the emission spectrum for the particular application. In further work will be studied various types of QDs and mechanism responsible for fluorescence changes induced by UV.

Acknowledgement

The work was supported by V4 Metallomic Scientific Network TD 11440027.

References

[1] O.C. Farokhzad, R. Langer, Acs Nano 3 (2009) 16.
[2] Q. Chaudhry, M. Scotter, J. Blackburn, B. Ross, A. Boxall, L. Castle, R. Aitken, R. Watkins, Food Additives and Contaminants Part a-Chemistry Analysis Control Exposure & Risk Assessment 25 (2008) 241.
[3] X. Wang, L.L. Yang, Z. Chen, D.M. Shin, Ca-a Cancer Journal for Clinicians 58 (2008) 97.
[4] M. Bruchez, M. Moronne, P. Gin, S. Weiss, A.P. Alivisatos, Science 281 (1998) 2013.
[5] S.M. Farkhani, A. Valizadeh, Iet Nanobiotechnology 8 (2014) 59.
[6] L. Nejdl, L. Richtera, D. Wawrzak, V. Milosavljevic, P. Kopel, J. Kudr, B. Ruttkay-Nedecky, V. Adam, R. Kizek, International Journal of Electrochemical Science 10 (2015) 1696.
[7] I. Porcar, P. Perrin, C. Tribet, Langmuir 17 (2001) 6905.
[8] T.A. Kandiel, R. Dillert, A. Feldhoff, D.W. Bahnemann, Journal of Physical Chemistry C 114 (2010) 4909.
[9] X.J. Liu, L.K. Pan, Q.F. Zhao, T. Lv, G. Zhu, T.Q. Chen, T. Lu, Z. Sun, C.Q. Sun, Chemical Engineering Journal 183 (2012) 238.
[10] H. Schmidt, M. Akarsu, T.S. Muller, K. Moh, G. Schafer, D.J. Strauss, M. Naumann, Research on Chemical Intermediates 31 (2005) 535.
[11] X.B. Chen, S.H. Shen, L.J. Guo, S.S. Mao, Chemical Reviews 110 (2010) 6503.
[12] J. Aldana, Y.A. Wang, X.G. Peng, Journal of the American Chemical Society 123 (2001) 8844.
[13] A.C.S. Samia, X.B. Chen, C. Burda, Journal of the American Chemical Society 125 (2003) 15736.
[14] A.O. Choi, S.E. Brown, M. Szyf, D. Maysinger, Journal of Molecular Medicine-Jmm 86 (2008) 291.
[15] C.X. Yin, T. Yang, W. Zhang, X.D. Zhou, K. Jiao, Chinese Chemical Letters 21 (2010) 716.

[16] M.I. Litter, Applied Catalysis B-Environmental 23 (1999) 89.
[17] Y. Ku, I.L. Jung, Water Research 35 (2001) 135.
[18] G. Williams, B. Seger, P.V. Kamat, Acs Nano 2 (2008) 1487.

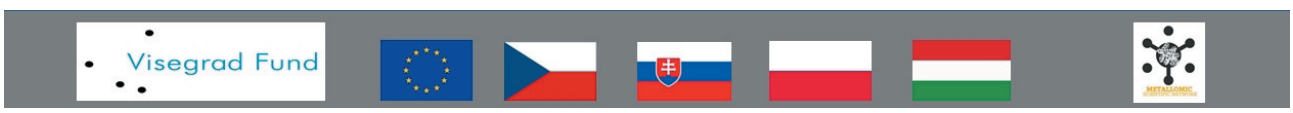

Quantum dots in fluorescence resonance energy transfer-based nanosensors and their application

Marketa VACULOVICOVA[1,2], Maja STANISAVLJEVIC[1], Sona KRIZKOVA[1,2], Marta KEPINSKA[3], Anna BIZON[3], Rene KIZEK[1,2], Vojtech ADAM[1,2]*

[1] Department of Chemistry and Biochemistry, Faculty of Agronomy, Mendel University in Brno, Zemedelska 1, CZ-613 00 Brno, Czech Republic, European Union
[2] Central European Institute of Technology, Brno University of Technology, Technicka 3058/10, CZ-616 00 Brno, Czech Republic, European Union
[3] Department of Biomedical and Environmental Analyses, Wroclaw Medical University, Borowska 211, PL-50-556 Wroclaw, Poland, European Union

*vojtech.adam@mendelu.cz

Abstract

Due to the numerous benefits, QD-FRET based sensors gained a wide spread popularity in a variety of scientific areas. As a number of other areas, also FRET-based sensors have been affected by nanotechnology development. Nanoscale materials with their uniqueness have become a new challenge for biosensors designing

Introduction

Nanotechnology - the development of materials at the nanoscale - is one of the most prominent advancing technologies today. Novel nanomaterials have found their place in improvement of biosensors including well-known and widespread technologies. Biosensors classification is done according to multiple criteria like transduction mechanism and/or biorecognition principles. Further fluorescence-based technique, which rises great interest, is Förster resonance energy transfer (FRET) as a specific mechanism of energy transfer between two molecules, called fluorophores, which can be easily excited with photon.

Fret basics

FRET is acronym for Förster resonance energy transfer named according to its discoverer German scientist Theodor Förster [1]. In the presence of two fluorophores, the energy donor and acceptor, FRET will occur after fulfilling certain conditions and the most important will be presented here. Detailed explanation of the fluorescence and FRET has been published in the past [2-4].

FRET involves non-radiative transfer of energy between donor and acceptor fluorophores, also called FRET pairs. Energy transfer between FRET pair is the result of long-range dipole–dipole interaction between them and does not include a photon emission.

FRET will occur when overlap of the emission spectrum of the donor and absorption spectrum of the acceptor is bigger than 30% and the distance is less than 10 nm. Fulfilling this conditions the mutual dipole orientation will be satisfied as well [5]. The distance between FRET pair is not only defining whether FRET occurs or not, but the efficiency of energy transfer have the same dependence of the distance and mathematically is expressed with the following equation:

$$E = R_o^6 / (R_o^6 + r^6)$$

where E is efficiency of energy transfer, R_o is Förster distance (the distance at which energy efficiency is 50%) and r is the donor-acceptor distance.

The other, but not less important properties are quantum yield and fluorescence lifetime of the fluorophores. Larger quantum yield means approaching to the unity and displaying the brighter emission and represents number of emitted photons relative to the number of absorbed ones. The more photons are emitted from the donor the better energy transfer will occur. Fluorescence lifetime, on the other hand, defines an average time that molecule spends in the excited state before relaxation. Both of these properties are dependent on rates of radiative and non-radiative decay because they are tightly connected to depopulation of excited state which determinate fluorescent characteristic of the fluorophores [3,6].

FRET can be detected by monitoring the acceptor fluorescence and/or the acceptor quenching. In FRET system, quenching will be observed when the acceptor belongs to the family of molecules called quenchers which after excitation are returned to their ground state via non-radiative decay pathways [7].

Due to aforementioned conditions, that fluorophores have to achieve it is obvious that designing FRET encounter a lot of limitations and shortcomings as well as fluorophores as an inevitable part. Regarding improvement of its characteristics beside improvement of existing fluorophores, new nanomaterials have been explored and used for the sensing.

Quantum dots and new fluorophores

Regarding FRET, one of the most interesting nanomaterials are nanoparticles, especially quantum dots (QDs). QDs are semiconductors made out of the elements from groups II and VI or groups III and V in periodic table. They are known for their small size (1-10 nm) and size-dependent optical and electronic properties caused by quantum confinement [8]. By now, QDs have been confirmed as suitable alternative to fluorophores used in FRET based biosensors and other fluorescence techniques. They offer several advantages over organic dyes.

QDs as new generation of fluorophores have several advantages over conventional ones. In addition, QDs have one unique characteristic incomparable with organic fluorophores, the ability of tuning the emission range as a result of core size regulation during synthesis follows quantum confinement. QDs broad excitation spectra and narrow defined emission peak allow multicolor QDs to be excited from one source without emission signal overlap [9,10], also 10-100 times lager molar extinction coefficient than fluorophores has as a result brighter probes comparing the conventional fluorophores [11,12]. This induce large Stokes shift (difference between peak absorption and peak emission wavelengths) of QDs in a range of 300-400 nm as well valuable for multiplexing [13]. These advantages enable imaging and/or tracking multiple molecular targets at the same time as well as elimination of background autofluorescence, which can emerge in biological samples causing detection of mixed signals from autofluorescence and fluorophores fluorescence. Therefore, fluorescence lifetime plays an important role and QDs, with their lifetime of 20-50 ns, have superiority over fluorophores with their few-nanosecond fluorescence lifetime, as well as size-tunable absorption and emission spectra [14]. Further notable advantage is the high quantum yield ranging from 40% to 90% and due to their inorganic core; they are highly resistant to the photobleaching and/or chemical degradation [15].

QDs are not flawless, they suffer of luminescence intermittency known as blinking which can cause problems in applications and usually have been overcome by shell engineering and/or decreasing the excitation intensity [16,17], and then their inorganic nature and in-

solubility has been successfully mitigated by different coating and capping agents. QDs are an order of magnitude bigger that organic dyes, which represents a problem if the probe size is important [14]. Further as shortcomings, their synthesis costs and high toxicity of the used precursors are usually stated. Their overall toxicity remains a subject of discussions although possible solutions are given by development of alternative ways of synthesis such as "green synthesis" [18-20] or biosynthesis [21-23] of QDs. The overall summary of applications is given in Fig. 1.

Figure 1: Summary of application fields of QD-FRET sensors.

Conclusion

FRET has gained a huge importance in different research fields and improved detection sensitivity in various analytical techniques since its first description. As it is presented in this review, FRET in combination with QDs and their superior properties, such as long fluorescence lifetime and resistance to photobleaching, has enabled designing of the new and improved sensors. QD-FRET-based sensor are giving a great contribution to the miniaturization of the sensors. Moreover, QDs immobilization to the inexpensive materials and employing phone cameras as detectors leads toward cheaper detections possibilities, which is a solid proof of their immense potential to be affordable and perhaps applied in everyday life in the future.

We suggest that FRET-based biosensors could be a key for point-of-care diagnostics, which has to be low cost, easy-to-use (color change) and sensitive. Besides this *in vitro* diagnostics, there is an ocean of fields in *in vivo* diagnostics, where FRET would find a good place including tracking of the target molecules, studying of changes in biochemical pathways and cell structures.

Acknowledgement

The work was supported by V4 Metallomic Scientific Network TD 11440027.

References

[1] T. Förster, Annalen der Physik 437 (1948) 55.
[2] P.R. Selvin, Nat. Struct. Biol. 7 (2000) 730.
[3] J.R. Uhl, Y.W. Tang, E.R. Cockerill, Fluorescence Resonance Energy Transfer, Amer Soc Microbiology, Washington, 2011.
[4] N. Shanker, S.L. Bane, in J.J. Correia, H.W. Detrich (Editors), Biophysical Tools for Biologists: Vol 1 in Vitro Techniques, Elsevier Academic Press Inc, San Diego, 2008, p. 213.
[5] M. Elangovan, R.N. Day, A. Periasamy, J. Microsc.-Oxf. 205 (2002) 3.
[6] J. Lakowicz, Principles of Fluorescence Spectroscopy, Kluwer Academic/Plenum Publishers, New York, Boston, Dordrecht, London, Moscow, 1999.
[7] G. Leriche, G. Budin, Z. Darwich, D. Weltin, Y. Mely, A.S. Klymchenko, A. Wagner, Chem. Commun. 48 (2012) 3224.
[8] F.C. Adams, C. Barbante, Spectrochim. Acta B 86 (2013) 3.
[9] A.P. Alivisatos, W.W. Gu, C. Larabell, Annual Review of Biomedical Engineering 7 (2005) 55.
[10] C.E. Probst, P. Zrazhevskiy, V. Bagalkot, X.H. Gao, Adv. Drug Deliv. Rev. 65 (2013) 703.
[11] W.W. Yu, L.H. Qu, W.Z. Guo, X.G. Peng, Chem. Mater. 15 (2003) 2854.
[12] J.J. Sun, E.M. Goldys, J. Phys. Chem. C 112 (2008) 9261.
[13] A.H. Fu, W.W. Gu, C. Larabell, A.P. Alivisatos, Curr. Opin. Neurobiol. 15 (2005) 568.
[14] M.A. Walling, J.A. Novak, J.R.E. Shepard, Int. J. Mol. Sci. 10 (2009) 441.
[15] P. Zrazhevskiy, M. Sena, X.H. Gao, Chem. Soc. Rev. 39 (2010) 4326.
[16] L. Li, G.J. Tian, Y. Luo, H. Brismar, Y. Fu, J. Phys. Chem. C 117 (2013) 4844.
[17] M.H.W. Stopel, J.C. Prangsma, C. Blum, V. Subramaniam, RSC Adv. 3 (2013) 17440.
[18] P.C. Huang, Q. Jiang, P. Yu, L.F. Yang, L.Q. Mao, ACS Appl. Mater. Interfaces 5 (2013) 5239.
[19] R.K. Beri, P.K. Khanna, J. Nanosci. Nanotechnol. 11 (2011) 5137.
[20] M. Ahmed, A. Guleria, M.C. Rath, A.K. Singh, S. Adhikari, S.K. Sarkar, J. Nanosci. Nanotechnol. 14 (2014) 5730.
[21] H.F. Bao, N. Hao, Y.X. Yang, D.Y. Zhao, Nano Res. 3 (2010) 481.
[22] H.Q. Huang, M.X. He, W.X. Wang, J.L. Liu, C.C. Mi, S.K. Xu, Spectrosc. Spectr. Anal. 32 (2012) 1090.
[23] S.R. Sturzenbaum, M. Hockner, A. Panneerselvam, J. Levitt, J.S. Bouillard, S. Taniguchi, L.A. Dailey, R.A. Khanbeigi, E.V. Rosca, M. Thanou, K. Suhling, A.V. Zayats, M. Green, Nat. Nanotechnol. 8 (2013) 57.

Zinc resistant prostate cancer cell lines and methods for their analysis – workshop

Monika HOLUBOVA[1,2], Marketa SZTALMACHOVA[1,2], Kristyna HUDCOVA[1], Jan BALVAN[1,2], Jaromir GUMULEC[1,2], Vojtech ADAM[2,3*], Michal MASARIK[1,2]

[1] Department of Pathological Physiology, Faculty of Medicine, Masaryk University, Kamenice 5, CZ-612 00 Brno, Czech Republic, European Union
[2] Central European Institute of Technology, Brno University of Technology, Technicka 3058/10, CZ-616 00 Brno, Czech Republic, European Union
[3] Department of Chemistry and Biochemistry, Mendel University in Brno, Zemedelska 1, CZ-613 00 Brno, Czech Republic, European Union

*vojtech.adam@mendelu.cz

Zinc and its role in cancer and non-cancer cells

Zn(II) ions contribute to a number of biological processes including DNA synthesis, gene expression, enzymatic catalysis, neurotransmission, and apoptosis. It is not surprising that zinc as a trace element is the second to most abundant metal in a human. Approximately 90 % of zinc(II) ions is tightly bound most of all by cysteine, histidine and asparagine residues of peptides and proteins and the rest (10 %) is bound with relatively low affinities, forming reactive zinc(II) pool able to interact with other intracellular substances and compartments [1]. The last, very small fraction (approx. < 0.01 ‰ of total cellular zinc(II), ranging from pM to single digit nM) includes free zinc(II) ions [2]. Due to the abundance of zinc(II) ions more than ten percents of mammalian proteome consist from zinc-containing proteins involved in cell signalling, gene expression, membranes structure stability and function, cell respiration and modulation of the redox state. From those, zinc is required for the activity of more than 300 enzymes, interacting with zinc-binding domains such as zinc fingers, RING fingers, and LIM domains [3].

Zn^{2+}dysregulation, deficiency and over-supply are connected with various pathologies as diseases of the immune, gastrointestinal, endocrine and nervous system, heart failures, hematologic diseases, wound healing, ocular functions and neoplasms [4-6]. Displacement of Zn^{2+} from zinc-binding structures as zinc fingers in DNA repairing enzymes, may even be a major mechanism for carcinogenicity of other metals such as cadmium, cobalt, nickel, and arsenic [7]. The role of zinc in cancer has received increasing attention. A link between zinc deficiency and cancer has been shown in numerous clinical studies [8,9], and it was found that zinc status is compromised in cancer patients compared to healthy people [10]. This is clearly indicated in the ecological study, which was conducted using state-averaged cancer mortality rate data for white Americans for 1970-94 with indices for alcohol consumption, smoking, Hispanic heritage, urban residence and dietary factors for four large U.S. regions. The dietary zinc index was inversely correlated with 12 types of cancer (Hodgkin's lymphoma, bladder, breast, colon, oesophageal, gastric, rectal, laryngeal, nasopharyngeal, oral, skin and vulvar cancer) [11]. These results were also confirmed by Zuo et al. and by Unal et al., who found decreased zinc levels in serum of leukemic patients [12] and in serum of Hodgkin disease patients respectively [13]. Moreover, decreased blood levels of antioxidants (retinol, a-tocopherol, b-carotene) and zinc were found in childhood malignancies [14,15], which could be one of the negative effects of zinc metabolism alterations. Zinc deficiency has been also associated with oxidative stress [16] and oesophageal, head and neck cancer, prostate and other cancer types especially in their development and progression [17-21].

The cancer risk due to zinc deficiency and oxidative stress was also positivelly correlated with lack in DNA repairing [22]. One of possible explanations is that the oxidative stress under the low zinc concentrations is caused by damaging of the mitochondrial functions, because zinc is necessary for mitochondrial functions [16]. In addition, cancer patients with zinc deficiency exhibited increased paraneoplastic cachexia and treatment-associated morbidity [6].

One may suggest that zinc excessive supplementation would be beneficial, but this feature depends on the type of tumour disease, because Plum et al. and Ko et al. showed that zinc excessive supplementation may be immunosuppressive and may therefore increase the risk of prostate cancer [23,24], because of unique prostate cancer zinc metabolism [4]. In spite of the situation in prostate cancer, it could be concluded that some supplementation with zinc(II) ions could be beneficial [25]. However, this is limited by the absence of a marker of its deficiency because decreased serum zinc concentrations are late sign of its deficiency. Depression of immune-stimulated TNFα secretion by leukocytes seems to be such a marker, but there are some technical disadvantages of this method [26].

It is clear that the role of zinc in tumour diseases is still not satisfactory answered and need to be further investigated. One piece of puzzle could be maintaining of zinc homeostasis, which is critical under normal and disease conditions [27], because zinc must be available in proper concentrations on the right place in the right time. There are no specific zinc storage systems, therefore its homeostasis is achieved by regulation of zinc uptake, distribution and excretion [28]. Membrane transporters and intracellular regulators, from which (apo) metallothioneins seems to be the most important ones, are of great interest [29]. Various types of tumour cell lines have been used to investigate the cellular effects of zinc(II) ions and its connection with metallothioneins, because it has not still been clarified whether zinc may directly act on cancer cells and what are the molecular mechanisms involved in this effect. Apoptosis belongs to the mostly targeted issue relating to Zn(II). It was found that zinc concentrations within the range from 33.7 to 75 μM induced apoptosis in mouse TS/A mammary adenocarcinoma cells and that the induced apoptosis was associated with the increased production of intracellular reactive oxygen species (ROS), and p53 and Fas/Fas ligand mRNA and protein. Zn^{2+} induced only a faint MT response in cancer cells in comparison with mouse lymphocytes. The treatment of tumour cells with the antioxidant N-acetylcysteine was able to prevent zinc-induced apoptosis, as well as the increase in p53 and Fas ligand proteins induced by zinc. This indicates that zinc exerts a direct action on mammary cancer cells inducing ROS-mediated apoptosis and that the effect may be mediated by the ROS-dependent induction of p53 and Fas/Fas ligand [30]. Variability of responses to increased external zinc concentration was shown in three colon cancer cell lines with different sensitivities to zinc representing different stages of carcinogenesis. The most sensitive cell lines exhibited the increased levels of the intracellular free zinc and the inability to overexpress MTs. Mechanisms of zinc-induced cell injury and cell death revealed oxidative stress as the most important underlying mechanism activating stress kinase-dependent signalling, perturbation of mitochondria and plasma membrane damage. In addition, observed cell death in individual cell populations was cell line-dependent and variable including cells displaying features of apoptosis, necrosis, autophagy and other mixed-types of cell death [31]. Based on the mentioned facts, there are some connections between MTs and zinc and/or oxidative stress, which are summarized in the following chapters of this review.

Metallothioneins

Metallothioneins (MTs) are ubiquitous metal-binding proteins that have been highly conserved throughout evolution. These proteins were discovered by Margoshes and Valee as cadmium-binding proteins isolated from horse kidney in 1957 [32]. Later on, their involving in heavy metal homeostasis, oxidative stress coping, gene expression and transcription regulation, enzymes activation, apoptosis and cell proliferation have been found [33,34]. Four major isoforms (MT-1 through MT-4) have been identified in mammals [35-37]. MTs genes are tightly linked, and at a minimum they consist of eleven MT-1 genes (MT-1A, -B, -E, -F, -G, -H, -I, -J, -K, -L, and -X) encoding functional or non-functional RNAs, and one gene for each of the other MTs isoforms (the MT-2 A, MT-3, and MT-4 gene) [38]. The nomenclature for MTs isoforms has not been standardized until now [38]. A gene called MT-like 5 (MTL-5) that encodes a testis-specific MT-like protein called tesmin was described in the q13 region of chromosome 11 [39]. Tesmin plays a specific role in both male and female meiotic prophasis [39]. The specific functional roles of MTs isoforms and their molecular interactions are still unclear [40]. MT-1 and MT-2 are the most widely distributed MT isoforms. They are expressed in many cell types in different tissues and organs. Contrariwise, MT-3 and MT-4 demonstrate very limited cell-specific pattern of expression. MT-3 represents a unique metalloprotein called also neuronal-growth inhibitory factor, which inhibits outgrowth of neuronal cells [41]. In comparison with MT-1 and MT-2, MT-3 shows distinct chemical, structural and biological properties [42-46]. Moreover, connection of MT-3 to neurodegenerative processes is discussed. In addition, MT-4 belongs to noninducible proteins, with its expression primarily confined to certain squamous epithelia [47].

MTs and zinc in inhibition of apoptosis

The ability of MTs to bind toxic heavy metals and detoxify free radicals can be both beneficial and deleterious. According to the titles of two popular reviews, MT is a multipurpose protein with two faces [48,49]. In healthy cells MTs protect the cells against heavy metals and ROS action [50], but in cancer cells increased expression of MTs during chemotherapy or irradiation allows the cells to survive and to develop a resistance to chemo- and radiotherapy [51,52]. MTs can also help the cancer cell to survive by inhibition of apoptosis [49,53]. The two main roles of MTs are regulation of intracellular zinc concentration and interaction of MTs with some proteins involved in apoptosis. Zinc is an intracellular mediator of apoptosis, which can interfere with action of Ca^{2+}. Zinc addition prevents DNA fragmentation and inhibits many proteins connected to apoptosis, like caspases and calcium-magnesium dependent proteases [10]. Moreover zinc induces a transcription of the p53 gene, with increased expression of p53 mRNA and protein [54]. Some interactions between zinc, MTs and some genes and proteins involved in apoptosis must be considered, because MTs interact with the p50 subunits of a nuclear factor κB (NF-kB), with a kinase domain of PKCl, with GTPase Rab3A and protein p53. Those interactions are important for tumour growth, because activation and/or inactivation of these proteins may mediate antiapoptotic effect of MTs.

Nuclear factor κB (NF-κB)

MT-1 and MT-2 regulate the level, activity and cellular location of the transcription factor NF-kB [55-58]. NF-kB is necessary to ensure cell protection from the apoptotic cascade induced by tumour necrosis factor (TNF) and other stimuli through activation of antiapop-

totic genes and protooncogenes such as Bcl-2, c-myc and TRAF-1. Overexpression of MT-2 sensitized rodent cells to apoptosis induced by DNA cross-linking agent through inhibition of NF-κB activation [59]. Zinc has been suggested to be an important regulator of NF-κB. In HeLa cells, pyrrolidinedithiocarbamate (PDTC), a zinc ionophore, and zinc itself inhibited NF-κB activity. When the cells were pretreated with MT-inducers, PDTC did not inhibit NF-κB activity. HeLa cells overexpressing MT-2A did not exhibit inhibition of NF-κB activity by PDTC. These results implicate MTs in the zinc regulation of NF-κB and identify MTs as one of the potential intracellular modulators of NF-κB activation [56].

Zinc fingers

MTs can transfer zinc to zinc fingers of transcription factors. Therefore MTs influence binding of transcription factors to DNA and thus they regulate transcription [60]. Zinc transfer from transcription factor-IIIA fingers to thionein clusters was observed [61,62], as well as at transcription factor IIA [61], zinc finger transcription factor Zn(3)-SP1 [63] and oestrogen receptor zinc finger [64]. Zinc fingers, in which zinc is replaced with cadmium, exhibit lower affinity to DNA due to different conformation of DNA-binding domains [65]. It was observed that binding of zinc finger peptides to DNA can be modulated by the metallothionein-thionein conjugate pair [66].

PKC

PKC contain zinc finger-like domains [67]. Interaction of MTs with zinc fingers is known via zinc administration. It was found that MT-2A interacts with the kinase domain of PKC in prostate cancer [68]. There is supposed that this interaction contributes to induction of chemoresistance and/or androgen independence of prostate cancer cells. Moreover, zinc enhances the activity of protein kinase C that leads to induction of MT mRNA [69].

ECRG

ECRG2, a novel candidate of a tumour suppressor gene in the oesophageal carcinoma, interacts directly with MT-2A and links to apoptosis [70]. The interaction of ECRG2 and MT-2A was confirmed by glutathione S-transferase pull-down assays *in vitro* and co-immunoprecipitation experiments *in vivo*. ECRG2 co-localized with MT-2A mostly to nuclei and slightly to cytoplasm, as shown by confocal microscopy. Transfection of ECRG2 gene inhibited cell proliferation and induced apoptosis in oesophageal cancer cells [70].

p53

The p53 tumour suppressor protein has achieved stardom in molecular oncology owing to frequent inactivation in a large range of cancers. This apoptosis-inducing guardian of genome integrity binds to DNA via a sequence-specific DNA-binding domain and is stabilized by the coordination of an atom of zinc within a Cys_3His_1 cluster [71]. This binding to DNA is necessary for its function. Structure and function of p53 is controlled by zinc binding and redox conditions [72]. Properties of p53 can be regulated through two integrated biochemical systems: the redox-sensing capacity of the p53 protein (due to its structural features and its regulation by redox factors such as thioredoxin, MTs, or the redox-repair enzyme APE1/ref-1) and the expression of p53 as multiple isoforms with antagonist effects [73]. Surface plasmon resonance was used to study the specific interaction of p53 with apo-MT (metal-free form of MT-). Interaction was originated from the high binding affinity of free sulfhydryl groups of apo-MT with Zn^{2+} of p53, causing p53 to adopt a "mutant like" form with loss of sequence-specific DNA-binding activity [74]. In other *in vitro* studies, apo-MT-1

but not MT-1 (MT-1 with metal ion) forms a complex with p53 [57,75,76]. Further, recombinant MT, a metal chelator protein, was found to modulate p53 conformation *in vitro* [77]. One may conclude that in cultured cells, transfection with MT gene could modulate p53 transcriptional activity. Therefore, some data to support this speculation has to be needed. Thus, the potential role of p53 in regulation of MTs in the p53 positive MN1 and parental MCF7 cells was investigated. Zinc and copper increased activity of metal response elements (MREs) and MTF-1 expression and inactivation of p53 or the presence of inactive p53 inhibited MRE-dependent reporter gene expression in response to metals. This indicates that activation of p53 is an important factor in metal regulation of MTs [78]. In addition, removing of Zn^{2+} from protein p53 by MTs leads to its inactivation and therefore to inhibition of p53 mediated apoptosis [54] by inhibition of its binding to DNA [79] and proteins [80]. Persistent apo-MT overexpression in the cells may therefore promote their accelerated growth through the induction of a p53-null state [81].

The hypothesis of interactions between MTs and protein p53 has been also verified using the animal experiments. In p53 deficient mice with zinc deficiency, which were exposed to carcinogen 4-nitroquinoline 1-oxide, a significantly greater development of tumours was observed. In those tumours and in preneoplastic lingual and oesophageal lesions, overexpression of cytokeratin 14, cyclooxygenase-2 and MT that correlates with increased cellular proliferation, was detected [82]. MTs and p53 were colocalized in nuclei of canine mammary tumours, subcellular accumulation of p53 protein and MTs was associated with tumour malignancy and in part of benign tumours there was detected low to moderate intensity of MTs and the p53 protein. The authors found these results speculated that this expression in benign tumours would evolve into malignant ones [83].

Analysis of human cancer patients showed also interesting correlations between p53 and MTs gene expressions. In pancreatic serous cystadenomas, the increased expressions of MTs and p53 were observed in the less differentiated tumours. Thus the mRNA expression of MTs may be a potential prognostic marker for these tumours [84]. In oral squamous cell carcinoma frequent localization of MTs in nuclei was associated with the increased expression gene TP53. MT and p53 co-expression can be therefore considered as a sign of shorter survival of patients with advanced disease [85].

Conclusion

Zinc(II) ions contribute to a number of biological processes such as DNA synthesis, gene expression, enzymatic catalysis, neurotransmission, and apoptosis. Both zinc deficiency and zinc overload elicits oxidative stress that can lead to the cell death. These pro-oxidant functions contrast with pro-antioxidant functions in a range of physiological zinc concentrations. Oxidative or nitrosative stress can cause a release of zinc from proteins containing zinc-fingers and cluster motifs and its re-distribution, thereby alter the functions of those proteins, from which it is released and/or to which it binds. The transduction of redox signals into zinc signals and vice versa affects mitochondrial functions and signalling pathways including alterations in NF-kappa B, p53 and AP-1 activities and levels. Zinc sensors for cellular and organ physiology, improved analytical tools to approach zinc proteome, biomarkers of zinc deficiencies, methods for zinc imaging, obtaining more complex information on polymorphisms in zinc transporters, importers and binding proteins and on methods of targeting specific subcellular pools of zinc will be needed to develop for achieving this goal [3,86].

Acknowledgement

The work was supported by V4 Metallomic Scientific Network TD 11440027.

References

[1] R.B. Franklin, L.C. Costello, J. Cell. Biochem. 106 (2009) 750.
[2] R.A. Colvin, W.R. Holmes, C.P. Fontaine, W. Maret, Metallomics 2 (2010) 306.
[3] E. John, T.C. Laskow, W.J. Buchser, B.R. Pitt, P.H. Basse, L.H. Butterfield, P. Kalinski, M.T. Lotze, J. Transl. Med. 8 (2010) 1.
[4] J. Gumulec, M. Masarik, S. Krizkova, V. Adam, J. Hubalek, J. Hrabeta, T. Eckschlager, M. Stiborova, R. Kizek, Curr. Med. Chem. 18 (2011) 5041.
[5] P. Babula, V. Kohoutkova, R. Opatrilova, I. Dankova, M. Masarik, R. Kizek, Chim. Oggi-Chem. Today 28 (2011) 18.
[6] J.E. Cummings, J.P. Kovacic, J. Vet. Emerg. Crit. Care 19 (2009) 215.
[7] D. Beyersmann, A. Hartwig, Arch. Toxicol. 82 (2008) 493.
[8] B.N. Ames, Mutation Research-Fundamental and Molecular Mechanisms of Mutagenesis 475 (2001) 7.
[9] Y.Z. Fang, S. Yang, G.Y. Wu, Nutrition 18 (2002) 872.
[10] D.K. Dhawan, V.D. Chadha, Indian J. Med. Res. 132 (2010) 676.
[11] W.B. Grant, Anticancer Res. 28 (2008) 1955.
[12] X.L. Zuo, J.M. Chen, X. Zhou, X.Z. Li, G.Y. Mei, Biol. Trace Elem. Res. 114 (2006) 41.
[13] E. Unal, A.O. Cavdar, E. Babacan, S. Gozdasoglu, G. Yavuz, A. Ikinciogullari, E. Akar, S. Cin, J. Trace Elem. Med. Biol. 14 (2001) 25.
[14] D.J.M. Malvy, B. Burtschy, J. Arnaud, D. Sommelet, G. Leverger, L. Dostalova, J. Drucker, O. Amedeemanesme, Int. J. Epidemiol. 22 (1993) 761.
[15] D.J.M. Malvy, J. Arnaud, B. Burtschy, D. Sommelet, G. Leverger, L. Dostalova, O. AmedeeManesme, Med. Pediatric Oncol. 29 (1997) 213.
[16] D.J. Eide, Metallomics 3 (2011) 1124.
[17] R.B. Franklin, L.C. Costello, Arch. Biochem. Biophys. 463 (2007) 211.
[18] C. Hogstrand, P. Kille, R.I. Nicholson, K.M. Taylor, Trends Mol. Med 15 (2009) 101.
[19] E.A. Ostrakhovitch, Curr. Cancer Drug Targets 11 (2011) 479.
[20] T. Fukada, S. Yamasaki, K. Nishida, M. Murakami, T. Hirano, J. Biol. Inorg. Chem. 16 (2011) 1123.
[21] M.O. Pedersen, A. Larsen, M. Stoltenberg, M. Penkowa, Prog. Histochem. Cytochem. 44 (2009) 29.
[22] E. Ho, J. Nutr. Biochem. 15 (2004) 572.
[23] L.M. Plum, L. Rink, H. Haase, Int. J. Environ. Res. Public Health 7 (2010) 1342.
[24] Y.H. Ko, Y.J. Woo, J.W. Kim, H. Choi, S.H. Kang, J.G. Lee, J.J. Kim, H.S. Park, J. Cheon, Asian J. Androl. 12 (2010) 164.
[25] A.S. Prasad, O. Kucuk, Cancer Metastasis Rev. 21 (2002) 291.
[26] M.S. Ryu, B. Langkamp-Henken, S.M. Chang, M.N. Shankar, R.J. Cousins, Proc. Natl. Acad. Sci. U. S. A. 108 (2011) 20970.
[27] M. Murakami, T. Hirano, Cancer Sci. 99 (2008) 1515.
[28] W. Maret, A. Krezel, Mol. Med. 13 (2007) 371.
[29] Q. Hao, W. Maret, J. Alzheimers Dis. 8 (2005) 161.
[30] M. Provinciali, A. Donnini, K. Argentati, G. Di Stasio, B. Bartozzi, G. Bernardini, Free Radic. Biol. Med. 32 (2002) 431.
[31] S. John, T. Briatka, E. Rudolf, Oncol. Rep. 25 (2010) 769.
[32] M. Margoshes, B.L. Vallee, J. Am. Chem. Soc. 79 (1957) 4813.
[33] N. Thirumoorthy, K.T.M. Kumar, A.S. Sundar, L. Panayappan, M. Chatterjee, World J. Gastroenterol. 13 (2007) 993.
[34] S.E. Theocharis, A.P. Margeli, A. Koutselinis, Int. J. Biol. Markers 18 (2003) 162.
[35] A.T. Miles, G.M. Hawksworth, J.H. Beattie, V. Rodilla, Crit. Rev. Biochem. Mol. Biol. 35 (2000) 35.
[36] C.O. Simpkins, Cell. Mol. Biol. 46 (2000) 465.
[37] R. Kizek, L. Trnkova, E. Palecek, Anal. Chem. 73 (2001) 4801.
[38] K. Ghoshal, S.T. Jacob, Prog. Nucleic Acid Res. Mol. Biol. 66 (2001) 357.
[39] C. Olesen, M. Moller, A.G. Byskov, Molecular Reproduction and Development 67 (2004) 116.
[40] J.H.R. Kagi, A. Schaffer, Biochemistry 27 (1988) 8509.
[41] Z.X. Huang, Febs Journal 277 (2010) 2911.

[42] P. Faller, Febs Journal 277 (2010) 2921.
[43] Z.C. Ding, F.Y. Ni, Z.X. Huang, Febs Journal 277 (2010) 2912.
[44] G.J. Brewer, Metallomics 1 (2009) 199.
[45] R. Bofill, M. Capdevila, S. Atrian, Metallomics 1 (2009) 229.
[46] L.A. Ba, M. Doering, T. Burkholz, C. Jacob, Metallomics 1 (2009) 292.
[47] M. Vasak, G. Meloni, J. Biol. Inorg. Chem. 16 (2011) 1067.
[48] P. Coyle, J.C. Philcox, L.C. Carey, A.M. Rofe, Cell. Mol. Life Sci. 59 (2002) 627.
[49] H.M. McGee, G.M. Woods, B. Bennett, R.S. Chung, Photochem. Photobiol. Sci. 9 (2010) 586.
[50] C.D. Klaassen, J. Liu, B.A. Diwan, Toxicol. Appl. Pharmacol. 238 (2009) 215.
[51] M. Knipp, Curr. Med. Chem. 16 (2009) 522.
[52] T. Boulikas, M. Vougiouka, Oncol. Rep. 10 (2003) 1663.
[53] M. Dutsch-Wicherek, J. Sikora, R. Tomaszewska, Front. Biosci. 13 (2008) 4029.
[54] L.Z. Fan, M.G. Cherian, Br. J. Cancer 87 (2002) 1019.
[55] H.L. Butcher, W.A. Kennette, O. Collins, R.K. Zalups, J. Koropatnick, J. Pharmacol. Exp. Ther. 310 (2004) 589.
[56] C.H. Kim, J.H. Kim, J. Lee, Y.S. Ahn, Toxicol. Appl. Pharmacol. 190 (2003) 189.
[57] A.B. Abdel-Mageed, K.C. Agrawal, Cancer Res. 58 (1998) 2335.
[58] C.Y. Wang, J.C. Cusack, R. Liu, A.S. Baldwin, Nat. Med. 5 (1999) 412.
[59] E. Papouli, M. Defais, F. Larminat, J. Biol. Chem. 277 (2002) 4764.
[60] B.L. Vallee, J.E. Coleman, D.S. Auld, Proc. Natl. Acad. Sci. U. S. A. 88 (1991) 999.
[61] J. Zeng, B.L. Vallee, J.H.R. Kagi, Proc. Natl. Acad. Sci. U. S. A. 88 (1991) 9984.
[62] M. Huang, C.F. Shaw, D.H. Petering, J. Inorg. Biochem. 98 (2004) 639.
[63] R. Kothinti, A. Blodgett, N.M. Tabatabai, D.H. Petering, Chem. Res. Toxicol. 23 (2010) 405.
[64] D.F. CanoGauci, B. Sarkar, FEBS Lett. 386 (1996) 1.
[65] G. Malgieri, L. Zaccaro, M. Leone, E. Bucci, S. Esposito, I. Baglivo, A. Del Gatto, L. Russo, R. Scandurra, P.V. Pedone, R. Fattorusso, C. Isernia, Biopolymers 95 (2011) 801.
[66] G. Roesijadi, R. Bogumil, M. Vasak, J.H.R. Kagi, J. Biol. Chem. 273 (1998) 17425.
[67] S. Kuroda, C. Tokunaga, Y. Kiyohara, O. Higuchi, H. Konishi, K. Mizuno, G.N. Gill, U. Kikkawa, J. Biol. Chem. 271 (1996) 31029.
[68] P.S. Rao, M. Jaggi, D.J. Smith, G.P. Hemstreet, K.C. Balaji, Biochem. Biophys. Res. Commun. 310 (2003) 1032.
[69] M. Ebadi, M.A. Elsayed, M.H.M. Aly, Neuroendocrinol. Lett. 15 (1993) 69.
[70] Y.P. Cui, J.B. Wang, X.Y. Zhang, R.G. Lang, M.X. Bi, L.P. Guo, S.H. Lu, Biochem. Biophys. Res. Commun. 302 (2003) 904.
[71] C. Meplan, P. Hainaut, J. Trace Elem. Med. Biol. 12 (1999) 337.
[72] P. Hainaut, K. Mann, Antioxid. Redox Signal. 3 (2001) 611.
[73] H. Hafsi, P. Hainaut, Antioxid. Redox Signal. 15 (2011) 1655.
[74] N. Xia, L. Liu, X.Y. Yi, J.X. Wang, Anal. Bioanal. Chem. 395 (2009) 2569.
[75] M. Knipp, G. Meloni, B. Roschitzki, M. Vasak, Biochemistry 44 (2005) 3159.
[76] E.A. Ostrakhovitch, P.E. Olsson, S. Jiang, M.G. Cherian, FEBS Lett. 580 (2006) 1235.
[77] C. Meplan, M.J. Richard, P. Hainaut, Oncogene 19 (2000) 5227.
[78] E.A. Ostrakhovitch, P.E. Olsson, J. von Hofsten, M.G. Cherian, J. Cell. Biochem. 102 (2007) 1571.
[79] E. Palecek, M. Brazdova, H. Cernocka, D. Vlk, V. Brazda, B. Vojtesek, Oncogene 18 (1999) 3617.
[80] J.X. Wang, J.L. Yang, Curr. Pharm. Biotechnol. 11 (2010) 122.
[81] Y. Kondo, J.M. Rusnak, D.G. Hoyt, C.E. Settineri, B.R. Pitt, J.S. Lazo, Mol. Pharmacol. 52 (1997) 195.
[82] L.Y.Y. Fong, Y.B. Jiang, J.L. Farber, Carcinogenesis 27 (2006) 1489.
[83] S.A. Vural, M.R. Vural, S. Kuplulu, M.E. Alcigir, M. Kaymaz, Rev. Med. Vet. 160 (2009) 300.
[84] M. Sliwinska-Mosson, H. Milnerowicz, J. Rabczynski, S. Milnerowicz, Arch. Immunol. Ther. Exp. 57 (2009) 295.
[85] S.V. Cardoso, J.B. Silveira, V.D. Machado, A.M.B. De-Paula, A.M. Loyola, M.C.F. De Aguiar, Anticancer Res. 29 (2009) 1189.
[86] S. Krizkova, M. Ryvolova, D. Hynek, T. Eckschlager, P. Hodek, M. Masarik, V. Adam, R. Kizek, Electrophoresis in press (2012).

CONFERENCE PROCEEDINGS
Metallomics Technology Conference 2015: Recent Advances and Strategies
Editors: Vojtěch Adam, René Kizek
Publisher: Mendel University in Brno, Zemědělská 1, 613 00 Brno
Print: Mendel University Press, Zemědělská 1, 613 00 Brno
Edition: 1st Edition, 2015
No. of pages: 80
No. of copies: 20

ISBN 978-80-7509-309-7
ISBN 978-80-7509-314-1 (on-line)

The project is supported by International Visegrad Fund.
www.visegradfund.org